Analysis and Manipulation of Specialized Metabolism in Solanaceae

A Dissertation
SUBMITTED TO THE FACULTY OF THE UNIVERSITY
OF MINNESOTA
BY

VINCENZO AVERELLO IV

IN PARTIAL FULFILLMENT OF THE REQUIREMENTS
FOR THE DEGREE OF
DOCTOR OF PHILOSPHY

ADRIAN D. HEGEMAN

2024

Acknowledgements

My time as a graduate student and worker in the Department of Horticultural Science at the University of Minnesota was supported and connected to more people than I can name. However, I am stubborn and will still try.

Thank you to my advisors, Changbin Chen and Adrian Hegeman. Thank you Changbin for bringing me to the University of Minnesota, teaching me tissue culture, gene transfer, and molecular biology. You are the most supportive advisor I could have. Thank you, Adrian Hegeman for bringing me into your lab after Changbin moved his lab to Arizona State University in 2021 and teaching me metabolomics and allowing me the space to apply the techniques I learned to research questions in his lab. I need to thank Emily Hoover who facilitated the transition between advisors and labs during the depths of COVID19.

Thank you to everyone in the Chen Lab, the post-docs and researchers Nelson Garcia, Penny Kianian, Stefanie Dukowic-Schulze, and Ryan Murphy who all helped me get settled into the Chen Lab and learn molecular biology techniques. I want to thank my fellow grad student in the Chen Lab Clair Milstead who was a huge support at times while we worked together, particularly during COVID as the Chen Lab wound down its time in Minnesota.

When I moved into the Hegeman Lab during the depths of COVID, Kate Freund Saxhaug and Kate Sammons were there to get me started working the lab during the difficult time for all of us. Thank you for teaching me how to perform LC-MS and getting started in the Hegeman Lab. Thank you to Emily Juhl and Daniel Bacher for being great lab mates, officemates and friends. Thank you to Evan Larson who helped me in the lab since he joined and helped advance my knowledge of LC-MS and helping with research questions.

Jayanti Suresh has been the biggest support and help during my entire time in the department. For every time I broke the autoclave or dishwasher or needed to order something or 1,000 other requests, thank you so much. Thank you for all the food and gifts you have brought over the years.

Thank you to everyone who served on my preliminary exam committee and dissertation committee. Thank you to Eric Watkins and Laura Shannon for serving as committee chairs and providing research help and space when needed. Thank you to Neil Olszewski and Clay Carter for being fantastic resources for the past several years for questions about genetics and molecular biology.

Thank you to Jerry Cohen and Gary Gardner who have been supportive faculty in the department when I have questions directly related to my research or anything that could come up. Also thank you Gary for your support of graduate student fellowships that I have been

awarded while here. Thank you to Alan Smith, Cindy Tong, Neil Anderson, and Matthew Clark for allowing me to use lab space and laminar flow hoods through this time.

The APS and Horticultural Science Staff have been massively helpful with any number of issues that have arisen. Special thanks to Lynne Medgaarden, Lauren Matsushin, Alicia McCann, Serena Jones, Kelsey Bogdanovich, Echo Martin, and Sam Grover.

The APS Grad Program is one of the best communities of friends and scholars of which I can be a member. As someone who moved here with no social network, the grad students here made me feel welcomed and embraced. Special thanks go to Jeff Neyhart, John Hill, Austin Dobbels, Kayla Altendorf, Garrett Heineck, Vivian Wauters, Sharon Perrone, Seth Wannemuehler, Sarah Moore, Mjay Espina, Julian Cooper, Lucas Roberts, Lori Crogan, James Bowdin and so many, many more than can be named. And to all my officemates, Matthew Gullickson, Andrew Sherwood, Michael Laskowski, and Leisl Litshewski.

Thank you to all the fellow organizers of GLU-UE Local 1105 who did what we were told could not be done, organizing a graduate labor union at the University of Minnesota and winning a contract. Thank you to Noah Wexler, Anya Auerbach, Matthew Kornberg, Alex Provan, David Wolfson, Andrew Mann, Phoebe Keyes, Casey McNichols, Julia Baker, and hundreds of others who worked together to make this change happen.

Special thanks to those friends who broke bread together. Max Fraser, James Wolfin, Elizabeth Blissett, Baylee Miller, Rebecca Fudge, Eitan Jaffe thank you for the friendship and companionship provided over the years.

To my friends around the country who came back together especially during COVID, thank you for being an outlet of connection in those times. To Ed Chavez, Bradley Meek, Patrick Sutton who watched movies on Friday nights. To those who played games together Christopher Baldi, Carol Baldi, Christopher Aa, Christopher Wysznski, Lee Markison, Laura Kenny, and Patrick Kenny. Most of all to David Bopp and Daniel Clark.

Finally, I want to thank my family, my mom, my dad, my sister, Aunt Diane, and grandma for the support you've given during this degree and my whole life.

Abstract

Plants produce a wide range of specialized metabolites. These compounds act in a myriad of ways producing attractive colors and aromas for pollinators and seed dispersal, flavor volatiles, and defensive compounds. Steroidal glycoalkaloids (SGAs) are biosynthetically produced from a cholesterol backbone. Most plants produce phytosterols, including β-sitosterol, stigmasterol, and campesterol, from a single sterol pathway, while *Solanum* has a branch off of the main sterol biosynthetic pathway that generates cholesterol and SGAs. Squalene is a terpene precursor of all phytosterols. The cholesterol branch shares several enzymes while several key steps are performed by enzymes that are duplicated from genes in the main branch. Cholesterol is modified, nitrogen is incorporated, and the resulting SGAs are glycosylated. Jasmonic acid responsive ethylene response factor 4 (JRE4) is a major regulator of the cholesterol branch and SGA biosynthesis. SGAs can impart bitter flavors and also provide defense against insect herbivory and fungal infection. The duplicated genes are *DWARF5* (in general phytosterol biosynthesis) and *7DHCR* (in the cholesterogenesis pathway). *Arabidopsis dwf5* mutants have a short stature and smaller dark green leaves due to deficiencies in brassinosteroid production. CS72 carries a single nucleotide polymorphism in *DWF5*, *dwf5-4. 7DHCR* was cloned from MTX-851 and transformed into a *dwf5-4* line. Relative sterol content was measured using UHPLC-HRAMS, and a Zorbax SB-CN column with an APCI source. Squalene content increased in the *dwf5-4* line compared to the *7DHCR* complementation line, while β-sitosterol and campesterol content decreased. These results suggest *7DHCR* has a broader substrate specificity than previously understood. Several species in the genus *Jaltomata*, a close relative of tomato, produce a red nectar. *Jaltomata bohsiana* produces a clear nectar and lacks a protein found in red-nectared species. To better understand this trait, an *Agrobacterium*-mediated transformation protocol was developed. *J. bohsiana* seeds were germinated in sterile Magenta boxes to produce explants from the cotyledons and hypocotyl. After 48 hours, these were co-cultured with AGL1 carrying a binary vector based on pDIRECT21_C. TAIL-PCR showed the insert was present with plant DNA from most closely matches data from fully sequenced *Solanum* relatives as one would expect given the lack of available *Jaltomata bohsiana* genomic sequence information.

Table of Contents

List of Tables

List of Figures

Chapter 1

Chapter 2

Introduction

Plants produce a wide range of specialized metabolites to enable interaction with their environment. These metabolites are connected to many processes in the plant's life cycle, including pollination, dispersal, defense, and abiotic stress. Beyond the plant's use of these compounds, humans have taken interest in these compounds for millenia. They are used as dyes, flavoring, medicine, and recreation. Because of the importance of specialization metabolism to plants, humans, and other organisms, they are an exciting area of research.

One plant family, Solanaceae, has been of particular interest, often because of its specialized metabolites. This has led to the family being over-represented in the number of assembled genomes, second only to Brassicaea (Pasin et al. 2024). Among well-known species in Solanaceae there are major vegetable species like tomato (*Solanum lycopersicum*), potato (*Solanum tuberosum*), pepper (*Capsicum* sp.), ornamental species like *Petunia*, other important species like tobacco (*Nicotiana tabacum*), and belladonna (*Atropa belladonna*). These are just some examples of a large plant family with many other species, currently estimated to number near 2,700 (Huang et al., 2023).

In particular, because of robust genomic resources available several tomato lines have been released or could be released soon that have been modified to produce either specialized metabolites in tissue where they were not previously or one that were not present before genetic modification. Among modifications that have been made is the development of a purple fleshed tomato, produced by the expression of two transcription factors from snapdragon (*Antirrhinum majus*) to enhance the levels of anthocyanins in the tomato fruit (Tohge et al., 2015). To produce a tomato fruit with increased ɣ-aminobutyric acid (GABA) levels two genes were modified at the C-terminus to reduce auto-inhibitory function (Nonaka et al. 2017; 2019). Vitamin D_3 was produced in tomato by knocking-out one gene in the cholesterol biosynthesis pathway (Li et al. 2022).

Chapter 1 of this dissertation reviews the current understanding of the SGA pathway. This pathway produces provitamin D_3 in tomato is also the pathway that syntheses steroidal glycoalkaloids (SGAs). SGAs are important defensive compounds that protect plants in *Solanum* against herbivory and fungal stress. *Solanum* has an additional branch of sterol biosynthesis which produces cholesterol, the backbone of SGAs. Nitrogen is incorporated from GABA and that core is glycosylated (Grzech et al., 2024; Itkin et al., 2013). As a pathway with several steps, it presents many opportunities for manipulation and modification to affect human nutritional interest and flavor as well as investigating the cell biology of the storage and transport of SGAs.

Chapter two explores the substrate specificity of a tomato gene, *7-dehdyrocholesterol reductase*. In tomato, one of the reactions in the cholesterol branch of the sterol biosynthesis pathway is the reduction of 7-dehydrocholesterol to cholesterol. This is performed by *7-DHCR*, which is the product of a gene duplication event from *DWARF5*. Both of these genes

reduce the 7-carbon of $\Delta^{5,7}$ sterols, the current understanding in *Solanum* is *7-DHCR* only performs the reduction of 7-dehydrocholesterol while *DWARF5* performs the remaining $\Delta^{5,7}$ sterol reductions (Sonawane et al., 2016). Additionally, there is evidence that *7-DHCR* has broader substrate specificity than solely 7-dehydrocholesterol (Sonawane et al., 2016). There are open questions as to the substrate specificity of *7-DHCR*. In *Arabidopsis*, mutations in *DWARF5* cause a stunted phenotype with shorter stature with smaller darker leaves due to deficiencies in brassinosteroid production (Choe et al., 2000). With this in mind, understanding the difference in substrate specificity between *7-DHCR* and *DWARF5* in tomato could inform further research into neofunctionalization of duplicated genes and enzyme promiscuity (Ji et al., 2024).

Chapter three describes the development of a transformation protocol for *Jaltomata bohsiana*. A trait of particular interest in the Solanaceae is the red nectar trait in *Jaltomata*. Nesocodin was recently identified as the compound that produces this red color. Nesocodin is produced by the reaction of sinapaldehyde and proline (Roy et al., 2024). Also, there are two enzymes expressed in the nectar, one, sinapyl alcohol oxidase, produces sinapaldehyde from sinapyl alcohol and the other carbonic anhydrase, which works in to increase the pH of the nectar to 9.0 and which is needed for the full development of the red pigmentationthe reaction between sinapaldehyde and proline. Unlike tomato and *Arabidopsis*, no transformation protocol has been developed for any *Jaltomata* species. Genetics transformation is an important technique that enables research into the function of genes and the proteins they encode.

The genetics of plant specialized metabolism are often a complex process of many enzymes and transcription factors working to produce these compounds from core metabolism. As many of these enzymes are the product of gene duplication, there are interesting questions related to these enzyme groups to learn about how they have neofunctionalized, including relating substrate specificity. Specialized metabolism genetics research cannot be limited to index species, like corn, tomato, and *Arabidopsis*, so developing the tools, like genetic transformation, is needed to research the genetics of specialized metabolism is still needed and important to learn about how these plants interact with their environment through the production of specialized metabolites.

Worked Cited

Averello, V., A. D. Hegeman, and C. Chen. 2024. Finding the balance: modifying the cholesterol and steroidal glycoalkaloid synthesis pathway in tomato (*Solanum lycopersicum* L.) for human health, fruit flavor, and plant defense. Horticultural Plant Journal.

Choe, S., A. Tanaka, T. Noguchi, S. Fujioka, S. Takatsuro, A.S. Ross, F.E. Tax, S. Yoshida, K.A. Feldmann. 2000. Lesions in the sterol Δ^7 reductase gene of *Arabidopsis* cause dwarfism to a block in brassinosteroid biosynthesis. The Plant Journal 21: 431-443. doi: https://doi.org/10.1046/j.1365-313x.2000.00639.x

Grzech D., S.J. Smit, R. M. Alam, M. Boccia, Y. Nakamura, B. Hong, R. Barbole, S. Heinicke, M. Kunert, W. Seibt, V. Grabe, L. Caputi, B. R. Lichman, S. E. O'Connor, A. Aharoni, and P. D. Sonawane. 2024. Incorporation of nitrogen in antinutritional *Solanum* alkaloid biosynthesis. Nature Chemical Biology. doi: https://doi.org/10.1038/s41589-024-01735-w.

Huang, J., W. Xu, J. Zhai, Y. Hu, J. Guo, C. Zhang, Y. Zhao, L. Zhang, C. Martine, H. Ma, and C.-H. Huang. 2023. Nuclear phylogeny and insights into whole-genome duplications and reproductive development of Solanaceae plants. Plant Communications 4. doi: https://doi.org/10.1016/j.xplc.2023.100595.

Itkin M., U. Heinig, O. Tzfadia, A.J. Bhide, B. Shinde, P.D. Cardenas, S.E. Bocobza, T. Unger, S. Malitsky, R. Finkers, Y. Tikunov, A. Bovy, Y. Chikata, P. Singh, I. Rogachev, J. Beekwilder, A.P. Giri, and A. Aharoni. 2013. Biosynthesis of antinutritional alkaloids in solanaceous crops is mediated by clustered genes. Science 341: 175-179. doi: https://doi.org/10.1126/science.1240230

Ji, W., A. Osbourn, and Z. Liu. 2024 Understanding metabolic diversification in plants: branchpoints in the evolution of specialized metabolism. Philosophical Transactions of the Royal Society B 379:

Li, J., A. Scarano, N. Mora Gonzalez, F. D'Orso, Y. Yue, K. Nemeth, G. Saalbach, L. Hill, C. de Oliveira Martins, R. Moran, A. Santino, C. Martin. 2022. Biofortified tomatoes provide a new route to vitamin D sufficiency. Nature Plants 8: 611-616. doi: https://doi.org/10.1038/s41477-022-01154-6.

Nonaka S., C. Arai, M. Takayama, C. Matsukura, and H. Ezura. 2017. Efficient increase of ɣ-aminobutyric acid (GABA) content in tomato fruits by targeted mutagenesis. Scientific Reports 7. doi: https://doi.org/10.10138/s41598-017-06400-y.

Nonaka S., C. Arai, M. Takayama, C. Matsukura, and H. Ezura. 2019. Author correction: efficient increase of ɣ-aminobutyric acid (GABA) content in tomato fruits by targeted mutagenesis. Scientific Reports 9. doi: https://doi.org/10.10138 /s41598-019-55119-5.

Pasin, F., M. Uranga, R. Charudattan, C.-T. Kwon. 2024. Deploying deep Solanaceae domestication and virus biotechnology knowledge to enhance food system performance and diversity. Horticulture Research 11. doi: https://doi-org/10.1093/hr/uhae205.

Roy, R., N. Moreno, S.A. Brockman, A. Kostanecki, A. Zambre, C. Holl, E.M. Solhaug, A. Minami, E.C. Snell-Rood, M. Hampton, M.A. Bee, Y. Chiari, A.D. Hegeman, and C.J. Carter. 2022. Convergent evolution of a blood-red nectar pigment in vertebrate-pollinated flowers. Proceedings of the National Academy 119. doi: https://doi.org/10.1073/pnas.2114420119.

Sonawane, P.D., J. Pollier, S. Panda, J. Szymanski, H. Massalha, M. Yona, T. Unger, S. Malitsky, P. Ardent, L. Pauwels, E. Almekias-Siegel, I. Rogachev, S. Meir, P.D. Cardenas, M. Athar, M. Petrikov, H. Schaller, A.A. Schaffer, A. Kamble, A.P. Giri, A. Goossens, and A. Aharoni. 2016. Plant cholesterol biosynthetic pathway overlaps with phytosterol metabolism. Nature Plants 3. doi: 10.1038/nplants.2016.205

Tohge, T., Y. Zhang, S. Peterek, A. Matros, G. Rallapalli, Y. A. Tandrón, E. Butelli, K. Kallam, N. Hertkorn, H.-P. Mock, C. Martin, A. R. Fernie. 2015. Ectopic expression of snapdragon transcription factors facilitates the identification of genes encoding enzymes of anthocyanin decoration in tomato. The Plant Journal 83: 686-704. doi: https://doi.org/10.1111/tpj.12920.

Chapter One: Finding the Balance: Modifying the Cholesterol and Steroidal Glycoalkaloid Synthesis Pathway in Tomato (*Solanum lycopersicum* L.) for human health, fruit flavor, and plant defense

Abstract

Unlike most plants, members of the genus *Solanum* produce cholesterol and use this as a precursor for steroidal glycoalkaloids. The production of the compounds begins as a branch from brassinosteroid biosynthesis, which produces cholesterol that is further modified to produce steroidal glycoalkaloids. During the cholesterol biosynthesis pathway, genetic engineering could alter the formation of cholesterol from provitamin D_3 (7-dehydrocholesterol) and produce vitamin D_3. Cholesterol is a precursor for many steroidal glycoalkaloids, including α-tomatine and esculeoside A. Alpha-tomatine is consumed by mammals and it can reduce cholesterol content and improve LDL:HDL ratio. When there is a high α-tomatine content, the fruit will have a bitter flavor. The compounds of α-tomatine and several other glycoalkaloids serve as a protective and defensive compound for tomato against insect, fungal, and bacterial pests. These compounds also affect the rhizosphere bacteria, recruiting beneficial bacteria. One of the steroidal glycoalkalaids, esculeoside A increases while fruit ripening. This review focuses on recent studies that uncovered key reactions of the production of cholesterol and steroidal glycoalkaloids in tomato connecting to human health, fruit flavor, and plant defense and the potential application for tomato crop improvement.

Introduction

This chapter has been published in Horticultural Plant Journal. Tomato (*Solanum lycopersicum* L. syn. *Lycopersicon esculentum* Mill.) is among the most grown and consumed vegetables in the United States and around the world (Bentley, 2017; Fao, 2020). Tomato contains many compounds that are beneficial to human health including vitamin C, folate, and a small amount of vitamin A (Beecher, 1998). Lycopene, which is abundant in tomato, has been connected to improved outcomes of several cancers (Rao and Agarwal, 2000, Song et al., 2021). Tomato also contains steroidal glyoalkaloids (SGAs), which confer a bitter taste to the fruit, protect the plant from pests, and have been connected to improved human health (Friedman, 2002).

The SGAs serve to protect the plant from herbivory and fungal diseases, have been found to improve cholesterol levels, and affect the flavor of tomato fruits (Figure 1). The primary mode action of α-tomatine was to form a complex with 3β-hydroxysteroids, which caused damage to the cell membrane (Roddick, 1974). The growth of many fungal species (with exceptions of *Stemphylium solani* and *Verticillium dahliae*) were inhibited by α-tomatine and it could induce apoptosis in some strains of *Fusarium oxysporum* (Sandrock and Vanetten, 1998; Ito et al., 2007).

In *Solanum*, these SGAs are produced from cholesterol as the sterol core. Sterols are tetracyclic triterpenes with a hydroxyl group attached to the C3 position of the steroid (Fig. 1). SGAs were presented in all organs of the tomato plant but not at all stages of development (Kozukue et al., 2004). The highest levels of α-tomatine and dehydrotomatine were found in the green fruit, flowers, calyxes, and leaves (Kozukue et al., 2004). The amount and particular profiles of sterols and SGAs changed as the fruit ripens (Ijima et al., 2009). As the fruit matures, the amount of α-tomatine decreased and esculeoside A increased (Yamanaka et al., 2009).
During the processes of domestication and improvement, there has been selection against high levels of SGAs (Zhu et al., 2018). There are some varieties that may have been selected to accumulate certain compounds over others, like the bitter-when-ripe fruits found in the Andes (Rick et al., 1994). In commercial fresh fruit, the most prominent SGA is either esculeoside A, lycoperoside F, or lycoperoside G with 1589.4±1738.3 µg in a 126 g serving of fresh tomato (Dzakovich et al., 2020). The authors did not discuss how a serving size was determined. This work was not able to distinguish esculeoside A, lycoperoside F and lycoperoside G from one another by ultra-high performance liquid chromatography (UHPLC). In processed tomato products such as juice, ketchup, and sauce, the most common SGA is α-tomatine (Dzakovich et al., 2020). The content of α-tomatine could vary by year and has been shown to be higher when organic practices are used for cultivation (Koh et al., 2012). The total amount of α-tomatine per green fruit increases as the fruit size increases. For example, a 1.5g-1.9 g fruit has an average of 1.6 mg of α-tomatine per fruit while 218.0g-220.5 g fruit having an average 32.6 mg of α-tomatine per fruit. However, concentration decreases as fruit size increase with small fruit having (89.9±3.6) mg/100g pericarp and the large fruit having (14.9±0.3) g/100 g pericarp (Kozukue and Friedman, 2003).

Several reviews of phytosterol biosysnthesis have been published in the last 20 years. For instance, Benveniste (2004) presented a review of the general phytosterol synthesis based on mutant analysis available at that time. Cardenas et al.(2015) resented a similar scope of cholesterol and SGA synthesis, but new discoveries have been made since that publication. Recent reviews have covered both the production of cholesterol and the production of SGAs all from cholesterol, and the modes of action and properties of α-tomatine (You and van Kan, 2020; Vriese et al., 2021). This review will include new developments in the understanding of tomato SGA biosynthesis.

By understanding the processes that produced the many important compounds that effect fruit flavor, the plant's ability to defend itself and the most nutritious fruit possible, we may be able to manipulate this pathway to find new balances between these three important features of tomato and many horticultural crops. We focused on progress made recent years using molecular, genetic and biochemistry tools and the implications on tomato improvement (Table 1).

Reactions in the production of cholesterol from isoprenoid metabolism

From terpenoid building blocks to the first dedicated steps to produce cholesterol

Terpenes are a broad class of compounds which include carotenoids, which provide color as well as being potent antioxidants through compounds like lycopene and β-carotene, and apocarotenoids which provide flavor through compounds like β-ionone, and sterols (Fig. 1) (Paparella et al, 2021). The cytoplasmic mevalonic acid pathway (MVA) was the source of farnesyl pyrophosphate (FPP) (Closa et al., 2010; Vriese et al., 2021). Two molecules of FPP were joined by squalene synthase to produce squalene (Fig. 2) (Nakashima et al., 1995; Devarenne et al., 1998). In potato, when squalene synthase was more highly expressed either due to a genotypic difference or being driven by a 35S promoter, more SGAs were accumulated (Krits et al., 2007; Ginzberg et al., 2012). An oxygen was attached to the 2 and 3 carbons of squalene to form 2,3-oxidosqualene (sometimes called epoxysqualene) by squalene epoxidase (also called squalene monooxygenase or SQE) which had a cyclic structure that included the 2 and 3 carbons and the newly attached oxygen. There were at least three *SQE* genes with this activity in *Arabidopsis* and two *SQE* genes in *Medicago truncatula*, however, there is no report of SQE being characterized in tomato (Suzuki et al., 2002; Rasbery et al., 2007). Then the 2,3-oxidosqualene was converted to cycloartenol by cycloartenol synthase (CAS) (Raederstorff and Rohmer, 1987; Corey et al., 1993; Gas-Pascual et al., 2014). In tomato, 2,3-oxidosqualene also serves as a precursor of cuticle wax components β-amyrin and δ-amyrin (Wang et al., 2011). Cycloartenol serves as the beginning of sterol production in plants (Fig. 2).

The first dedicated step to the production of cholesterol and its downstream products is reducing the C24-C25 bond of cycloartenol to form cycloartanol (Fig. 2) (Sawai et al., 2014). The pentacyclic steroid, cycloartenol is the beginning of steroid synthesis in plants. This

reduction was performed by sterol sidechain reductase 2 (SSR2) (Sawai et al., 2014). When SSR2 was not actived, there was a significant reduction of cholesterol (Sawai et al., 2014). Cycloartenol represents the branch point between cholesterogenesis and brassinosteroid and other sterol biosynthesis. This step could be a key point of regulation if one wanted to adjust cholesterol, SGAs, or brassinosteroid production. If an ethyl group is attached to C24 by sterol methyltransferase 1 (SMT1) forming 24-methylenecycloartanol, then it will no longer be used to produce cholesterol (Diener et al., 2000). Additionally, if SMT1 is non-functional, the most abundant sterol in *Arabidopsis* will be cholesterol not sitosterol (Diener et al., 2000). This branch could be an important point of control between sterols and brassinosteroids on one branch and cholesterol and SGAs on the other.

In plants, the two methyl groups at C-4 of sterols are removed in two separate reactions. In cholesterol, the first was performed by sterol methyl oxidase 3 (SMO3), a homolog of SMO1, which performed the same reaction in the general sterol pathway (Sonawane et al., 2016). SMO3 uses cycloartanol to produce 31-norcycloartanol. Unlike animals and fungi where a single SMO enzyme performs both oxidations serially, in plants these oxidations occurred at two separate points in sterol metabolism (Darnet and Rahier, 2004). When SMO1 was disrupted by virus induced gene-silencing (VIGS) in leaves and green fruit, an increased accumulation in α-tomatine and when SMO3 was disrupted in the same tissues, there was decreased accumulation of α-tomatine (Sonawane et al., 2016). *In vitro* SMO1 had been found to catalyze an NADPH-dependent reaction, when NADH is substituted, cycloeucalenone is produced instead of cycloeucalenol (Pascal et al., 1990; Pascal et al., 1993; Pascal et al., 1994).

Along with SMO3, the production of 31-norcycloartanol involves at least one and up to three more genes. In tomato, there are two 3β-hydroxysteroid dehydrogenase/C-4 decarboxylase (*3βHSD/D*) genes. When *3βHSD/D2* was silenced, there was a reduction of α-tomatine in the leaves and green fruit. In the leaves, there was also a reduction in cholesterol, campesterol, β-sitosterol, isofucsterol, and Δ^7 avenasterol suggesting this gene was active in both cholesterol biosynthesis and the general sterol metabolism (Sonawane et al., 2016). When both *3βHSD/D* were silenced in *Nicotiana benthimiana*, there was an increase in 4,4-dimethylsterols and the addition of a novel sterol derivative, 4α-carboyx-4β,14α-dimethyl-9β-19-cyclo-ergost-24(24^1)-en-3β-ol (Rahier et al., 2006). C-4 sterol demethylation has been reviewed by Rahier(2011) and another gene may be involved in this process of demethylation (Sonawane et al., 2016).

A putative side chain oxidoreductase (SDR) was found to co-express with SSR in tomato fruits. When this gene was silenced there were decreased in cholesterol, campesterol, stigmasterol, β-sitosterol, and isofucosterol (Sonawane et al., 2016). This suggested this gene was involved in both phytosterol and cholesterol pathways. In yeast, there are three components to the C4 demethylation complex, Sonawane et al. (2016) suggest that this *SDR* gene was a third gene in the plant sterol metabolism pathway (Pascal et al., 1994).

General sterol production and cholesterol/SGA biosynthesis share several enzymes

The next four enzymes in the cholesterol biosynthesis process were shared with the general sterol biosynthesis pathway (Sonawane et al., 2016). The first of these steps is the

oxidation of C8 of 31-norcycloartanol to form 31-nor-24(45)-dihydrolanosterol by cyclopropylsterol isomerase (CPI). In CPI-silenced leaves, there was a significant accumulation of 31-norcycloartanol substrates (Sonawane et al., 2016). The second shared step is the demethylation of C14 of 31-nor-24(25)-dihydrolanosterol to 4*α*-methylcholesta-8,14-dien-3*β*-ol by sterol C-14-demethylase (CYP51). In tomato when this gene was silenced, there was an accumulation of 31-norcycloartanol, the predicted precursor, not 31-nor-24(25)-dihydrolanosterol. However, in *N. benthamiana*, there was accumulation of 31-nor-24(25)-dihydrolanosterol and obtusifoliol, the predicted substrates of CYP51 (Sonawane et al., 2016). This followed by reduction of C14 of 4*α*-methylcholesta-8,14-dien-3*β*-ol to form 4*α*-methyl-24(25)-dihydrozymosterol by sterol C-14 reductase (C14-R). When C14-R was silenced in leaves, there was substantial accumulation of 4*α*-methylcholesta-8,14-dien-3*β*-ol (Sonawane et al., 2016). The final shared step is an isomerization, shifting the double carbon-carbon bond from C-8 of 4*α*-methyl-24(25)-dihydrozymosterol to the C-7 of 4*α*-methyl-5*α*-cholest-7-en-3*β*-ol by 8,7-sterol isomerase (8,7-SI). In *Saccharomyces,* 8,7-SI could complement ERG2, which performed an 8,7-isomerization (Sonawane et al., 2016).

The production of cholesterol

After the four shared reactions, the biosynthesis pathway divides. The methyl group attached to C-4 of 4*α*-methyl-5*α*-cholest-7-en-3*β*-ol was removed by the same process as the removal of a methyl group from C-4 from cycloartanol with the only difference being SMO4 used 4*α*-methyl-5*α*-cholest-7-en-3*β*-ol as a substrate to produce cholesta-7-en-3*β*-ol (Sonawane et al., 2016).

In the same way, the remaining enzymes to produce cholesterol were homologs of enzymes in the general plant sterol pathway, SMO3 was a homolog of SMO1 and SMO4 was a homolog of SMO2 (Sonawane et al., 2016). The next reaction was the oxidation of C-5 of cholesta-7-en-3β-ol to form 7-dehydrocholesterol by C5-sterol desaturase-2 (C5-SD2) (Sonawane et al., 2016). C5-SD2 required NADH to perform this reaction (Sonawane et al., 2016). The transcription factors glycoalkaloid metabolism 9 (GAME9) and MYC2 directly targeted the promoter of *C5-SD2*, working synergistically increasing transcription of C5-SD2 (Cardenas et al., 2016). MYC2 has been identified as a regulator of jasmonate-mediated stress response and termination of jasmonate signaling in tomato (Du et al., 2017), which also plays roles in plant development (Gupta et al., 2014, Kazan and Manners, 2013). C5-SD2 is homologous to STE1/DWARF7 in *Arabidopsis* and ERG3 in *Saccharomyces.* Plants deficient in *STE1/DWARF7* accumulate Δ^7 sterols, such as Δ^7-cholestenol, Δ^7-campestenol, Δ^7-sitosterol, and avenasterol instead of cholesterol, campesterol, sitosterol, and iosfucosterol (Gachotte et al., 1996). STE1/DWARF7 and EFG3 had been found to complement each other (Gachotte et al., 1995, 1996).

GAME9 was also co-expressed with RING membrane-anchor E3 ubiquitin ligase 1 (RMA1), also called MAKIBISHI 1 (MKB1) (Shoji and Saito, 2022). RMA1 is thought to be involved in endoplasmic reticulum (ER) associated degradation (ERAD). *RMA1* had lower relative expression in plants with reduced *GAME9* expression and expression was induced by treating leaves with methyl-jasmonate (MeJA) (Shoji and Saito, 2022). Currently RMA1 has not been functionally characterized in tomato.

In the general plant sterol pathway, phytosterol C7 reduction was performed by DWARF5 (DWF5) and in the cholesterol pathway 7-dehydrocholesterol reductase (7-DHCR), homolog of DWARF5, reduced C7 of 7-deyhydrocholesterol to form cholesterol (Fig. 2) (Sonawane et al., 2016). Cholesterol could be reduced to cholestanol which might serve as a precursor to castasterone and brassinolide (Nakajima et al., 2002; Kim et al., 2004). In *Nicotiana tabacum* and *Phaseolus vulgarus*, cholesterol was the dominant sterol in the phloem, predominantly in glycosylated forms, as well as free sterol and acylated forms (Behmer et al., 2013). The free and acylated forms suggested there may be shuttle proteins for these to travel in the phloem because the acylated cholesterol likely serves as a deterrent from phloemfeeding insects (Behmer et al., 2013). This has not yet been shown in tomato but given the presence of cholesterol in tomato and it being in the same family as *Nicotiana*, it may have a similar composition of sterols in the phloem and could be a future research direction.

Like other genes in brassinosteroid synthesis, mutations in *Arabidopsis DWF5* caused stunted growth and darker rounder leaves (Choe et al., 2000). It was found that *Saccharomyces cerevisiae* expressing the *Arabidopsis* DWARF5 could reduce the C7 bond in producing ergosterol, the major fungal sterol (Lecain et al., 1996).

7-dehydrocholesterol is also called provitamin D_3. When exposed to UVB light (280 nm - 315 nm) provitamin D_3 can be converted to vitamin D_3, which is rarely found in plants. However, there is very little 7-dehydrocholesterol present at any one time in tomato. To increase the pool of 7-dehydrocholesterol available in tomato, 7-DHCR could be disrupted by methods like gene editing with CRISPR-Cas9 (Li et al., 2022). When 7-DHCR was disrupted, the amount of 7-dehydrocholesterol was increased in the fruit at all life stages of tomato (Li et al., 2022). In *Arabidopsis*, when DWF5 mutants were exposed to UVB, 7-dehydrositosterol was converted to vitamin D_5 (Silvestro et al., 2018).

7-DHCR was upreguated by jasmonate-responsive ethylene response factor (ERF) 4 (JRE4) also called Glycoalkaloid Metabolism 9 (GAME9) (Thagun et al., 2016; Nakayasu et al., 2018). When *JRE4* was overexpressed, there was a small but significant increase in cholesterol in the plant (Cardenas et al., 2016). JRE4 occurred in a region of the genome that had been selected against detected by comparisons to genomes of wild and ancestral tomatoes (Zhu et al., 2018). An allelic variant of JRE4 had been characterized which has lower binding efficiency to GAME17 (Yu et al., 2020). JRE4 was regulated by CORONATINE INSENSITIVE1 (COI) (Abdelkareem et al., 2017). COI1 was needed for the perception of jasmonic acid, a stress response hormone, and the upregulating of JRE4 to stimulate production of SGAs (Abdelkareem et al., 2017). COI1 and jasmonic acid have been associated with many traits including smaller fruits, decreased pollen and seed viability, lack of trichome development, decreased production of the monoterpenes, α-pinene, β-pinene, limonene, and *cis*-β-ocimene, as well as weakened jasmonic acid induced defense response (Li et al., 2004). At this time, current research has not identified which steps in the production of sterols limit production or are rate limiting, a possible method of learning about this would be to measure the flux through the pathway using stable isotope labelled compounds that could be measured at different points in development.

Producing SGAs from cholesterol

Modifying the sterol backbone and incorporating nitrogen

In *Solanum*, cholesterol served as the substrate to produce SGAs, which acted as protective compounds in tomato and potato (Itkin et al., 2013; Sonawane et al., 2016). The production of *α*-tomatine and dehydrotomatine proceed in the same pathway but depend on different substrates, tomatidine or dehydrotomatidine respectively (Lee et al., 2019). Many of the *GAME* genes involved in the production of SGAs from cholesterol occurred in gene clusters on chromosome 7 and chromosome 12 (Itkin et al., 2013). In particular, GAME1 GAME2, GAME6, GAME7, GAME11, GAME17, GAME18 occurred clustered on chromosome 7 and GAME4 and GAME12 occurred in a gene cluster on chromosome 12 (Itkin et al., 2013).

The first step in the process of producing SGAs from cholesterol began with the hydroxylation of C22 for cholesterol by GAME7, a CYP72, forming 22-hydroxycholesterol (Itkin et al., 2013). *GAME7* has been found to be upregulated when the tomato fruit is infected with *Colletotricum gloeosporoides* (Alkan et al., 2015). When tomato roots were colonized with the endophytic fungus *Serendipita indica*, there was a significant downregulation of many genes related to SGA metabolism in the leaves, however, only two were downregulated in the roots, *GAME7* and *GAME12* (Ntana et al., 2022). These changes in transcription upon interaction with different species suggested that GAME7 maybe be a point of regulation that can be manipulated for changes in tomato flavor or defense. A recent study showed that SGAs contributed to anthracnose resistance (Fabian, et al., 2022). In the anthracnose-susceptible tomato line, enhanced expression of *GAME* genes, especially *GAME5* and *GAME31* were detected in mature fruits that contain higher esculeoside A and barely detected tomatine and acetoxytomatine (Fig. 2) (Fabian et al., 2022). Mature fruits of the anthracnose-resistant line, however, had significantly reduced the *GAME5* expression level and the fruits contained high level of *α*-tomatine and no detected esculeoside A (Fig. 2) (Fabian et al., 2022). In addition, fruits of *GAME5* and *GAME31* silenced plants showed significant enhancement of anthracnose-resistance (Fabian et al., 2022). Because the GAME31 and GAME5 processed *α*-tomatine to esculeoside A (Fig. 2), which suggests that SGAs, especially *α*-tomatine contribute to the resistance of anthracnose diseases caused by the infection of fungal pathogen *Colletotrichum ssp*.

The next step is the hydroxylation of C26 of 22-hydroxycholesterol by GAME8 forming 22,26-dihydroxycholesterol (Itkin et al., 2013). When this gene was silenced, the leaves of tomato will accumulated 22-(R)-hydroxychosterol (Itkin et al., 2013). In potato, there were two copies of GAME8, however, in tomato it is unclear if there are one or two copies of GAME8 (Itkin et al., 2013). 22,26-dihydroxycholesterol was further hydroxylated by GAME6 at the C22, and a fifth (E-ring) was formed by GAME11, a 2-oxoglutarate-dependant dioxygenase, to produce a furostanol-type saponin aglycone (Itkin et al., 2013; Wei et al., 2021). GAME11 was negatively regulated by TAGL1, a MADS-box gene that regulated ripening (Zhao et al., 2018). In plants with defective linolenic acid synthesis (*spr2* mutants), both *GAME6* and *GAME11* were less expressed (Montero-Vargas et al., 2018). These plants

also had lower relative abundance of tomatidine, tomatine, and dehydrotomatine (Montero-Vargas et al., 2018).

C26 of the aglycone was oxidized by GAME4, a CYP88, formed furostanol-26-aldehyde (Itkin et al., 2013). GAME4, like 7-DHRC, was regulated by JRE4/GAME9 (Thagun et al., 2016; Nakayasu et al., 2018). A key step in the production of any alkaloid is the incorporation of nitrogen, which was activated by GAME12 in tomato (Itkin et al., 2013; Nakayasu et al., 2021a; Nakayasu et al., 2021b). GAME12 transaminated furostanol-26-aldehyde produced 26-amino-furostanol (Nakayasu et al., 2021b). The reaction used γ-aminobutyric acid (GABA) as the nitrogen donor (Nakayasu et al., 2021b). *GAME4* and *GAME12* were expressed at lower levels in *spr2* mutants (Montero-Vargas et al., 2018). The formation of the final F-ring and water loss of tomatidenol occurred spontaneously by nucleophilic attack (Itkin et al., 2013).

Glycosylation

The final process in the production of α-tomatine is the addition of lycotetrose in a series of four reactions (Fig. 3). The first was performed by GAMEl, a galactosyltransferase which attached a galactose to the oxygen at C3 producing tomatidine galactoside (Itkin et al., 2013; Itkin et al., 2011). When *GAME1* was silenced, there was an increase in tomatidine, suggesting this played an early role in the production of α-tomatine (Itkin et al., 2011). These silenced plants had severe morphological changes with deformed leaves and small flower buds, possibly due to the altered membrane sterols, indicating a likely toxic compound (Itkin et al., 2011).

GAME17 was determined to be a glucosyltransferase based on *in vitro* enzyme activity (Itkin et al., 2013). GAME17 attaches a glucose moiety to galactose moiety, producing γ-tomatine (Fig. 3). Like 7-DHCR and GAME4, GAME17's promoter contained a binding domain for GAME9 (Yu et al., 2020). Naturally occurred variation in GAME9 that was more common in large fruited tomato varieties had reduced binding efficiency to the GAME17 promoter (Yu et al., 2020).

GAME18 attached a second glucose moiety to the first glucose moiety producing β1-tomatine (Fig. 3). Finally, GAME2 attached xylose to the first glucose moiety producing α-tomatine, the major SGA in tomato (Fig. 3) (Itkin et al., 2013). GAME1, GAME2, GAME17, GAME18, have all be identified using introgression lines with *Solanum pennelii* regions as having been selected against during domestication and improvement, particularly in the seed (Alseekh et al., 2020). Similarly, *GAME1* was found to have higher expression in the wild species *Solanum nigrum* than in cultivated tomato and potato (Abdelhaliem et al., 2021). *GAME1* and *GAME17* have been found to be less expressed in *spr2* mutants.

MYC2 has been identified as a regulator of jasmonate stress response (Du et al., 2017). The clade IIIe basic helix-loop-helix (bHLH) transcription factors MYC1 and MYC2 bound to the G-box portion of the C5-SD2 (Swinnen et al., 2022). MYC1 and MYC2 acted redundantly as part of the constitutive production of SGAs and the jasmonate inducible production of SGAs (Swinnen et al., 2022). MYC1 and MYC2 acted with GAME9 to increase production of SGAs. MYC1 and MYC2 also interacted with gibberellin signaling acting on DELLA and thus inhibiting GA response and plant growth (Panda et al., 2022).

Changes with ripening

As tomato fruit ripens, the *α*-tomatine content decreased and the esculeoside A content increased. In ripening mutants such as *rin*, however, this did not occur (Ijima et al., 2009). The first part of this process was the export of *α*-tomatine from the vacuole to the cytoplasm by GORKY (In Russian, GORKY means for bitter) (Kazachkova et al., 2021). GORKY mutants had a similar pattern of SGA changes as other bitter-when-ripe tomato fruit, that being an accumulation of *α*-tomatine (Kazachkova et al., 2021). GORKY began to act as the tomato moved from the breaker stage to the red ripe stage. In knock-out mutants, *GAME1* and *GAME4* expressions were not affected while there was a slight decrease in the expression of *GAME5*, the function of which is discussed later in this section (Kazachkova et al., 2021). At the current time, it has not been determined what regulates *GORKY* expression and how it can be used to improve tomato flavor, but it could be possible to create a range of bitterness based on different interests.

It is suggested that the first two reactions in this production are hydroxylation of C23 of *α*-tomatine and the isomerization of the C22 (Fig. 2; Fig. 3) (Yamanaka et al., 2009; Cárdenas et al., 2019; Nakayasu et al., 2020; Szymański et al., 2020). C23 was hydroxylated by 23DOX (GAME31), an *α*-tomatine 23-hydroxylase was found to catalyze this reaction (Cárdenas et al., 2019; Nakayasu et al., 2020). Additionally, the isomerization was thought to be spontaneous as the expected intermediate between *α*-tomatine and neorickiiloside B was not detected (Nakayasu et al., 2020).

The putative reactions to produce esculeoside A from neorickiioside B were acetylation of the C23 producing lycoperoside C, hydroxylation of C27, followed by a final glycosylation of C27 forming esculeoside A (Nakayasu et al., 2020). Hydroxylation of lycoperoside C (also called acetoxytomatine) was performed by E8/27DOX/GAME40, a hydroxylase in the 2-oxoglutarate-dependant dioxygenase (2-ODD) family producing prosapogenin A (acetoxy-hydroxytomatine) (Akiyama et al., 2021; Sonawane et al., 2022). E8/27DOX/GAME40 may be an important point for ripening flavor and defense regulation as it has been established to be ethylene responsive (Lincoln et al., 1987; Lincoln and Fisher, 1988). Glycosylation of C27 might be performed by GAME5, a UDP-glycosyltransferase, which transfered a glucose moiety to produce esculeoside A (Szymański et al., 2020). However, when this gene was silenced by VIGS there was no change in the amount of esculeoside A produced (Szymański et al., 2020). Further work on GAME5 led to the identification of both a *GAME5-like* gene which has a similar expression pattern to *GAME5* (Zhao et al., 2023). The presence of GAME5 and GAME5-like may explain why there was no decrease in esculeoside A when GAME5 was knocked out. Additionally, *DELAY OF GERMATION 1* (*DOG1*) was identified as a regulator of GAME1, GAME5, and GAME5-like because when *DOG1* was overexpressed there were increased in hydroxytomatine, lycoperside B, and lycoperside H in the leaves (Zhao et al., 2023). Additionally, DOG1 binds to the promoters of *GAME5* and *GAME5-like* (Zhao et al., 2023). In *E. coli*, GAME5 and GAME5-like both catalyzed the production of *α*-tomatine from tomatidine and were able to glucosylate the flavanols kaempferol and quercetin, the production of quercetin glucoside more efficient that the production of *α*-tomatine (Zhao et al., 2023). This opens the possibility to using these enzymes in other pathways and processes by changing expression and using different promoters to produce new chemical products.

Two alternative products from α-tomatine have recently been discovered and developed. Both of these reactions involve reduction of C22 of α-tomatine. The first of these is habrochaitoside A from α-tomatine by GAME34 (Sonawane et al., 2022). In cultivated tomato, habrochaitoside A only accumulated in the root, hypocotyl, and cotyledons of seven days to fifteen days old seedling and the stem and root of four weeks to six weeks old plants (Sonawane et al., 2022). When *GAME34* was overexpressed in tomato, leaves and green fruit would accumulate habrochaitoside A (Sonawane et al., 2022). The second of these is prashantoside A, which is produced by GAME33 from α-tomatine. This compound has not been reported in wild-type plants. However, when *GAME33* was over-expressed, prashantoside A was found in the leaves. Additionally, the green fruit of these plants showed a reduction in α-tomatine. The flavor of these fruits was not reported but as new compounds were found through adjusting the time and localization of gene expression, new flavors could be found in tomato.

Plant defense

The SGAs, particularly α-tomatine, have been investigated for their plant protective qualities. In potato (*Solanum tuberosum* L.), the most common SGA is α-solanine, which has been well characterized as toxic and a source of plant protection (McKee, 1959; Roddick, 1977; Dalvi and Bowie, 1983; Ginzberg et al., 2009; Friedman, 2015).

Alpha-tomatine complexes with free sterols in cells caused liposome membrane disruption and electrolyte leakage (Steel and Drysdale, 1988). It was first recognized as having fungistatic, the ability to stop the growth of fungi, against *Fusarium oxyporium*, the causal agent of wilt (Irving et al., 1945; Roddick, 1974). This is effective on a broad range of fungi, however many fungi that were pathogenic to tomato had tolerance or resistance mechanisms (Sandrock and Vanetten, 1998). Rasool et al.(2021) suggested that it may be possible that certain endophytic fungi including *Metarhizium robertsii* and *Beauveria bassiana* might induce production of dehydrotomatine and α-tomatine and had a protective effect against two-spotted spider mites (*Tatranychus urticae*). Leaf extracts from *GAME34* overexpression lines were found to have anti-fungal effects prevent the spores of *Puccinia* from germinating while wild-type extracts did not have this effect (Sonawane et al., 2022).

The amount of tomatidine and α-tomatine changed when the plant was infected with *Phytophthora infestans* (Galeano Garcia et al., 2018). Both α-tomatine and tomatidine inhibit the growth of a potato infecting strain of *P. infestans,* with a greater effect from α-tomatine (Dahlin et al., 2017). Tomatidine had been suggested as a biomarker of infection as it is produced when α-tomatine is degraded by bacteria and fungi (Galeano Garcia et al., 2018). Part of the response to fungal pathogens such as *P. infestans* and *Botrytis cinerea* were a reduction in express of microRNA1916 (miR1916), which led to an increase in strictosidine synthase (STR2; Solyc07g055740) and an increase in α-tomatine (Chen et al., 2019). When STR2 transcription was increased either through interfering with miR1916 or overexpressing *STR2*, there was an increase in α-tomatine and smaller disease lesions from exposure to pathogens (Chen et al., 2019).

Alpha-tomatine inhibited growth and colony formation of *Beauveria bassiana*, an entomopathogenic fungus of *Leptinotarsa decemlineata* (Colorado potato beetle) (Costa and Gaugler, 1989). Alpha-tomatine did not appear to have a detrimental effect on the Colorado potato beetle itself. Different levels of SGAs did not affect leaf consumption or significantly alter the beetle's behavior (Harrison and Mitchell, 1988). While the presence of trichomes affected feeding behavior, this was not correlated with the *α*-tomatine content (Barbour and Kennedy, 1991).

When tomato roots were inoculated with arbuscular mycorrhizal fungi (AMF) *Rizophagus irregularis*, *Funneliformis mosseae* and a combination of the two, there was a significant increase in *α*-tomatine under normal watering conditions, but not under drought conditions. Dehydrotomatine was only increased in the *Funnelformis* treatment under normal water conditions (Orine et al., 2022). When *Spodoptera littoralis* caterpillar were fed leaves of inoculated plants they had a 25% decrease in biomass (Orine et al., 2022). It is suggested that the AMF prepares the plant for stresses (Orine et al., 2022).

In addition to having a detrimental effect on several fungal species, *α*-tomatine has been found to have protective effects on the plant against insects. It has been found to have both deterrent and antifeedant of termites (*Odontotermes wallonesis*) of all castes (Nisha and Rajavel, 2016). Similarly, when *Spodoptera litura* were fed on leaves with a defective JRE4 gained more weight than those fed on wild-type or plants with JRE4 driven by the 35S promoter (Nakayasu et al., 2018). A point of concern was raised because *α*-tomatine can affect parasitic wasps (*Hyposoter exigue*) from their host *Heliothis zea*, suggesting these wasps may not be an effective control measure in a tomato system (Campbell and Duffey, 1979). When *Drosophila melanogaster* was exposed to tomato leaf extracts and *α*-tomatine, there was a decrease in the number of days between life stages at all concentrations tested (from 0.005 μM to 50 μM). At the highest concentrations of *α*-tomatine (5 μM and 50 μM), there was a significant increase in individuals with malformations (Ventrella et al., 2016). The progeny of the extract exposed individuals also showed a shortened time between life stages (Ventrella et al., 2016).

When *α*-tomatine was exuded into the soil it could inhibit root growth of plants including lettuce (*Lactuca sativa*), perennial ryegrass (*Lolium perenne*), and cockspur (*Echinochloa crus-galli*) (Rial et al., 2018). The exuded tomatine may serve as an attractant for Sphingomonadaceae bacteria, which were commonly found near tomato and used the *α*-tomatine as a carbon source (Nakayasu et al., 2021a).

Human and animal health

Rats that were fed a diet with *α*-tomatine had decreased absorption of cholesterol and decrease in serum cholesterol, both high-density lipoprotein (HDL) and low-density lipoprotein (LDL), without a significant change in food intake, liver weight, or weight gain (Cayen, 1971). Similarly, when hamsters were fed tomatine containing diets, there were no detected detrimental effects while a decrease in LDL was found, and a decrease in LDL:HDL (high density lipoprotein) ratio (Friedman et al., 2000b). Consumption of both red and green

tomatoes reduce LDL, very low density lipoprotein (VLDL), and triglycerides, however, green tomatoes had a more pronounced effect (Friedman et al., 2000a).

Glycoalkaloids' ability to form a complex with sterols and toxicity to other eukaryotes has led to investigation of human health, including fighting cancer. α-tomatine has been shown to inhibit colon cancer cell (HT29) and liver cancer cell (HepG2) growth. It was found to be more effective than SGAs α-chaconine and α-solanine and cancer drugs doxorubicin and camptothecin. However, it also inhibited non-cancerous HeLa cell growth, suggesting it also harms non-cancerous cells (Lee et al., 2004). Alpha-tomatine inhibited cell growth of pancreatic cancer (PC-3) cells by the inhibition of 1κBα kinase, which in turn inhibited nuclear factor kappa B (NF-κB) preventing apoptosis (Lee et al., 2011, 2013, 2022)

When α-tomatine was used as a vaccine adjuvant, it had been able to help induce an immune response (Rajananthanan et al., 2000; Morrow et al., 2004). The lycotetraose moiety of α-tomatine had been shown *in silico* to have strong binding ability to the binding cavity of coronavirus SARS-CoV-2 main protease (Vergoten and Bailly, 2022).

There is some evidence that glycoalkaloids may protect against UV damage to the skin. UVB-exposed mice that were fed tomatoes had reduced tumor incidence compared to UVB-exposed mice that were not fed tomatoes. This suggestion arose because glycoalkaloids were found in the skin of mice that were fed tomatoes (Cooperstone et al., 2017). Molecular docking analysis has suggested that α-tomatine binds with epidermal growth factors (EGFRs), which are a cause of non-small cell lung cancer, suggesting a role in preventing cancer (Amalia et al., 2020).

Conclusion and perspectives

SGAs have many different uses for plant defense, tomato flavor, and human health. Additionally, some of the intermediates in SGA production can be used to produce other important products. For example, 7-dehydrocholesterol is also a precursor to vitamin D_3, which is needed for good skeletal health in mammals (Fig. 2).

A thorough understanding of the biosynthetic pathway can allow researchers to identify targets for manipulation to produce more or less of the desired compounds. Additional work remains to be done to understand the full pathway as a QTL was recently detected and validated on chromosome 3 which controls the amount of several early SGA (Dzakovich et al., 2022). It may also be possible to investigate genes that are not normally expressed like GAME33, which produced new compounds not before found in nature (Sonawane et al., 2022). Beyond this, the flavor of these compounds and their effects on tomato pests, the silent metabolism of plants could be an important resource for plant improvement for new flavor profiles, new medicines, and new plant protective compounds. Many of the *GAME* genes occurred in two clusters on chromosome 7 and chromosome 12. These clusters collocated with gene clusters in the acyl sugar biosynthesis pathway, another class of defensive compounds in tomato (Fan et al., 2020). This colocation led to some questions that can investigate in the future, including any shared evolutionary history between the genes and possible synergistic effects of both classes of compounds on plant defense (Fan et al., 2020).

With effective transformation protocols for tomato and precise gene editing technology, researchers and breeders will be able to make predictable specific modifications (Cermak et al., 2017; Li et al., 2018; Chen et al., 2020; Kwon et al., 2020). This could allow for new traits like extra bitter tomatoes, enhanced resistance to pathogens and insects, or new molecules with properties and uses that can be discovered.

Table 1. A list of genes that were involved in the biosynthesis of cholesterol and SGAs in tomato

Gene name	Function	Gene number	Reference
Squalene Epoxidase (*SQE*)	Epoxidizes squalene forming 2,3-oxidosqualene	Solyc04g077440	Rasbery et al., 2007; Suzuki et al., 2002
Cycloartenol Synthase (CAS)	Converts 2,3-oxidosqualene to cycloartenol	Solyc04g070980	(Corey et al., 1993; Gas-Pascual et al., 2014; Raederstorff and Rohmer, 1987)
Sterol Side Chain Reductase-2 (SSR2)	Reduces C24 of Cycloartenol forming Cycloartanol	Solyc02g069490	(Sawai et al., 2014; Zheng et al., 2021)
Sterol methyltransferase (SMT1)	Methylates C24 of cycloartenol forming 24-methylenecycloartenol	Solyc10g080150	(Diener et al., 2000)
Sterol Methyl oxidase 3 (SMO3)	Demethylates C-4 of cycloartenol forming 31-norcycloartanol	Solyc01g091320	(Darnet and Rahier, 2004; Pascal et al., 1990; Pascal et al., 1993; Pascal et al., 1994; Sonawane et al., 2016)
3*β*-hydroxysteroid dehydrogenase/C-4 decarboxylase2 (*3βHSD2/D*)	Participates in demethylation with SMO3 and SMO4	Solyc02g081730	(Pascal et al., 1993; Rahier, 2011; Sonawane et al., 2016)
Side Chain Oxidoreductase (SDR)	Participates in demethylation with SMO3 and SMO4	Solyc01g073640	(Pascal et al., 1994; Rahier, 2011; Sonawane et al., 2016)
Cyclopropylsterol isomerase (CPI)	Oxidation of C-8 of 31-norcyloartanol forming 31-nor-24(25)-dihydroloanosterol	Solyc12g098640	(Sonawane et al., 2016)
Sterol C-14-demethylase (CYP51)	Demethylates C-14 of 31-nor-24(25)-dihydroloanosterol to	Solyc01g008110	(Sonawane et al., 2016)

	form 4α-methylcholesta-8,14-dien-3β-ol		
Sterol C-14 Reductase (C14-R)	Reduces C14 of 4α-methylcholesta-8,14-dien-3β-ol to form 4α-methyl-24(25)-dihyrozymosterol	Solyc09g009040	(Sonawane et al., 2016)
8,7-sterol isomerase (8,7-SI)	Transfers a double bond from C-8 of 4α-methyl-24(25)-dihyrozymosterol to C-7 of 4α-methyl-5α-cholest-7-en-3β-ol	Solyc06g082980	(Sonawane et al., 2016)
Sterol methyl transferase 4 (SMO4)	Removes the remaining C-4 methyl group of 4α-methyl-5α-cholest-7-en-3β-ol forming cholesta-7-en-3β-ol	Solyc06g005750	(Sonawane et al., 2016)
C-5-sterol desaturase-2 (C5-SD2)	Oxidizes C-5 of cholesta-7-en-3β-ol to product 7-dehycholesterol	Solyc02g086180	(Sonawane et al., 2016)
7-dehydrocholesterol reductase	Reduces C-7 of 7-dehydrocholesterol to form cholesterol	Solyc06g074090	(Li et al., 2022; Sonawane et al., 2016)
Jasmonic acid responsive Ethylene Response Factor transcription factor 4/ Glycoalkaloid Metabolism 9 (JRE4/GAME9)	Transcription factor of 7-dehydrocholesterol reductase, GAME4, GAME17	Solyc01g090340	(Cardenas et al., 2016; Nakayasu et al., 2018; Thagun et al., 2016; Yu et al., 2020; Zhu et al., 2018)
Coronatine Insensitive 1 (COI1)	Necessary for perception of jasmonic acid and activates JRE4	Solyc05g052620	(Abdelkareem et al., 2017)
Glycoalkaloid Metabolism 7 (GAME7)	A CYP72, hydroxylates C-22 of cholesterol	Solyc07g062520	(Alkan et al., 2015; Itkin et al., 2013; Ntana et al., 2022)

	forming 22-hydrocholesterol		
Glycoalkaloid Metabolism 8 (GAME8)	Hydroxylates C-26 of 22-hydrocholesterol to form 22,26-dihydroxycholesterol	SGN-U578058	(Itkin et al., 2013)
Glycoalkaloid Metabolism 6 (GAME6)	Hydroxylation of C-22 of 22,26-dihydrocholesterol	Solyc07g043460	(Itkin et al., 2013; Montero-Vargas et al., 2018)
Glycoalkaloid Metabolism 11 (GAME11)	Facilitates E-ring closure of 22,26-dihydrocholesterol	Solyc07g043420	(Itkin et al., 2013; Montero-Vargas et al., 2018; Wei et al., 2021)
Glycoalkaloid Metabolism 4/ CYP88	Oxidizes C26 of furostanol-type saponin aglycone forming furostanol-26-aldehyde	Solyc12g006460	(Itkin et al., 2013; Montero-Vargas et al., 2018; Nakayasu et al., 2018; Thagun et al., 2016)
Glycoalkaloid Metabolism 12	Transaminates C26 of furostanol-26-aldehyde forming 26-amino-furostanol	Solyc12g006470	(Itkin et al., 2013; Montero-Vargas et al., 2018; Nakayasu et al., 2021a; Nakayasu et al., 2021b)
Glycoalkaloid Metabolism 1 (GAME1)	Galactosylates oxygen at C-3 of tomatidine forming tomatidine galactoside	Solyc07g043490	(Abdelhaliem et al., 2021; Alseekh et al., 2020; Itkin et al., 2013; Itkin et al., 2011; Zhu et al., 2018)
Glycoalkaloid Metabolism 17 (GAME17)	Attaches a glucose to tomatine galactoside forming γ-tomatine	Solyc07g043480	(Alseekh et al., 2020; Itkin et al., 2013; Yu et al., 2020)
Glycoalkaloid Metabolism 18 (GAME18)	Attaches a glucose to the glucose of γ-tomatine forming β1-tomatine	Solyc07g043500	(Alseekh et al., 2020; Yu et al., 2020)

Glycoalkaloid Metabolism 2 (GAME2)	Attaches a xylose to the first glucose forming α-tomatine	Solyc07g043410	(Itkin et al., 2013)
23-Hydroxylase/Glycoalkaloid Metabolism 31 (23DOX/GAME31)	Hydroxylates C23 of *α*-tomatine forming neonickiiloside B	Solyc02g062460	(Nakayasu et al., 2020; Szymański et al., 2020)
Glycoalkaloid Metabolism 33 (GAME33)	Desaturates C22 of *α*-tomatine forming prashantoside A. The same reaction occurs with dehydrotomatine as a substrate and forms prashantoside B.	Solyc00g138060	(Sonawane et al., 2022)
Glycoalkaloid Metabolism 34 (GAME34)	Desaturates C22 of *α*-tomatine forming Habrochaitoside A. The same reaction occurs with dehydrotomatine as a substrate and forms habrochaitoside B.	Solyc01g006580	(Sonawane et al., 2022)
E8/27DOX/GAME40	Hydroxylation of C27 of lycoperoside C (acetoxytomatine) forming prosapogenin A (acetoxy-hydroxytomatine)	Solyc09g08980	(Akiyama et al., 2021, Sonawane et al., 2022)
Glycoalkaloid Metabolism 5 (GAME5)	Glycosylates C27 of sapogenin A forming esculeoside A. Also capable of catalyzing the production of *α*-tomatine from tomatidine and glucosylating kaempferol and quercetin	Solyc10g08530	(Sonawane et al., 2016, Szymański et al., 2020, Zhao et al., 2023)
Gylcoalkaloid Metabolism 5-like (GAME5-like)	Similar expression pattern to GAME5 and substrate specificity	Solyc10g085240	(Zhao et al., 2023)

Delay of Germination 1 (DOG1)	bZIP family transcription factor which binds to the promoters of GAME5 and GAME5-like to enhance expression	Solyc10g085210	(Zhao et al., 2023)

Figures

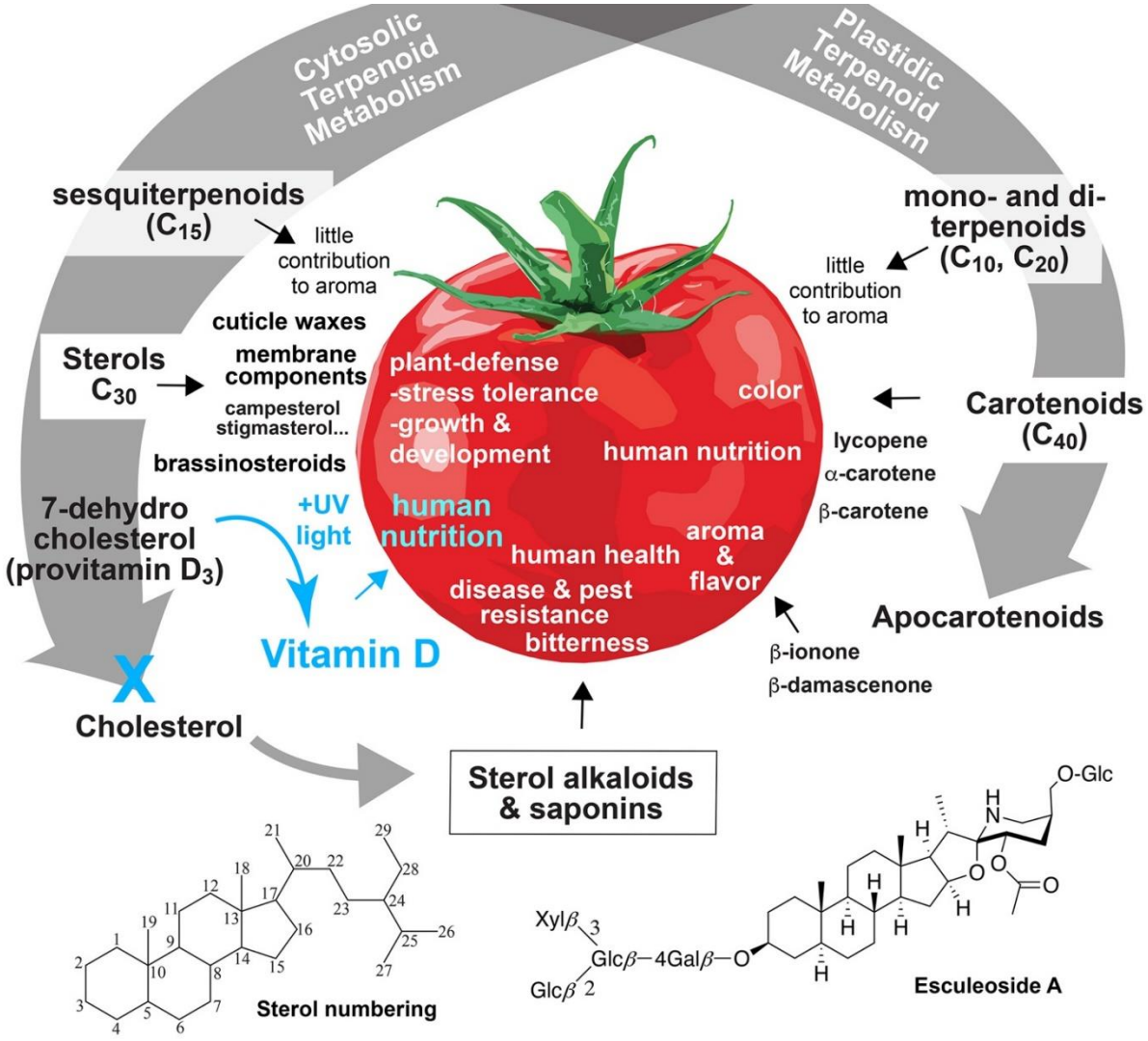

Figure. 1 Tomato quality traits linked through terpenoid metabolism – potential for engineering vitamin D_3 production

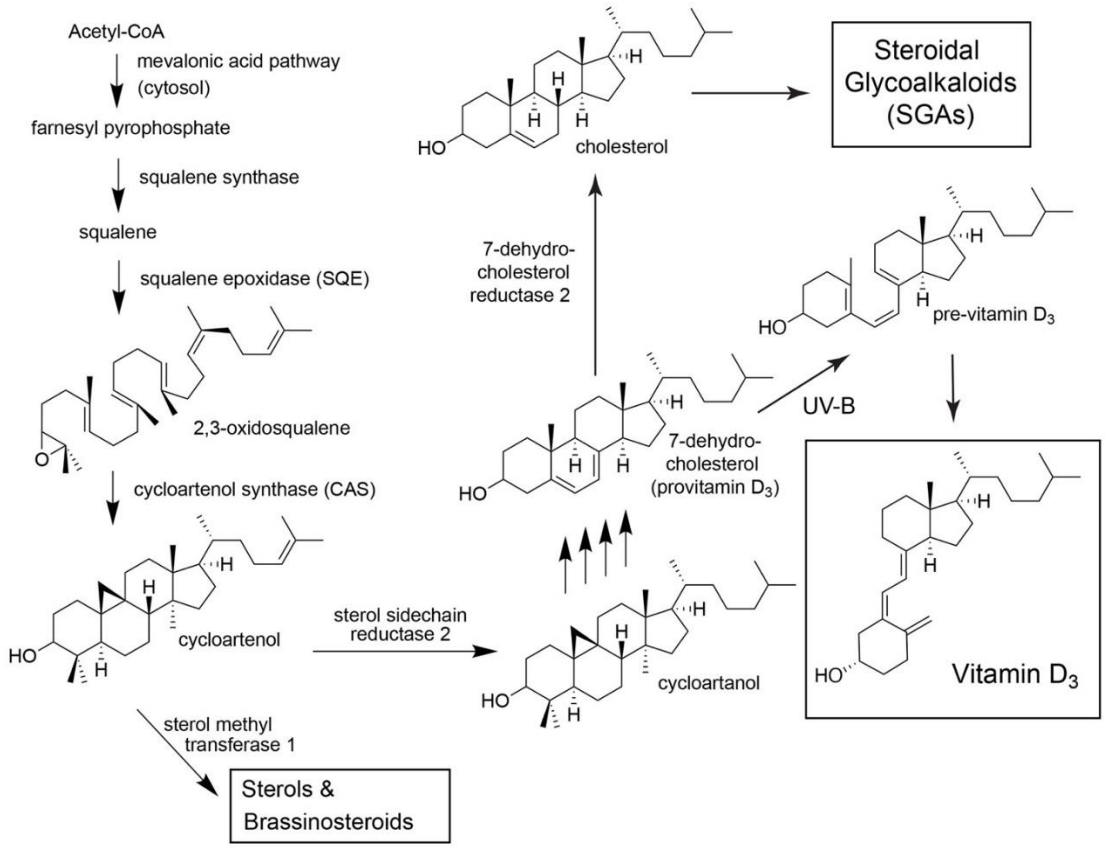

Figure. 2 Cholesterol biosynthesis pathway, in which 7-dehydro-cholesterol (provitamin D_3) can be processed with the function of 7-dehydro-cholesterol reductase 2 (7-DR2) to form cholesterol. 7-dehydro-cholesterol can also be processed into pre-vitamin D_3, then vitamin D_3 with the treatment of UV-B. Theoretically, knocking down 7-DR2 would enrich provitamin D_3, then possibly yield more vitamin D_3

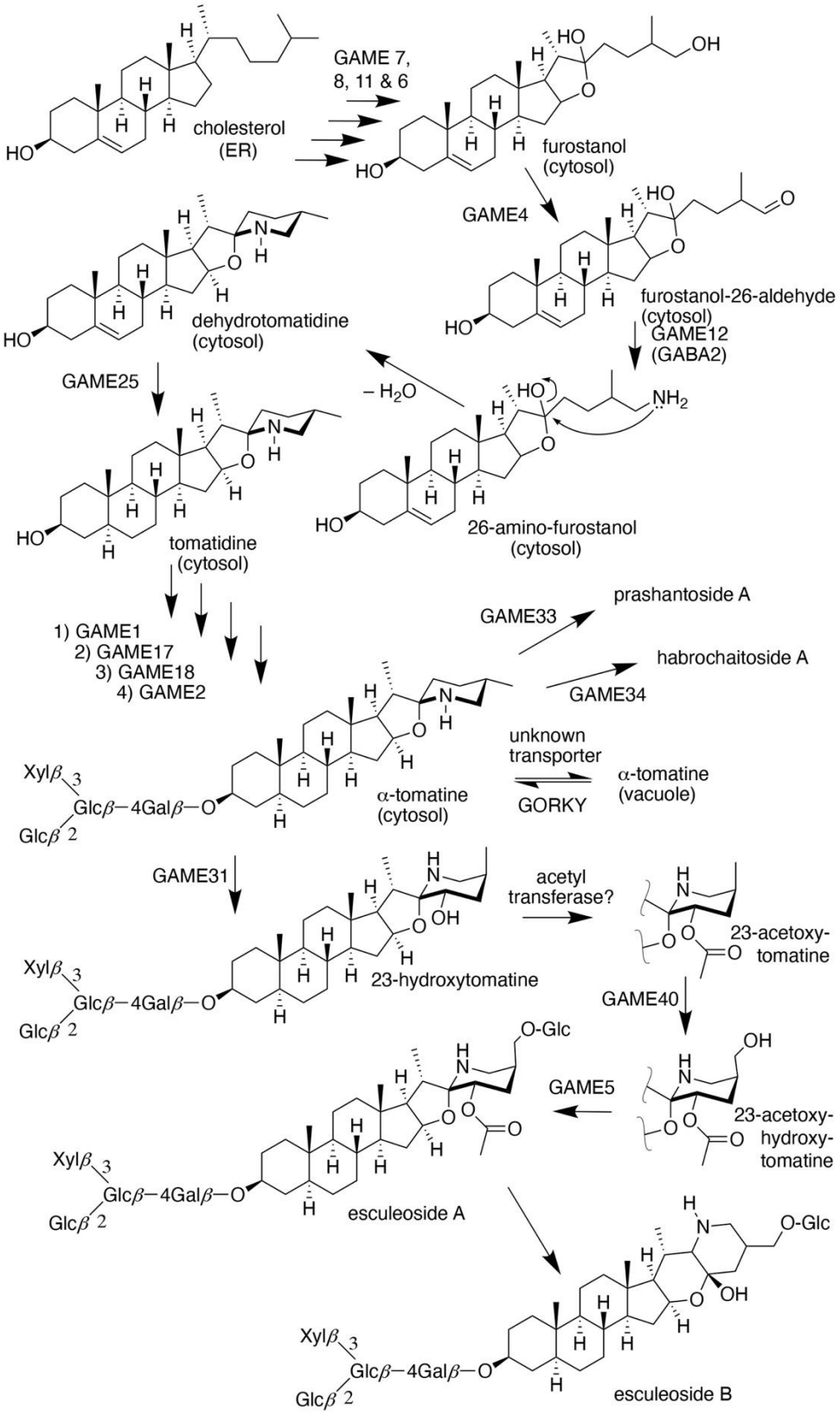
cholesterol
(ER)
GAME 7,
8, 11 & 6
furostanol
(cytosol)
GAME4
furostanol-26-aldehyde
(cytosol)
GAME12
(GABA2)
dehydrotomatidine
(cytosol)
GAME25
– H2O
26-amino-furostanol
(cytosol)
tomatidine
(cytosol)
1) GAME1
2) GAME17
3) GAME18
4) GAME2
GAME33
prashantoside A
habrochaitoside A
GAME34
α-tomatine
(cytosol)
unknown
transporter
GORKY
α-tomatine
(vacuole)
GAME31
23-hydroxytomatine
acetyl
transferase?
23-acetoxy-
tomatine
GAME40
GAME5
23-acetoxy-
hydroxy-
tomatine
esculeoside A
esculeoside B
Xylβ 3
Glcβ–4Galβ–O
Glcβ 2

Figure. 3 Steroidal glycoalkaloid synthesis pathway

Modifying the SGA synthesis pathway could improve tomato nutrational value, flavor and pest resistence.

References

Abdelhaliem, E., El-haleem, M.A., George, N.M., 2021. Transcriptional expression of genes involved in steroidal glycoalkaloid biosynthesis in three wild *Solanum* species. Annals of the Romanian Society of Cell Biology, 25: 8010-8019.

Abdelkareem, A., C. Thagun, M. Nakayasu, M. Mizutani. 2017. Jasmonate-induced biosynthesis of steroidal glycoalkaloids depends on COI1 proteins in tomato. Biochemical and Biophysical Research Communications, 489: 206-210.

Akiyama, R., M. Nakayasu, N. Umemoto, J. Kato, M. Kobayashi, H.J. Lee, Y. Sugimoto, Y. Iijima, K. Saito, T. Muranaka, M. Mizutani. 2021. Tomato E8 encodes a C-27 hydroxylase in metabolic detoxification of α -tomatine during fruit ripening. Plant and Cell Physiology, 62: 775-783.

Alkan, N., G. Friedlander, D. Ment, D. Prusky, and R. Fluhr. 2015. Simultaneous transcriptome analysis of *Colletotrichum gloeosporioides* and tomato fruit pathosystem reveals novel fungal pathogenicity and fruit defense strategies. New Phytologist, 205:801-815.

Alseekh, S., I. Ofner, Z. Liu, S. Osorio, J. Vallarino, R.L. Last, D. Zamir, T. Tohge, and A.R. Fernie. 2020. Quantitative trait loci analysis of seed-specialized metabolites reveals seed-specific flavonols and differential regulation of glycoalkaloid content in tomato. The Plant Journal, 103: 2007-2024.

Amalia, I.F., A. Sayyidah, K.A. Larasati, and S.F. Budiarti. 2020. Molecular docking analysis of alpha-tomatine and tomatidine to inhibit epidermal growth factor receptor (EGFR) activation in non-small-cell lung cancer (NSCLC). Journal of smart bioprospecting and techology, 2: 1-6.

Barbour, J.D., Kennedy, G.G., 1991. Role of steroidal glycoalkaloid alpha-tomatine in host-plant resistance of tomato to colorado potato beetle. Journal of Chemical Ecology, 17: 989-1005.

Beecher, G.R., 1998. Nutrient content of tomatoes and tomato products. Experimental Biology and Medicine, 218: 98-100.

Behmer, S.T., N. Olszewski, J. Sebastiani, S. Palka, G. Sparacino, E. Sciarrno, and R.J. Grebenok. 2013. Plant phloem sterol content: forms, putative functions, and implications for phloem-feeding insects. Frontiers in Plant Science, 4: 370.

Bentley, J. 2017., U . S . Trends in Food Availability and a Dietary Assessment of Loss-Adjusted Food Availability , 1970-2014. Economic Information Bulletin - USDA Economic Research Service, 166: iv + 32 pp.

Benveniste, P., 2004. Biosynthesis and accumulation of sterols. Annual Review of Plant Biology, 55: 429-457.

Campbell, B.C., Duffey, S.S., 1979. Tomatine and parasitic wasps : potential incompatibility of plant antibiosis with biological control. Science, 205: 700-702.

Cárdenas, P.D., P.D. Sonawane, U. Heinig, S.E. Bocobza, S. Burdman, and A. Aharoni. 2015. The bitter side of the nightshades: genomics drives discovery in S*olanaceae* steroidal alkaloid metabolism. Phytochemistry, 113: 24-32.

Cárdenas, P.D., P.D. Sonawane, U. Heinig, A. Jozwiak, S. Panda, B. Abebie, Y. Kazachkova, M. Pliner, T. Unger, D. Wolf, I. Ofner, E. Vilaprinyo, S. Meir, O. Davydov, A. Gal-

On, S. Burdman, A. Giri, D. Zamir, T. Scherf, J. Szymanski, I. Rogachev, and A. Aharoni. 2019. Pathways to defense metabolites and evading fruit bitterness in genus *Solanum* evolved through 2-oxoglutarate-dependent dioxygenases. Nature Communications, 10: 5169.

Cárdenas, P.D., P.D. Sonawane, J. Pollier, R.V. Bossche, V. Dewangan, E. Weithorn, L. Tal, I. Rogachev, S. Malitsky, A.P. Giri, A. Goossens, S. Burdman, and A. Aharoni. 2016. GAME9 regulates the biosynthesis of steriodal alkaloids and upstream isoprenoids in the plant mevalonate pathway. Nat Commun, 7: 10654.

Cayen, M.N., 1971. Effect of dietary tomatine on cholesterol metabolism in the rat. Journal Lipid Research, 12: 482-490.

Cermak, T., S.J. Curtin, J. Gil-Humanes, R. Čegan, T.J.Y. Kono, E. Konečná, J.J. Belanto, C.G. Starker, J.W. Mathre, R.L. Greenstein, and D.F. Voytas. 2017. A multi-purpose toolkit to enable advanced genome engineering in plants. The Plant Cell, 29: 1196-1217.

Chen, L., J. Meng, X.L. He, M. Zhang, and Y.S. Luan. 2019. *Solanum lycopersicum* microRNA1916 targets multiple target genes and negatively regulates the immune response in tomato. Plant, Cell & Environment, 42: 1393-1407.

Chen, Y., W. Mao, T. Liu, Q. Feng, L. Li, and B. Li. 2020. Genome editing as a versatile tool to improve horticultural crop qualities. Hortic Plant J, 6: 372-384.

Choe, S., A. Tanaka, T. Noguchi, S. Fujioka, S. Takatsuto, A.S. Ross, F.E. Tax, S. Yoshida, and K.A. Feldmann. 2000. Lesions in the sterolΔ^7 reductase gene of *Arabidopsis* cause dwarfism due to a block in brassinosteroid biosynthesis. Plant Journal, 21: 431-443.

Closa, M., E. Vranova, C. Bortolotti, L. Bigler, M. Arro, A. Ferrer, and W. Gruissem. 2010. The *Arabidopsis thaliana* FPP synthase isozymes have overlapping and specific functions in isoprenoid biosynthesis and complete loss of FPP synthase activity causes early developmental arrest. The Plant Journal, 63: 512-525.

Cooperstone, J.L., K.L. Tober, K.M. Riedl, M.D. Teegarden, M.J. Cichon, D.M. Francis, S.J. Schwartz, and T.M. Oberyszyn. 2017. Tomatoes protect against development of UV-induced keratinocyte carcinoma via metabolomic alterations. Scientific Reports, 7: 1-9.

Corey, E.J., S.P.T. Matsuda, and B. Bartel. 1993. Isolation of an *Arabidopsis thaliana* gene encoding cycloartenol synthase by functional expression in a yeast mutant lacking lanosterol synthase by the use of a chromatographic screen. Proceedings of the National Academy of Sciences, 90:11628-11632.

Costa, S.D., Gaugler, R.R., 1989. Sensitivity of *Beauveria bassiana* to solanine and tomatine : plant defensive chemicals inhibit an insect pathogen. Journal of Chemical Ecology 15: 697-706.

Dahlin, P., M.C. Muller, S. Ekengren, L.S. McKee, and V. Bulone. 2017. The impact of steroidal glycoalkaloids on the physiology of phytophthora infestans, the causative agent of potato late blight. Molecular Plant-Microbe Interactions, 30: 531-542.

Dalvi, R.R., Bowie, W.C. 1983. Toxicology of solanine: an overview. Veterinary and human toxicology, 25: 13-15.

Darnet, S., Rahier, A., 2004. Plant sterol biosynthesis: identification of two distinct families of sterol 4 α-methyl oxidases. Biochemical Journal, 378: 889-898.

Devarenne, T.P., D.H. Shin, K. Back, S. Yin, and J. Chappell. 1998. Molecular characterization of tobacco squalene synthase and regulation in response to fungal elicitor. Archives of Biochemistry and Biophysics, 349: 205-215.

Diener, A.C., H. Li, W.X. Zhou, W.J. Whoriskey, W.D. Nes, G.R. Fink. 2000. *STEROL METHYLTRANSFERASE 1* controls the level of cholesterol in plants. Plant Cell, 12: 853-870.

Du, M., J. Zhao, D.T.W. Tzeng, Y. Liu, L. Deng, T. Yang, Q. Zhai, F. Wu, Z. Huang, Q. Wang, Q. Chen, S. Zhong, C.B. Li, C. Li. 2017. MYC orchestrates a hierarchical transcriptional cascade that regulates jasmonate-mediated plant immunity in tomato. The Plant Cell, 29: 1883-1906.

Dzakovich, M.P., D.M. Francis, J.L. Cooperstone. 2022. Steroidal alkaloid biosynthesis is coordinately regulated and differs among tomatoes in the red-fruited clade. The Plant Genome, 15: e20192.Dzakovich, M.P., J.L. Hartman, and J.L. Cooperstone. 2020. A high-throughput extraction and analysis method for steroidal glycoalkaloids in tomato. Frontiers in Plant Science, 11: 1-12.

Fan, P., P. Wang, Y.R. Lou, B.J. Leong, B.M. Moore, C.A. Schenck, R. Combs, P. Cao, F. Brandizzi, S.H. Shiu, and R.L. Last. 2020. Evolution of a plant gene cluster in Solanaceae and emergence of metabolic diversity. eLife 9: e56717.

Fao. 2020. FAOSTAT.

Friedman, M., 2015. Chemistry and anticarcinogenic mechanisms of glycoalkaloids produced by eggplants, potatoes, and tomatoes. Journal of Agricultural and Food Chemistry, 63: 3323-3337.

Friedman, M., T.E. Fitch, C.E. Levin, and W.H. Yokoyama. 2000a. Feeding tomatoes to hamsters reduces their plasma low-density lipoprotein cholesterol and triglycerides. Journal of Food Science, 65: 897-900.

Friedman, M., T.E. Fitch, and W.E. Yokoyama. 2000b. Lowering of plasma LDL cholesterol in hamsters by the tomato glycoalkaloid tomatine. Food and Chemical Toxicology, 38: 549-553.

Gachotte, D., T. Hussselstein, M. Bard, F. Lacroute, and P. Benveniste. 1996. Isolation and characterization of an *Arabidopsis thaliana* cDNA encoding a Δ^7-sterol-C-5-desaturase by functional complementation of a defection yeast mutant. The Plant Journal, 9: 391-398.

Gachotte, D., R. Meens, and P. Beneveniste. 1995. An *Arabidopsis* mutant deficient in sterol biosynthesis: heterologous complementation by ERG 3 encording a Δ^7-sterol-C-5-desaturase from yeast. The Plant Journal, 8: 407-416.

Galeano Garcia, P., F. Neves dos Santos, S. Zanotta, M. Nogueira Eberlin, and C. Carazzone. 2018. Metabolomics of *Solanum lycopersicum* infected with *Phytophthora infestans* leads to early detection of late blight in asymptomatic plants. Molecules, 23: 3330.

Gas-Pascual, E., A. Berna, T.J. Bach, and H. Schaller. 2014. Plant oxidosqualene metabolism: cycloartenol synthase-dependent sterol biosynthesis in *Nicotiana benthamiana*. PLoS ONE, 9: e109156.

Ginzberg, I., M. Thippeswamy, E. Fogelman, U. Demirel, A.M. Mweetwa, J. Tokuhisa, and R.E. Veilleux. 2012. Induction of potato steroidal glycoalkaloid biosynthetic pathway by overexpression of cDNA encoding primary metabolism HMG-CoA reductase and squalene synthase. Planta, 235: 1341-1353.

Ginzberg, I., J.G. Tokuhisa, and R.E. Veilleux. 2009. Potato steroidal glycoalkaloids : biosynthesis and genetic manipulation. Potato Research, 52: 1-15.

Harrison, G. and B.K. Mitchell. 1988. Host-plant acceptance by geographic populations of the colorado potato beetle , *Leptinotarsa decemlineata*: role of solanaceous alkaloids as sensory deterrents. Journal of Chemical Ecology, 14: 777-788.

Ijima, Y., Y. Fujiwara, T. Tokita, T. Ikeda, T. Nohara, K. Aoki, and D. Shibata. 2009. Involvement of ethylene in the accumulation of esculeoside A during fruit ripening of tomato (*Solanum lycopersicum*). Journal of Agricultural and Food Chemistry, 57: 3247-3252.

Irving, G.W., T.D. Fontaine, and S.P. Doolittle. 1945. Lycopersicin , a fungistatic agent from the tomato plant. Science, 102: 9-11.

Itkin, M., U. Heinig, O. Tzfadia, A.J. Bhide, B. Shinde, P.D. Cardenas, S.E. Bocobza, T. Unger, S. Malitsky, R. Finkers, Y. Tikunov, A.G. Bovy, Y. Chikate, P. Singh, I. Rogachev, J. Beekwilder, A.P. Giri, and A. Aharoni. 2013. Biosynthesis of antinutritional alkaloids in solanaceous crops is mediated by glustered genes. Science, 341: 175-180.

Itkin, M., I. Rogachev, T. Rosenberg, S. Malitsky, L. Masini, S. Meir, Y. Iijima, K. Aoki, R. de Vos, D. Prusky, S. Burdman, J. Beekwilder, and A. Aharoni. 2011. GLYCOALKALOID METABOLISM1 is required for steroidal alkaloid glycosylation and prevention of phytotoxicity in tomato. The Plant Cell, 23: 4507-4525.

Ito, S., T. Ihara, H. Tamura, S. Tanaka, T. Ikeda, H. Kajihara, C. Dissanayake, and F.F. Abdel-Motall. 2007. α-Tomatine , the major saponin in tomato , induces programmed cell death mediated by reactive oxygen species in the fungal pathogen *Fusarium oxysporum*. FEBS Letters, 581:3217-3222.

Kazachkova, Y., I. Zemach, S. Panda, S. Bocobza, A. Vainer, I. Rogachev, Y. Dong, S. Ben-dor, D. Veres, C. Kanstrup, S.K. Lambertz, C. Crocoll, Y. Hu, E. Shani, S. Michaeli, H.H. Nour-eldin, D. Zamir, and A. Aharoni. 2021. The GORKY glycoalkaloid transporter is indispensable for preventing tomato bitterness. Nature Plants, 7: 468-480.

Kim, T.W., S.C. Chang, J.S. Lee, S. Takatsuto, T. Yokota, S.K. Kim. 2004. Novel biosynthetic pathway of castasterone from cholesterol in tomato. Plant Physiology, 135: 1231-1242.

Koh, E., S. Kaffka, and A.E. Mitchell. 2012. A long-term comparison of the influence of organic and conventional crop management practices on the content of the glycoalkaloid α-tomatine in tomatoes. Journal of the Science of Food and Agriculture, 93: 1537-1542.

Kozukue, N. and M. Friedman. 2003. Tomatine, chlorophyll, β-carotene and lycopene content in tomatoes during growth and maturation. Journal of the Science of Food and Agriculture, 200: 195-200.

Kozukue, N., J.S. Han, K.R. Lee, M. Friedman. 2004. Dehydrotomatine and α -tomatine content in tomato fruits and vegetative plant tissues. Journal of Agricultural and Food Chemistry, 52: 2079-2083.

Krits, P., E. Fogelman, and I. Ginzberg. 2007. Potato steroidal glycoalkaloid levels and the expression of key isoprenoid metabolic genes. Planta, 227: 143-150.

Kwon, C.T., J. Heo, Z.H. Lemmon, Y. Capua, S.F. Hutton, J.V. Eck, S.J. Park, and Z.B. Lippman. 2020. Rapid customization of Solanaceae fruit crops for urban agriculture. Nature Biotechnology, 38: 182-188.

Lecain, E., X. Chenivesse, R. Spagnoli, and D. Pompon. 1996. Cloning by metabolic interference in yeast and enzymatic characterization of *Arabidopsis thaliana* sterol Δ^7-reductase. The Journal of biological chemistry, 271: 10866-10873.

Lee, H.J., M. Nakayasu, R. Akiyama, M. Kobayashi, H. Miyachi, Y. Sugimoto, N. Umemoto, K. Saito, T. Muranaka, and M. Mizutani. 2019. Identification of a 3β -hydroxysteroid dehydrogenase / 3-ketosteroid eeductase involved in α -tomatine biosynthesis in tomato. Plant and Cell Physiology, 12: 1304-1315.

Lee, K.R., N. Kozukue, J.S. Han, J.H. Park, E.Y. Chang, E.J. Baek, J.S. Chang, M. Friedman. 2004. Glycoalkaloids and metabolites inhibit the growth of human colon (HT29) and liver (HepG2) cancer cells. Journal of Agricultural and Food Chemistry, 52: 2832-2839.

Lee, S.T., P.F. Wong, S.C. Cheah, and M.R. Mustafa. 2011. Alpha-tomatine induces apoptosis and inhibits nuclear factor-kappa B activation on human prostatic adenocarcinoma PC-3 cells. PLoS One, 6: e18915.

Lee, S.T., P.F. Wong, H. He, J.D. Hooper, and M.R. Mustafa. 2013. Alpha-tomatine attenuation of *in vivo* growth of subcutaneous and orthotopic xenograft tumors of human prostate carcinoma PC-3 cells is accompanied by inactivation of nuclear factor-kappa B signaling. PLoS One, 8: e57708.

Lee, S.T., P.F. Wong, H. He, J.D. Hooper, and M.R. Mustafa. 2022. Correction: Alpha-tomatine attenuation of *in vivo* growth of subcutaneous and orthotopic xenograft tumors of human prostate carcinoma PC-3 cells is accompanied by inactivation of nuclear factor-kappa B signaling. PLoS One, 17: e0268234.

Li, J., A. Scarano, N. Mora Gonzalez, F. D'Orso, Y. Yue, K. Nemeth, G. Saalbach, L. Hill, C. de Oliveira Martins, R. Moran, A. Santino, and C. Martin. 2022. Biofortified tomatoes provide a new route to vitamin D sufficiency. Nature Plants, 8: 611-616.

Li, L., Y. Zhao, B.C. McCaig, B.A. Winger, J. Wang, M.E. Whalon, E. Pichersky, and G.A. Howe. 2004. The tomato homolog of CORONATINE-INSENSITIVE1 is required for the maternal control of seed maturation, jasmonate-signaled defense responses, and glandular trichome development. The Plant Cell, 16: 126-143.

Li, X., Y. Wang, S. Chen, H. Tian, D. Fu, B. Zhu, Y. Luo, and H. Zhu. 2018. Lycopene is enriched in tomato fruit by CRISPR/Cas9-mediated multiplex genome editing. Frontiers in Plant Science, 9: 559.

Lincoln, J.E., S. Cordes, E. Read, and R.L. Fisher. 1987. Regulation of gene expression by ethylene during *Lycopersicon esculentum* (tomato) fruit development. Proceedings of the National Academy of Sciences, 84: 2793-2797.

Lincoln, J.E., Fisher, R.L., 1988. Diverse mechanisms for the regulation of ethylene-inducible gene expression. Molecular and General Genetics MGG, 212: 71-75.

McKee, R.K. 1959. Factors affecting the toxicity of solanine and related alkaloids to *Fusarium caeruleum*. Journal of general Microbiology, 20: 686-696.

Montero-Vargas, J.M., K. Casarrubias-Castillo, N. Martinez-Gallardo, J.J. Ordaz-Ortiz, J.P. Delano-Frier, and R. Winkler. 2018. Modulation of steroidal glycoalkaloid biosynthesis in tomato (*Solanum lycopersicum*) by jasmonic acid. Plant Science, 277: 155-165.

Morrow, W.J.W., Y.W. Yang, and N.A. Sheikh. 2004. Immunobiology of the tomatine adjuvant. Vaccine, 22: 2380-2384.

Nakajima, N., S. Fujioka, T. Tanaka, S. Takatsuto, and S. Yoshida. 2002. Biosynthesis of cholestanol in higher plants. Phytochemistry, 60: 275-279.

Nakashima, T., T. Inoue, A. Oka, T. Nishino, T. Osumi, and S. Hata. 1995. Cloning , expression , and characterization of cDNAs encoding *Arabidopsis thaliana* squalene synthase. Proceedings of the National Academy of Sciences, 92:2328-2332.

Nakayasu, M., R. Akiyama, M. Kobayashi, H.J. Lee, T. Kawasaki, B. Watanabe, S. Urakawa, J. Kato, Y. Sugimoto, Y. Iijima, K. Saito, T. Muranaka, N. Umemoto, and M. Mizutani. 2020. Identification of α -tomatine 23-hydroxylase involved in the detoxification of a bitter glycoalkaloid. Plant and Cell Physiology, 1777: 21-28.

Nakayasu, M., K. Ohno, K. Takamatsu, Y. Aoki, S. Yamazaki, H. Takase, T. Shoji, K. Yamazaki, and A. Sugiyama. 2021a. Tomato roots secrete tomatine to modulate the bacterial assemblage of the rhizosphere. Plant physiology, 186: 270-284.

Nakayasu, M., N. Shioya, M. Shikata, C. Thagun, and A. Abdelkareem. 2018. JRE4 is a master transcriptional regulator of defense-related steroidal glycoalkaloids in tomato. The Plant Journal, 94: 975-990.

Nakayasu, M., N. Umemoto, R. Akiyama, K. Ohyama, H.J. Lee, H. Miyachi, B. Watanabe, T. Muranaka, K. Saito, Y. Sugimoto, and M. Mizutani. 2021b. Characterization of C-26 aminotransferase , indispensable for steroidal glycoalkaloid biosynthesis. The Plant Journal, 108: 81-92.

Nisha, R., Rajavel, D.S., 2016. Effect of tomatine on termites *Odontotermes wallonensis* (Wasmann) vis-a-vis antifeedant and repellent activity. International Journal of Plant Protection, 9: 97-101.

Ntana, F., S.R. Johnson, B. Hamberger, B. Jensen, H.J.L. Jorgensen, and D.B. Collinge. 2022. Regulation of Tomato Specialised metabolism after establishment of symbiosis with the endophytic fungus *Serendipita indica*. microorganisms, 10: 194.

Orine, D., E. Defossez, F. Vergara, H. Uthe, N.M. van Dam, and S. Rsamann. 2022. Arbuscular mycorrhizal fungi prevent the negative effect of drought and modulate the growth-defence trade-off in tomato plants. Journal of Sustainable Agriculture and Environment, 1: 177-190.

Panda, S., A. Jozwiak, P.D. Sonawane, J. Szymanski, Y. Kazachkova, A. Vainer, H.V. Kilambi, E. Almekias-Siegl, V. Dikaya, S. Bocobza, H. Shohat, S. Meir, G. Wizler, A.P. Giri, R. Schuurink, D. Weiss, H. Yasuor, A. Kamble, and A. Aharoni. 2022.

Steroidal alkaloids defence metabolism and plant growth are modulated by the joint action of gibberellin and jasmonate signalling. New Phytologist, 233: 1220-1237.
Paparella, A., L. Shaltiel-Harpaza, M. Ibdah. 2021. *β*-Ionone: its occurrence and biological function and metabolic engineering. Plants, 10: 754.
Pascal, S., M. Taton, and A. Rahier. 1990. Oxidative C4-demethylation of 24-methylene cycloartanol by a cyanide-sensitive enzymatic system from higher plant microsomes. Biochemical and Biophysical Research Communications, 172: 98-106.
Pascal, S., M. Taton, and A. Rahier. 1993. Plant sterol biosynthesis: indentification and characterization of two distinct microsomal oxidative enzymatic systems involved in sterol C4-demethylation. The Journal of Biological Chemistry, 268: 11639-11654.
Pascal, S., M. Taton, and A. Rahier. 1994. Plant Sterol Biosynthesis: Identification of a NADPH dependent sterone reductase involved in sterol-4 demethylation. Archives of Biochemistry and Biophysics, 312:260-271.
Raederstorff, D. and M. Rohmer. 1987. Sterol biosynthesis via cycloartenol and other biochemical features related to photosynthetic phyla in the amoebae *Naegleria lovaniensis* and *Naegleria gruberi*. European Journal of Biochemistry, 434: 427-434.
Rahier, A., 2011. Dissecting the sterol C-4 demethylation process in higher plants . From structures and genes to catalytic mechanism. Steroids, 76: 340-352.
Rahier, A., S. Darnet, F. Bouvier, B. Camara, and M. Bard. 2006. Molecular and enzymatic characterizations of novel bifunctional 3*β* -hydroxysteroid dehydrogenases / C-4 decarboxylases from *Arabidopsis thaliana*, 281: 27264-27277.
Rajananthanan, P., G.S. Attard, N.A. Sheikh, W.J.W. Morrow. 2000. Novel aggregate structure adjuvants modulate lymphocyte proliferation and Th1 and Th2 cytokine profiles in ovalbumin immunized mice. Vaccine, 18: 140-152.
Rao, A.V. and S. Agarwal. 2000. Role of antioxidant lycopene in cancer and heart disease. Journal of the American College of Nutrition, 19: 563-569.
Rasbery, J.M., H. Shan, R.J. Leclair, M. Norman, S.P.T. Matsuda, and B. Bartel. 2007. *Arabidopsis thaliana* squalene epoxidase 1 is essential for root and seed development. The Journal of biological chemistry, 282: 17002-17013.
Rasool, S., P.D. Cardenas, D.I. Pattison, B. Jensen, and N.V. Meyling. 2021. Isolate-specific effect of entomopathogenic endophytic fungi on population growth of two-spotted spider mite (*Tetranychus urticae* Koch) and levels of steroidal glycoalkaloids in tomato. Journal of Chemical Ecology, 47: 476-488.
Rial, C., E. Go, R.M. Varela, J.M.G. Molinillo, and F.A. Mac. 2018. Ecological relevance of the major allelochemicals in *Lycopersicon esculentum* roots and exudates. Journal of Agricultural and Food Chemistry, 66: 4638-4644.
Rick, C.M., J.W. Uhligt, and A.D. Jones. 1994. High *α*-tomatine content in ripe fruit of Andean *Lycopersicon esculentum* var . cerasiforme : developmental and genetic aspects. Proceedings of the National Academy of Sciences, 91: 12877-12881.
Roddick, J.G. 1974. The steroidal glycoalkaloid *α*-tomatine. Phytochemistry, 13: 9-25.
Roddick, J.G. 1977. Subcellular localization of steroidal glycoalkaloids in vegetative organs of *Lycopersicon esculentum* and *Solanum tuberosum*. Phytochemistry, 16: 805-807.

Sandrock, R.W.,Vanetten, H.D., 1998. Fungal sensitivity to and enzymatic degradation of the phytoanticipin α -tomatine. Biochemistry and Cell Biology, 88: 137-143.

Sawai, S., K. Ohyama, S. Yasumoto, H. Seki, T. Sakuma, T. Yamamoto, Y. Takebayashi, M. Kojima, H. Sakakibara, T. Aoki, T. Muranaka, K. Saito, and Umemoto, N., 2014. Sterol side chain reductase 2 is a key enzyme in the biosynthesis of cholesterol, the common precursor of toxic steroidal glycoalkaloids in potato. The Plant Cell, 26: 3763-3774.

Shoji, T. and K. Saito. 2022. A RING membrane-anchor E3 ubiquitin ligase gene is co-expressed with steroidal glycoalkaloid biosynthesis genes in tomato. Plant Biotechnology, 39: 421-425.

Silvestro, D., C. Villette, J. Delecolle, C.E. Olsen, M.S. Motawia, P. Geoffroy, M. Miesch, P.E. Jensen, D. Heintz, and H. Schaller. 2018. Vitamin D-5 in *Arabidopsis thaliana*. Scientific Reports, 8: 16348.

Sonawane, P.D., A. Jozwiak, R. Barbole, S. Panda, B. Abebie, Y. Kazachkova, S.A. Gharat, O. Ramot, T. Unger, G. Wizler, S. Meir, I. Rogachev, A. Doron-Feigenboim, M. Petrikov, A. Schaffer, A.P. Giri, T. Scherf, and A. Aharoni. 2022. 2-oxoglutarate-dependent dioxygenases drive expansion of steroidal alkaloid structural diveristy in the genus *Solanum*. New Phytologist, 234:1394-1410.

Sonawane, P.D., J. Pollier, S. Panda, J. Szymanski, H. Massalha, M. Yona, T. Unger, S. Malitsky, P. Ardent, L. Pauwels, E. Almekias-Siegel, I. Rogachev, S. Meir, P.D. Cardenas, M. Athar, M. Petrikov, H. Schaller, A.A. Schaffer, A. Kamble, A.P. Giri, A. Goossens, and A. Aharoni. 2016. Plant cholesterol biosynthetic pathway overlaps with phytosterol metabolism. Nature Plants, 3: 17101.

Song, X., Luo, Y., Ma, L., Hu, X., Simal-Gandara, J., Wang, L.S., Bajpai, V.K.B., Xiao, J., Chen, F., 2021. Recent trends and advances in the epidemiology, synergism, and delivery system of lycopene as an anti-cancer agent. Seminars in Cancer Biology, 73: 331-346.

Steel, C.C., Drysdale, R.B., 1988. Electrolype leakage from plant and fungal tissues and disruption of liposome membranes by α-tomatine. Phytochemistry, 27: 1025-1030.

Suzuki, H., L. Achnine, R. Xu, S.P.T. Matsuda, and R.A. Dixon. 2002. A genomics approach to the early stages of triterpene saponin biosynthesis in *Medicago truncatula*. The Plant Journal, 32: 1033-1048.

Swinnen, G., M. De Meyer, J. Pollier, F.J. Molina-Hidalgo, E. Ceulemans, J. Venegas-Molina, L. De Milda, P. Fernandex-Calvo, M. Ron, L. Pauwels, and A. Goossens. 2022. The basic helix-loop-helix transcription factors MYC1 and MYC2 have a dual role in the regulation of constitutive and stress-inducible specialized metabolism in tomato. New Phytologist, 236: 911-928.

Szymański, J., S. Bocobza, S. Panda, P. Sonawane, P.D. Cárdenas, J. Lashbrooke, A. Kamble, N. Shahaf, S. Meir, A. Bovy, J. Beekwilder, Y. Tikunov, I.R. de la Fuenta, D. Zamir, I. Rogachev, and A. Aharoni. 2020. Analysis of wild tomato introgression lines elucidates the genetic basic of transcriptome and metabolome variation underlying fruit traits and pathogen response. Nature Genetics, 52: 1111-1121.

Thagun, C., S. Imanishi, T. Kudo, R. Nakabayashi, K. Ohyama, T. Mori, K. Kawamoto, Y. Nakamura, M. Katayama, S. Nonaka, C. Matsukura, K. Yano, H. Ezura, K. Saito, T.

Hashimoto, and T. Shoji. 2016. Jasmonate-responsive ERF transcription factors regulate steroidal glycoalkaloid biosynthesis in tomato. Plant and Cell Physiology, 57: 961-975.

Ventrella, E., Z. Adamski, E. Chudzinska, Maidowicz-Kobielska, P. Marciniak, E. Buyukguzel, K. Buyukguzel, M. Erdem, P. Falabella, L. Scrano, and S. Bufo. 2016. *Solanum tuberosum* and *Lycopersicon esculentum* Leaf Extracts and Single Metabolites Affect Development and Reproduction of *Drosophila melanogaster*. PLoSOne, 11: e0155958.

Vergoten, G. and C. Bailly. 2022. Contribution of the lycotetraose moiety of *α*-tomatine to the interaction with the main proteases of coronaviruses PEDV and SARS-CoV-2. Trends in Phytochemical Research , 6: 86-96.

Vriese, K.D., J. Pollier, A. Goossens, T. Beeckman, and S. Vanneste. 2021. Dissecting cholesterol and phytosterol biosynthesis via mutants and inhibitors. Journal of Experimental Botany, 72: 241-253.

Wang, Z., O. Guhling, R. Yao, F. Li, T.H. Yeats, J.K.C. Rose, and R. Jetter. 2011. Two oxidosqualene cyclases responsible for biosynthesis of tomato fruit cuticular terpenoids. Plant physiology, 155: 540-552.

Wei, S., W. Zhang, R. Fu, and Y. Zhang. 2021. Genome-wide characterization of 2-oxoglutarate and Fe(II)-dependent dioxygenase family genes in tomato during growth cycle and their roles in metabolism. BMC Genomics, 22: 126.

Yamanaka, T., J.-P. Vicken, H. Zuilhof, A. Legger, N. Takada, and H. Gruppen. 2009. C22 isomerization in *α* -tomatine-to-esculeoside A conversion during tomato ripening is driven by C27 hydroxylation of triterpenoidal skeleton. Journal of Agricultural and Food Chemistry, 57: 3786-3791.

You, Y. and J.A.L. van Kan. 2020. Bitter and sweet make tomato hard to (b)eat. New Phytologist, 230: 90-100.

Yu, G., C. Li, L. Zhang, G. Zhu, S. Munir, C. Shi, H. Zhang, and G. Ai. 2020. An allelic variant of GAME9 determines its binding capacity with the *GAME17* promoter in the regulation of steroidal glycoalkaloid biosynthesis in tomato. J Exp Bot, 71: 2527-2536.

Zhao, X., X. Yuan, S. Chen, L. Meng, and D. Fu. 2018. Role of the tomato *TAGL1* gene in regulating fruit metabolites elucidated using RNA sequence and metabolomics analyses. PLOS ONE, 13: e0199083.

Zhao, X., Y. Zhang, J. Lai, Y. Deng, Y. Hao, S. Wang, and J. Yang. 2023. The *SlDOG1* effect biosynthesis of steroidal glycoalkaloids by regulating *GAME* expression in tomato. International Journal of Molecular Sciences, 24: 3360.

Zheng, Z., G. Ye, Y. Zhou, X. Pu, W. Su, and J. Wang. 2021. Editing sterol side chain reductase 2 gene (*StSSR2*) via CRISPR / Cas9 reduces the total steroidal glycoalkaloids in potato. All Life, 14: 401-413.

Zhu, G., S. Wang, Z. Huang, S. Zhang, Q. Liao, C. Zhang, T. Lin, M. Qin, M. Peng, C. Yang, X. Cao, X. Han, X. Wang, E. van der Knaap, Z. Zhang, X. Cui, H. Klee, A.R. Fernie, J. Luo, and S. Huang. 2018. Rewiring of the fruit metabolome in tomato breeding. Cell, 172: 249-261.

Chapter Two: Tomato 7-Dehydrocholesterol Reductase (*Sl7DHCR*) Reduces $\Delta^{5,7}$ Sterols More Broadly than Previously Understood

Abstract

Tomato (*Solanum lycopersicum*) has a branch of the main sterol biosynthesis pathway which produces steroidal glycoalkaloids using a cholesterol backbone. Both the branch and the main sterol pathway contain a Δ^7-sterol reductase. Current understanding is 7-dehydrocholesterol reductase (*Sl7DHCR*) functions in the cholesterol branch while DWARF5 functions in the main pathway. *Sl7DHCR* was transformed into an *Arabidopsis thaliana dwf5* line. To analyze sterol content of these lines, LC-MS was performed. Chromatographic separation was performed using a SB-CN Zorbax column (with 1.8 µm particle size, 2.1 mm x 50 mm) with an atmospheric pressure chemical ionization (APCI) ion source. A total of 16 features with unique retention times and m/z were detected. We were able to identify three sterol-related metabolites, campesterol and β-sitosterol based on standards, and squalene based on mass and that it was the feature to occur at that mass and no other metabolites of interest share the same with mass as squalene. An increase in the amount of the sterol precursor squalene was observed in *dwf5* compared to *dwf5-7DHCR*, while a decrease was observed in end product sterols campesterol and β-sitosterol. This suggests that *Sl7DHCR* has a looser substrate specificity than was previously assumed.

Introduction

Tomato (*Solanum lycopersicum*) produces steroidal glycoalkaloids (SGAs). These are specialized metabolites derived from cholesterol, which contain nitrogen and have several sugar moieties attached to the sterol backbone by an O-glycosidic bond at the 3 carbon of the sterol. These SGAs impart a bitter taste on the tomato fruit and serve as defense against fungal infection and insect predation (McKee, 1959; Roddick, 1977; Dalvi and Bowie, 1983; Ginzberg et al., 2009; Friedman 2015). Tomato produces cholesterol through a branch off the main sterol biosynthesis pathway (Sonawane et al. 2016). The cholesterol branch starts with the production of cycloartanol from cycloartenol. Many of the parallel reactions are catalyzed by separate enzymes, often the product of a gene duplication event, while others share enzymes with the main sterol pathway.

One particular gene that is duplicated in tomato is 7-dehydrocholesterol reductase (*7DHCR*; Solyc06g074090), which catalyzes the reduction of 7-dehydrocholesterol to cholesterol. This gene is a result of a duplication of *DWARF5* (*DWF5*) which took place in an ancestral solanum species (Sonawane et al. 2016). The function of *DWF5* is thought to be catalyzation of the reduction of 5-dehydroavenasterol to isofucosterol and the reduction of 5-dehydroepisterol to 24-methylenecholesterol (Figure 1). Both *7DHCR* and *DWF5* catalyze Δ^7-sterol reductions of $\Delta^{5,7}$-sterols (Figure 1). When 7DHCR is silenced in tomato, there is a reduction of SGA accumulation as well as a reduction in stigmasterol and β-sitosterol, suggesting 7-DHCR may have function beyond the reduction of 7-dehydrocholesterol (Sonawane et al., 2016).

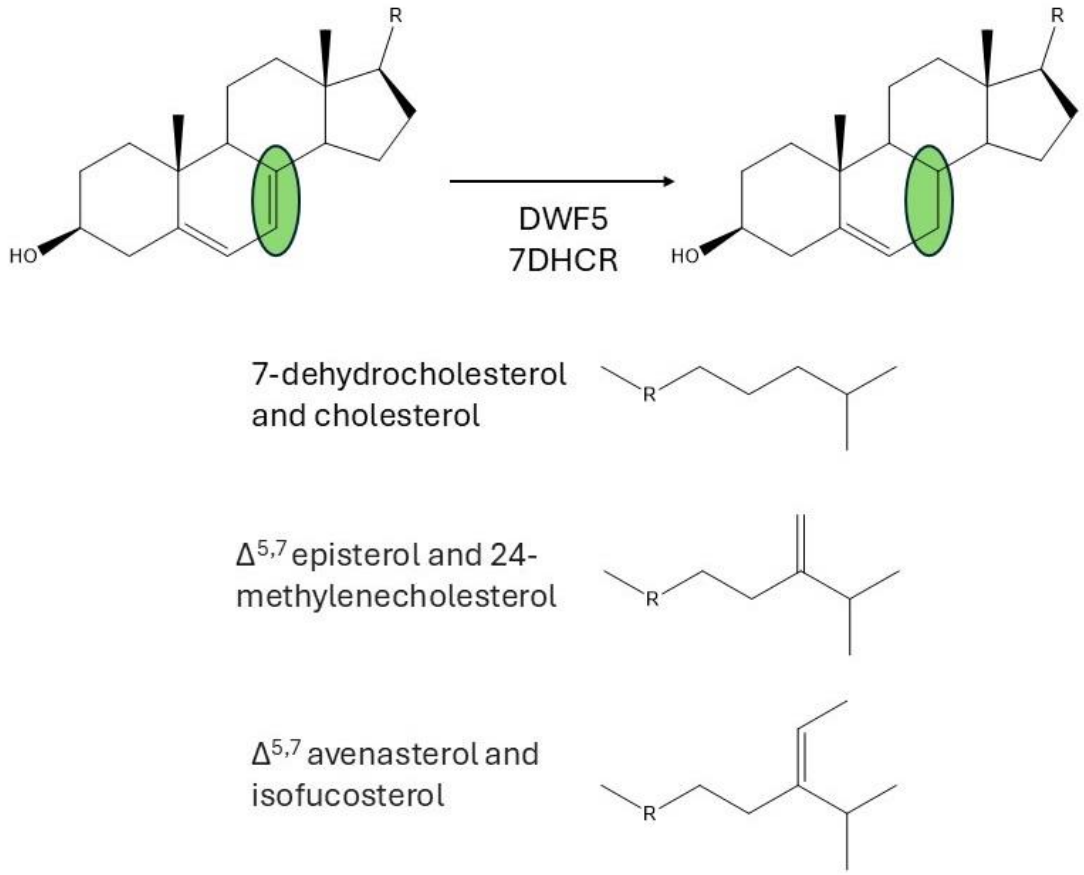

Figure 1 - Δ^7-sterol reductions of $\Delta^{5,7}$-sterols - Sterol backbone is shown with different side chains labeled below for the different substrates of *DWF5* and *7DHCR*. The site of the reduction is highlighted in green.

DWF5 was identified as a brassinosteroid synthesis gene (Choe et al 2000). Plants carrying a defective allele have shorter robust stature, increased number of inflorescences, round dark green leaves, and reduced germination. These mutants show reduced stomata opening and decreased expression of inward-rectifying K^+ rectifying channel activity (Inoue et al., 2017). *dwf5* plants recover WT phenotype when treated with exogenous brassinolide (Choe et al 2000). DWF5 is localized to the endoplasmic reticulum membrane (Silvestro et al., 2013).

At the current time, *SlDWF5* and *Sl7DHCR* are understood to have separate substrate specificities, however, because there is some preliminary evidence that Sl7DHCR may be more promiscuous than presented it is possible it can perform the same Δ^7 reductions as DWF5. In this study, Col-0 and *dwf5* lines were transformed to express *Sl7DHCR* and explore the range of substrates that *Sl7DHCR* is able to reduce and determine if it has broader Δ^7-sterol reductase activity than previously proposed.

Materials and Methods

Plant Material

Arabidopsis seed was acquired from the Arabidopsis Biological Resource Center (ABRC; Columbus, OH). We obtained *lepida (le)/dwf5-4,* which is one of several defective alleles of DWF5 available (McKelvie, 1961; Choe et al., 2000). Columbia-0 (Col-0) was used to compare to DWF5 for effects of *7-DHCR* in a plant with a functional *DWF5* allele.

Reagents

Taq polymerase and any restriction enzymes were purchased from New England Biolabs (Ipswich, MA). LC-MS and carotenoid extraction solvents other than water were purchased from Sigma (Saint Louis, MO). Optima LC-MS grade water was purchased from Fisher Chemical (Waltham, MA). All oligos were synthesized by Integrated DNA Technologies (Coralville, IA).

Generation of Plasmid

Tomato cv. MTX-851 was selected as the variety from which *Sl-7DR2* was cloned. Primers were designed from the tomato reference genome to amplify 7-DR-2 and its promoter region (Table 1). The predicted amplicon size is approximately 8 kb. To ensure accurate amplification, high-fidelity *Pfu* polymerase is used. The high-fidelity is ensured by the 3' → 5' proofreading exonuclease activity. The polymerase chain reaction (PCR) conditions follow the protocol available from New England Biolabs (Ipswich, MA). The reaction mixture contains 1x NEB HF buffer, 200 µM dNTPs, 0.5 µM of each of primer, which will be a OCC1237 and OCC1238 (Table 1), 50 ng of tomato genomic DNA, and 1 U of Phusion DNA polymerase (proprietary name used by New England Biolabs for *Pfu* polymerase). Total reaction volume is 50 µL. The reaction mixture is prepared on ice, before being transferred to a thermocycler. The PCR conditions are 98°C for 30s to denature the DNA, followed by 30 cycles of 98°C for 10s, 55°C for 30s, and 72°C for 5 min, and a final extension of 72°C for 10 min, before holding at 8°C.

The PCR product was analyzed on a 1% agarose gel to determine size and cleaned using a GenScript QuickCleanII PCR Extraction Kit (Piscataway, NJ) following the manufacturer's protocol. The gene was TA-cloned using the Promega (Madison, WI) pGEM®-T Easy Vector System II. Using the kit, the amplicon was inserted into the pGEM®-T Easy Vector, which contains an Ampicillin resistance gene and the LacZ operon to allow for efficient screening of bacterial colonies after transformation. The ligation mixture was transformed by heat shock into JM109 cells. The insert was sequenced using primers developed

Sl-7DR2 was removed from the pGEM®-T Easy Vector by restriction enzyme digestion. This was achievedperformed using manufacturer recommended double digestion. In brief, a double digest with SalI-HF and AscI was performed using CutSmart buffer following manufacturer recommendations, which is 5uL 10X rCutSmart Buffer, 10 units AscI, 20 units

SalI-HF, 1 ug plasmid DNA with a total reaction volume of 50 uL of H_2O. This was then cloned into a modified pCAMBIA1302 using T4 DNA ligase.

Plasmid Sequencing

After the amplified tomato gene was cloned into a pGEM®-T Easy Vector, Sanger Sequencing was performed at the University of Minnesota Genomics Center. Sequencing primers were designed based on the reference sequence of tomato *7DHCR* (Solyc06g07090.2) plus 2000 bp upstream and 1000 bp downstream using Primer3 (Untergasser et al, 2012; Korressar and Remm, 2007; Korressar et al, 2018). Sanger sequences were assembled using Geneious Prime 2025.0.3 (https://www.geneious.com) using the reference tomato gene.

Table 1 - Oligo Sequences

NAME	SEQUENCE	TM(°C)
OCC424	CGGCAAGACCATCACTCT	65
OCC425	TCATCAAGGAAGGCTCAA	60
OCC645	TCAAATGGACCGCTCTTATC	62
OCC646	CACAGACTGAAGCGTCCAAG	66
OCC1237	ACGCGTCGACGAGCCAACATACAACCCCCA	67
OCC1238	AGGCGCGCCTTGGAGATCCGTGGGAACTG	69
OCC1284	TATTGGAACACCATGGACATTGCATAT	55
OCC1285	AGAAGGCACCCACACTAGAC	54
OCC1307	CCTCGGTCCCTTTTTACTTG	52
OCC1308	CGTGCTGCAATCACAATCA	49
OCC1309	TTGGGCTTTTCCATCTCATC	50
OCC1310	TCCAATCTTGAAACACAGAAACA	50

OCC1311	AGAACAGGGAGGGAGGAAGA	54
OCC1312	AGCTAAACCAGCCCAGTGAA	52
OCC1315	TTGGGAAATGATTTGGGAAA	46
OCC1316	CCACCAAAGGCTGAGATAGG	54
OCC1317	TTTGTTTTCGTGACATGGTGA	49
OCC1318	TGAACCGTGATCAGTGGAAG	52
OCC1321	TTCCAGCTGTGCTTCTCAAG	52
OCC1322	TGGAGCCTACTGCATTTCAA	50
OCC1325	TGTTGCTAGCCCTCTTGTCA	52
OCC1326	GACAGATTGTTCGCCGAAAG	52
OCC1327	CCCTACCATGAACGCAAGAT	52
OCC1328	CGAAGGGGAAAGAGAATTTG	50
OCC1331	GAGTTCCGCAGAACAAATGG	52
OCC1332	AGGAGGCCCGTCAGATAGAT	54
OCC1333	ACCGTTTTGCTCTCATTTGC	50
OCC1334	CTTTTATGAGGGGCTGGACA	52
OCC1335	AGAGTTCTTGCCGGATGCTA	52
OCC1336	TCAAAAACGCTGCACGAATA	48
OCC1337	TTGCTTCTTTGCAGGTATGG	50
OCC1138	CCCGTGACTTTGTCCAATTT	50
OCC1341	AATCGCTTCCCTAGCAACAA	50

OVA0001	CACTCTGCTCACTTTAGTACCC	65
OVA0002	TGCAGGCCATTCTCCTTTAG	65
OVA0003	GACAGACAGAGGCAAGAGTTC	65
OVA0004	CGCCAGTTGTAGTAGTGTATGAG	65
OVA0005	TCAAAGATTGTCGCCTCATACA	64
OVA0006	CATAATGGAAATGCCGCGATAAG	64
OVA0007	ACCATTTCATGCCCTACATCTAT	63
OVA0008	CCATACTTTGACTTGCACCTTTC	64

Arabidiopsis growth conditions

Arabidopsis thaliana plants were grown in MAES Growth Chambers in Saint Paul, MN. The plants were grown in 16hr:8hr light:dark and 22°C/20°C light/dark temperatures with 50% relative humidity. PAR intensity was 200 µmol/m²/s.

Transformation of Arabidopsis

A floral spray method was used to transform *Arabidopsis* (Chung et al., 2000). Plants were grown in a growth chamber in Promix until a central bud formed. If any fruits or flowers had formed before *Agrobacterium* treatment they were removed immediately before treatment. 300 mL *Agrobacterium tumefaciens* cultures were grown overnight at 28°C in 1L conical flasks on an orbital shaker at 100 RPM. *Agrobacterium tumfaciens* AGL1 resuspended in 1X Murashige and Skoog media with 1% v/v Silwet-77 was applied using a spray bottle. The plants were then covered with black plastic to block light for 48 hours. *Agrobacterium* infection process was repeated twice more, after 2 days of exposure to normal light conditions for a total of 3 treatments with *Agrobacterium*. Both Col-0 and *dwf5-4* were transformed to carry *Sl7DHCR*.

Identifying Transformed Plants

Seed was collected from plants treated with *Agrobacterium*. *Arabidopsis* seeds were placed in a sterile microcentrifuge tube. 500 uL of sterilization solution was added to each tube. Sterilization solution was 3% sodium hypochlorite with 0.1% Tween-20. Samples were shaken for 7 min on an orbital shaker at 100 RPM. After shaking samples were centrifuged for 2 min at 3000 RPM. The supernatant was removed and replaced with 500 uL of sterile deionized H_2O and centrifuged for 2 min at 2500 RPM. The sterilization solution was replaced with water 4 times and incubated overnight at 4˚C. Seeds were transferred by sterile pipette to a 15x100 mm plate with 1x MS media with 25 mg/L Hygromycin B. Plates were sealed with micropore tape. Plates were stored in the dark for 48 hours after seeds were added. After this time, they were placed in the same growth chamber. When plants had grown roots, they were transferred to Promix and further grown in the growth chamber.

Plant DNA Extraction

100 mg of leaf tissue was collected in a 1.5 mL tube and flash frozen using liquid nitrogen. It was then ground to a fine powder using a pestle. 500 µL of extraction buffer was added to the leaf tissue. The extraction buffer contained 0.05M ethylenediaminetetraacetic acid (EDTA), 0.1M Tris-HCl, 0.5M NaCl, and 2% sodium dodecyl sulfate (SDS). The samples were mixed by vortex and then incubated at 70˚C for 60 minutes, mixing by inversion every 15 minutes. After the incubation, 130 µL of 0˚C 5M potassium acetate (KAc) was added to each sample, which were mixed by inversion and then incubated on ice for 5 min. Samples were centrifuged at 14000 g for 5 min. Supernatant was collected and transferred to a clean 1.5 mL tube. 30 µL of 3M Sodium Acetate (NaOAc) was added to each sample followed by 330 µL of 0˚C 2-propanol. Samples were incubated for 10 min on ice before centrifuging for 5 min at 14000 g. Supernatant was discarded and replaced with 700 µL of 70% EtOH. Samples were centrifuged for 5 minutes at 14000 g before the supernatant was removed and pellet was allowed to dry for 120 min and resuspended in H_2O. DNA content was determined using a ThermoScientific NanoDrop Spectrophotometer 2000c.

Polymerase Chain Reaction (PCR) and Derived Cleaved Amplified Polymorphic Sequences (dCAPS)

The PCR reaction mixture was 2.5 µL of 10X NEB ThermoPol Reaction Buffer, 200 µM of dNTPs, 0.2 µM primer 1, 0.2 µM primer 2, 1.0 µL of template DNA, 0.625 U of *Taq* polymerase, and a total reaction volume of 25 µL. PCR thermocycling conditions were 95°C for 30 seconds, followed by 30 cycles of 95°C for 15 seconds, 55°C for 30 seconds, 68°C for 1 minute followed by 68°C for 10 minutes before holding at 4°C. To test for the presence *Sl7DHCR*, OCC1307 and OCC1308 were used, with an expected product size of 898 bp. PCR products were visualized using a 1% agarose gel with NEB 1 kb DNA Ladder for determining product size.

Derived Cleaved Amplified Polymorphic Sequences (dCAPS) is a method of detecting single nucleotide polymorphisms (SNPs) performed in 2 steps, first PCR to amplify the reaction followed by a restriction enzyme digestion of the PCR product. The oligos for the PCR stage were OCC1284 and OCC1285, with a predicted product size of 307 bp. The digestion reaction was performed using 15 µL PCR product, 2.5 µL 10X rCutSmart^{TM} buffer, and 5U NdeI for 15 minutes at 37°C. For dCAPS, products of both PCR and digestion were analyzed using a 2% agarose gel. Oligos for the dCAPS assay as well as selection of restriction enzyme was performed using dCAPs Finder 2.0 (Neff et al. 2002).

RNA Extraction and Expression Analysis

RNA was extracted from leaves and flower buds of *Arabidopsis* plants using a Zymo (Irvine, CA) Direct-zol™ RNA MicroPrep kit following manufacturer's instructions. cDNA was produced using an Invitrogen™ (Waltham, MA) SuperScript™ IV First-Strand Synthesis System kit using the random hexamers provided. PCR was performed using intercalating primers designed for real-time qPCR using Integrated DNA Technology (Coralville, IA) PrimerQuest™ Tool. PCR was performed using cDNA as a template with OVA001 and OVA002 (expected fragment size 111 bp), OVA0003 and OVA0004 (expected fragment size 97 bp), OVA0005 and OVA0006 (expected fragment size 101 bp), OVA0007 and OVA0008 (expected fragment size 94 bp) targeted to the transcript sequence of *Sl7DHCR* and OCC424 and OCC425 and OCC645 and OCC646 targeting UBQ1 as controls (Ruppel et al., 2013).

Sterol Extraction

The sterol extraction method was based on Jäpelt et al. (2011). One basal leaf of an *Arabidopsis* plant was placed in a 2 mL centrifuge tube. Fresh leaf mass was collected at this time. 1 mL of methanol was added to each tube. These were stored at -80°C until extraction was performed (at least 72 hours). The conditions for saponification were 820 mM KOH and 192 mM ascorbic acid. 5 µL of 10 mM $^{13}C_3$-cholesterol was added to each sample. Samples were shaken overnight on an orbital shaker at 100 RPM. The next day samples were transferred to a glass tubes with a teflon-covered lid. 833 µL of 4:1 pentane:ethyl acetate (v:v) was added to each sample. Samples were shaken for 30 minutes at 100 RPM before centrifuging at 2000g for 5 min.The pentane layer was removed and collected in a glass tube. An additional 833 uL of 4:1 pentane:ethyl acetate (v:v) was added to each sample, shaking and centrifugation were repeated and pentane layers were pooled by sample. Samples were condensed under nitrogen and brought up to 1000 mL with methanol, samples were stored at -80°C.

UHPLC-HRAMS

Chromatographic separation and high-resolution accurate mass spectrometry (HRAMS) analysis were performed using an ultra high performance liquid chromatography system (UHPLC) connected to a hybrid quadrupole-Orbitrap mass spectrometer (Ultimate

3000 UHPLC, Q Exactive; Thermo Fisher Scientific, Waltham, MA)). Each sample (5 µL) was injected onto a SB-CN Zorbax column (with 1.8 µm particle size, 2.1 mm x 50 mm; Agilent, Santa Clara, CA). Column temperature was 40°C with a solvent flow rate of 0.400 mL/min. An 11-minute elution profile using solvent A, water with 0.1% formic acid and solvent B, acetonitrile with 0.1 formic acid was performed. From 0 minutes to 2 minutes the gradient was held at 60% solvent B, this increased linearly to 80% solvent B through minute 7 before increasing linearly to 98% solvent B through minute 9 followed by holding at 98% solvent B for 1 minute before returning to 60% solvent B at minute 11. This method is based on the carotenoid separation method described in Abate-Pella et al., 2017. Ionization was performed using an atmospheric-pressure chemical ionization (APCI) source. APCI conditions were sheath gas flow rate of 40 arbitrary units, capillary temperature 225 ℃, spray voltage of 5000 V, discharge current of 4.00 µA vaporizer temperature of 350℃ and MS Conditions are mass scan range of 100 to 1800 *m/z*, resolution of 70,000, positive polarity spectrum data type was profile, S-Lens RF level of 55.

MS Data Analysis

ThermoRaw files from the Ultimate 3000 UHPLC, Q Exactive were converted to mzML format using MSConvert filtering for peak picking using the Vendor Algorithm (Chambers et al, 2012). Data was extracted from these extracted ion chromatograms using MZMine 2.3 (Pluskal et al., 2010). Statistical analysis was performed in R 4.3.3. Peak area was normalized to the peak area of $^{13}C_3$-cholesterol-H_2O (m/z=372.3616) by dividing the sample peaks by the peak area of $^{13}C_3$-cholesterol-H_2O and multiplying by the mean of all samples peak area of $^{13}C_3$-cholesterol-H_2O. These were then normalized to mass of leaf (mg) in the same way, dividing the product of the $^{13}C_3$-cholesterol-H_2O normalization by the leaf mass and then multiplying by the mean of all leaf masses. The products of the leaf mass transformation were $\log_2$ transformed for further analysis. Leaf data are the mean of technical replicates of MS data and plant data are the mean of each leaf collected from that plant.

Results

Sanger Sequencing

Sanger sequencing of the complete genomic fragment of *7DHCR* of MTX-851 was completed using 30 fragments to assemble the complete sequence. The assembled sequence was 8031 bp long with a 3 bp gap between positions 2558-2560, a 12 bp gap between positions 4476 and 4487, and a 184 bp gap between positions 6415-6798. This equates to 95.3% identity between the sequences. When a MegaBLAST (performed on December 10, 2024) was performed using the consensus sequence the first 4 results were to tomato chromosome 6 as would be expected (Figure 2).

Description	Scientific Name	Max Score	Total Score	Query Cover	E value	Per. Ident	Acc. Len	Accession
Solanum lycopersicum cultivar I-3 chromosome 6	Solanum lycop…	11791	17191	97%	0.0	99.77%	49756038	CP023762.1
Solanum lycopersicum Micro-Tom DNA, chromosome 6, draft genome sequence	Solanum lycop…	11791	17213	97%	0.0	99.77%	52172941	AP028940.1
Solanum lycopersicum chromosome ch06, complete genome	Solanum lycop…	11791	17207	97%	0.0	99.77%	46045610	HG975518.1
Solanum lycopersicum genome assembly, chromosome: 6	Solanum lycop…	11791	17213	97%	0.0	99.77%	52221637	OU640349.1
Solanum verrucosum cultivar 11H23 chromosome 6	Solanum verruc…	6955	16397	75%	0.0	92.59%	55157000	CP133617.1
Solanum tuberosum cultivar Solyntus chromosome 6	Solanum tubero…	6628	16895	75%	0.0	91.59%	65489876	CP055239.1
Solanum tuberosum cultivar MSH/14-112 chromosome 6	Solanum tubero…	6567	15955	75%	0.0	90.92%	59526227	CP046692.1
Solanum tuberosum cultivar P8 chromosome 6	Solanum tubero…	6538	15583	75%	0.0	90.68%	59524932	CP046679.1
Solanum pennellii chromosome ch06, complete genome	Solanum pennellii	5005	24801	97%	0.0	97.29%	60730942	HG975445.1
Solanum nigrum genome assembly, chromosome: 32	Solanum nigrum	4602	6183	65%	0.0	89.19%	67870466	OZ176043.1

Figure 2 - BLAST results of consensus sequence showing high sequence similarity to *Solanum lycoperscium* chromosome 6 as well other *Solanum* species.

Genotyping

PCR based methods were successful to identify individuals carrying the *dwf5-4* allele and *Sl7DHCR*. The Col-0 with *7DHCR* and *dwf5* with *7DHCR* individuals showed a single band showing presence of *7DHCR* (Figure 3 and Figure 4). Based on the results of both *7DHCR* and *dwf5-4* PCR assays, 4 individuals were advanced for further analysis; there were CS72-7DHCR-11,-12,-13, and -14 (Figure 4). Individuals with the *dwf5* will have a band the same size after digestion as opposed to a smaller band or double band like seen in sample 1 (Figure 4).

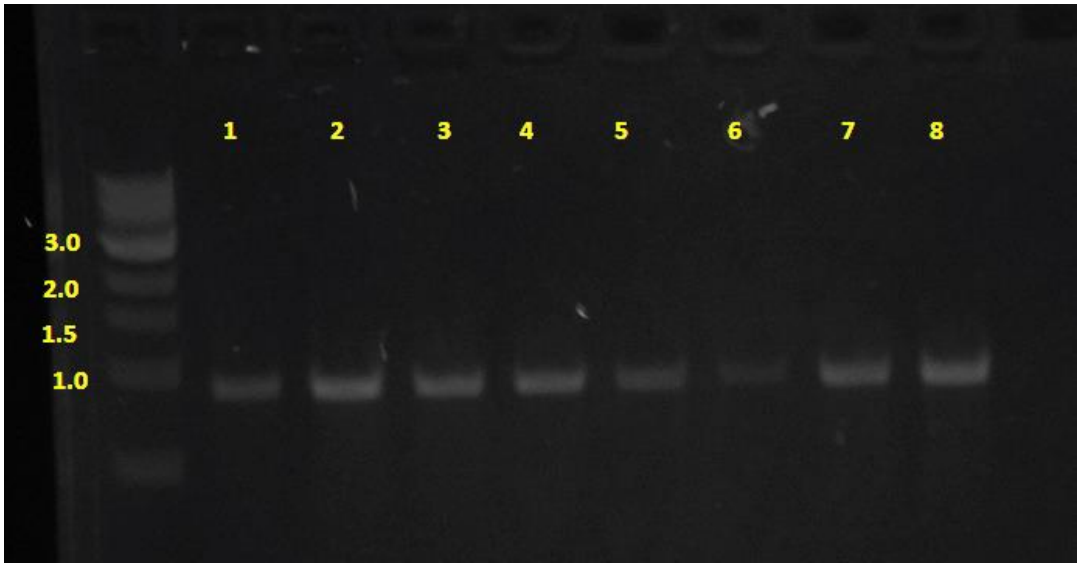

Figure 3 - 1% Agarose Gel of Col-0 individuals for *Sl7DHCR*. Each lane is a single individual with a band present showing the presence of *Sl7DHCR* in the individual. Numbers on the left side label a 1 kb ladder in kb. Each lane is a single plant.

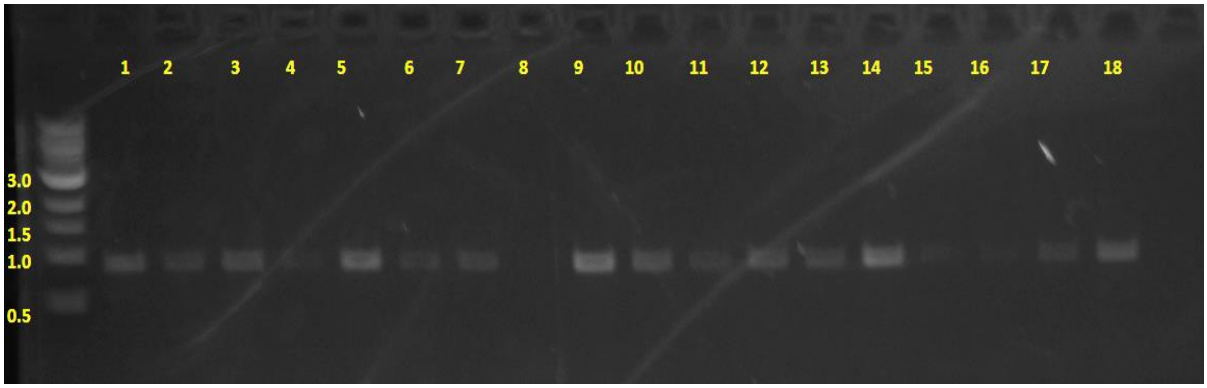

Figure 4- 1% Agarose Gel of possible *dwf5-4* individuals for *Sl7DHCR*. Each lane is a single individual with a band present showing the presence of *Sl7DHCR* in the individual. Numbers on the left side label a 1 kb ladder in kb.

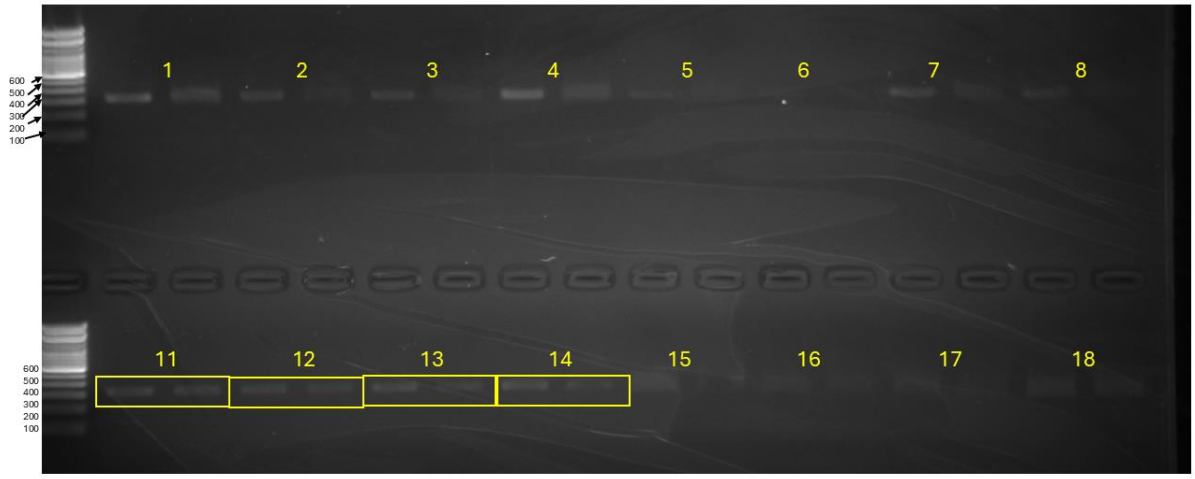

Figure 5- dCAPS to screen plants for *dwf5-4*. Samples are numbered for 2 lanes. The left of these is the PCR product before digestion with NdeI and the right lane is after digestion. When the bands are the same size, *dwf5-4* is present. Those samples marked with a yellow box are those that carry the *dwf5-4* allele.

Expression

To determine if *Sl7DHCR* is expressed in *Arabidopsis*, PCR was performed on cDNA derived from leaf and flower bud transcript. Four different individuals carrying *Sl7DHCR* were randomly selected to test expression. When visualized using gel electrophoresis, two bands are present which show the presence of *UBQ1* cDNA and four bands for *Sl7DHCR*.

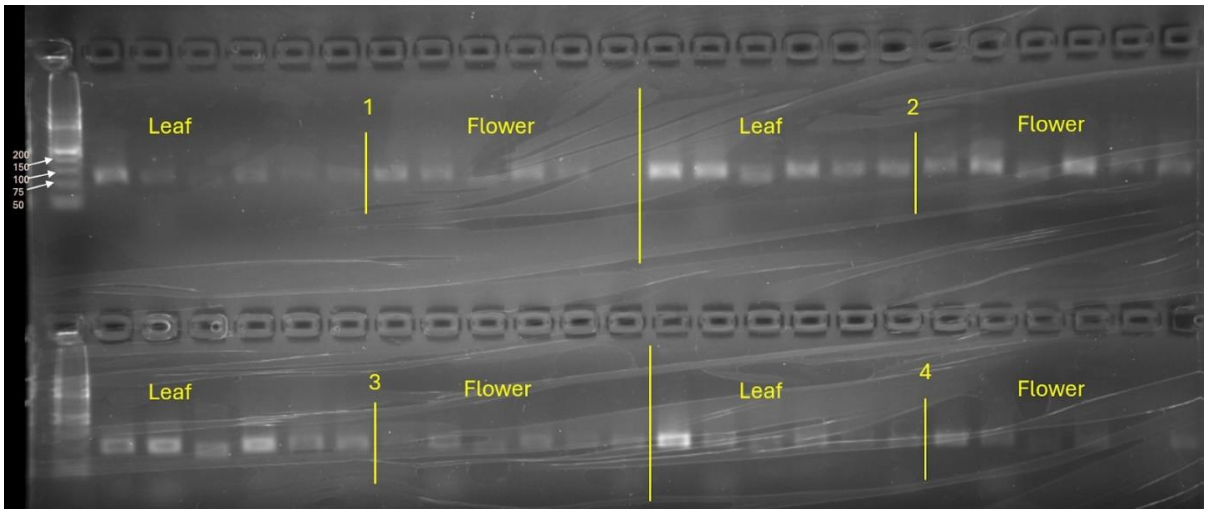

Figure 6- 2% agarose gel of PCR of cDNA from *Arabidopsis* plants that carry *Sl7DHCR*. Four different plants were used numbered 1, 2, 3, and 4, which two different organs, basal rosette leaves, and flower buds. The first two lanes of each organ are *AtUQB1* and the next four are to *Sl7DHCR*.

Sterol Analysis

Positive identification of two major sterols, campesterol and β-sitosterol, was done based on standards (Figure 7). Squalene was identified based on mass of a +H product and being the only metabolite of that mass screened. Sixteen features were detected (Table 2). Significant differences were found for all features except feature 8 (Ffigure 8). There are still several ambiguous features that cannot conclusively be assigned to a metabolite. For this reason, only select features are assigned to a metabolite (Figures 7, 8, 9). Features 15 and 16 are being treated as reflecting content of 2,3-oxidosqualene, cycloartenol, and obtusifoliol because these metabolites share a mass and are in the same portion of the sterol biosynthesis pathway. A pattern is evident in the content of squalene and features 15 and 16 of CS72 having higher content of these metabolites while campesterol and β-sitosterol are lower in CS72 than the other 3 genotypes. This suggests there may be a buildup of metabolites before DWF5 and a decrease in those after DWF5, and that *Sl7DHCR* complements the effects of *dwf5-4*.

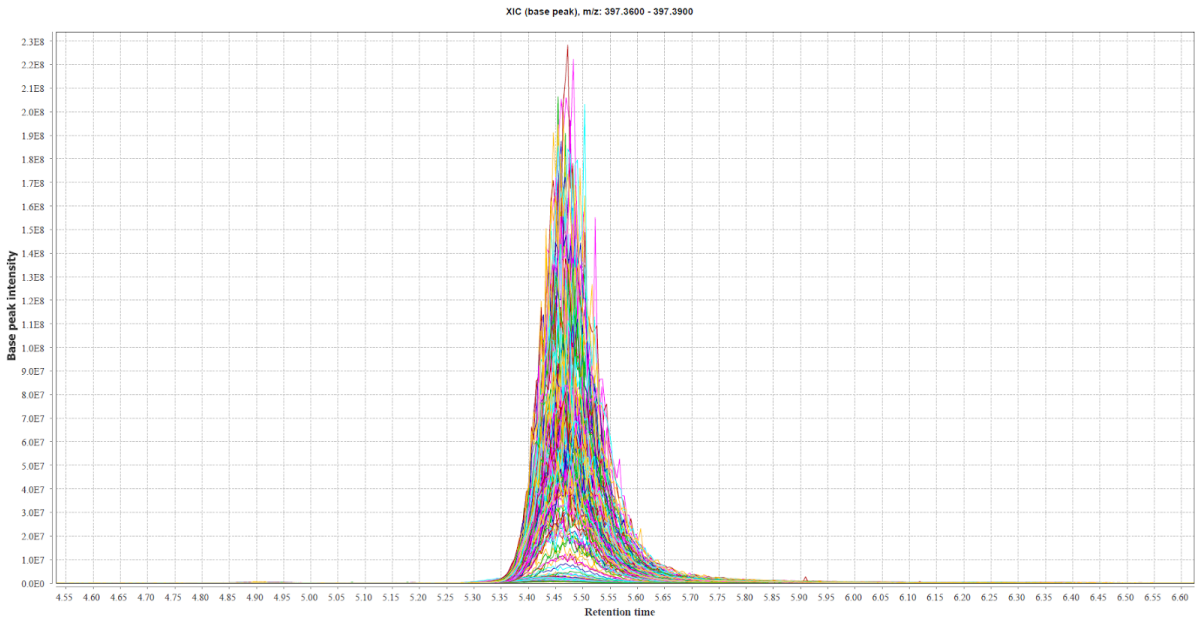

Figure 7 - Chromatogram of *m/z* 397.38. This *m/z* value is equivalent to that of β-sitosterol's water loss product +H. Produced by MzMine2.3

Table 2 - Features detected in sterol analysis.

Number	m/z	Retention Time (min)	Possible metabolite assignments	Possible Formula
1	383.3683	5.12	Campesterol - H_2O	$C_{28}H_{46}$
2	397.3840	5.46	β-sitosterol - H_2O	$C_{29}H_{48}$
3	399.3622	5.12	Episterol 24-methylene cholesterol	$C_{28}H_{46}O$
4	411.3622	1.99	4α-methyl-5α-ergosta-8,14,24(28)-trien-3β-ol 5-dehydroavenasterol	$C_{29}H_{46}O$
5	411.3622	4.95		
6	411.3622	5.47		
7	411.3986	5.69	Squalene	$C_{30}H_{50}$
8	413.3778	2.16	24-methylenephenol Δ^7-avenasterol Isofucosterol stigmasterol	$C_{29}H_{48}O$
9	413.3778	3.42		
10	413.3778	4.92		
11	413.3778	5.04		

12	413.3778	5.46		
13	415.3935	2.93	β-sitosterol	$C_{29}H_{50}O$
14	415.3935	6.36		
15	427.3935	5.45	2,3-oxidosqualene Cycloartenol Cycloeucalenol obtusifoliol	$C_{30}H_{50}O$
16	427.3935	5.55		

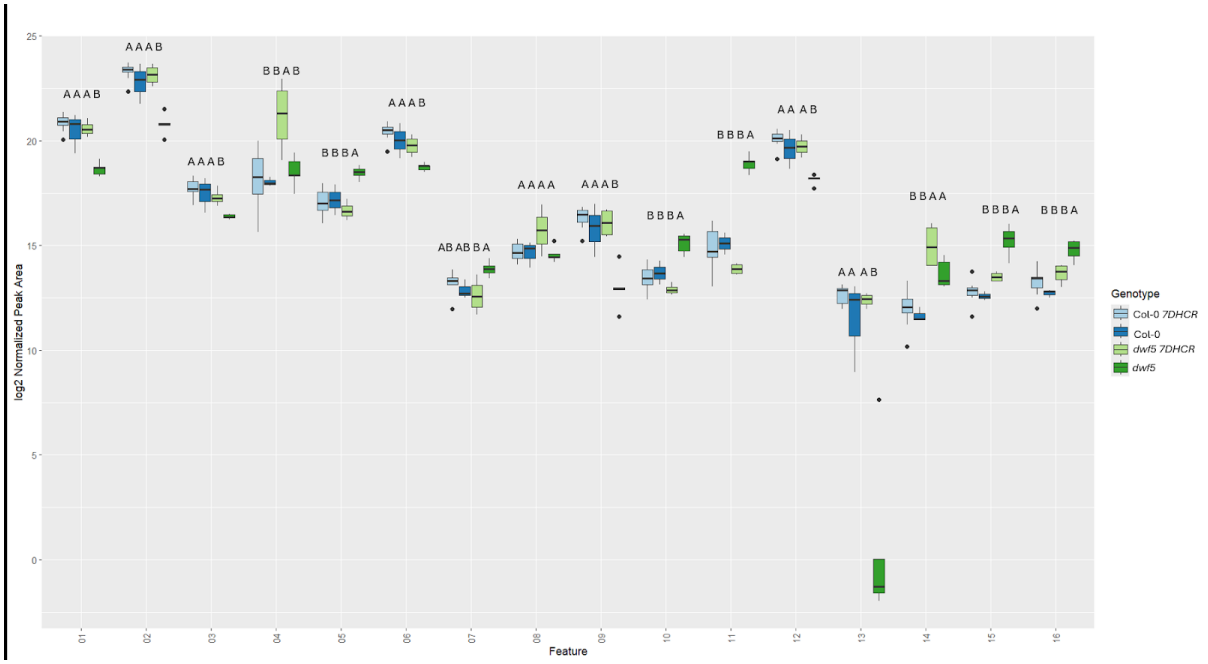

Figure 8 - Box plot of each feature. Letters represent a significant difference based on a means separation to show significant differences. Numbers on the X-Axis match numbers in Table 2. Feature m/z and retention times are 01: 383.3683 at 5.12 min, 02: 397.3840 at 5.46 min,03: 399.3622 at 5.12 min, 04: 411.3622 at 1.99 min, 05: 411.3622 at 4.95 min,06: 411.3622 at 5.47 min,07: 411.3986 at 5.69 min, 08: 413.3986 at 5.69 min,09: 413.3778 at 3.42 min,10: 413.3778 at 4.92 min,11: 413.3778 at 5.04 min, 12: 413.3778 min, 13: 415.3935 at 2.93 min, 14: 415.3935 min, 15: 417.3935 at 5.45 min, 16: 427.3935 at 5.55 min.

Squalene
410.3913

2,3-Oxidosqualene
426.3862

Cycloartenol
426.3862

24-methylenecyloartenol
440.4018

Cycloeucalenol
426.3862

Obtusifoliol
426.3862

DWARF5 *DWARF5*

β-sitosterol
414.3862

Campesterol
400.3705

AB AB B A

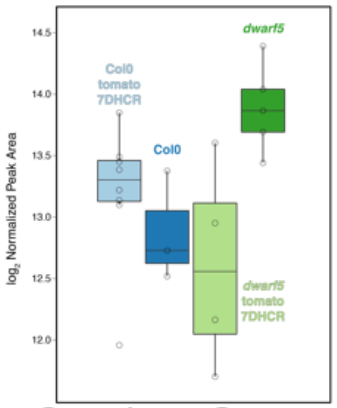

Squalene Content

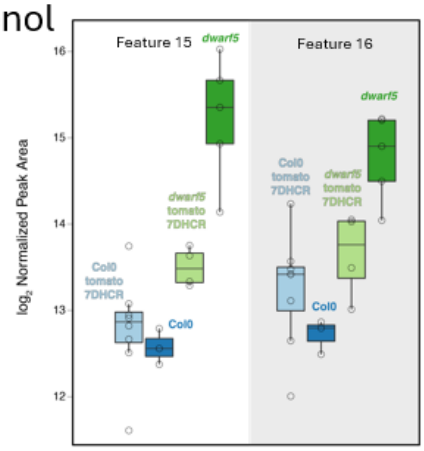

A A A B

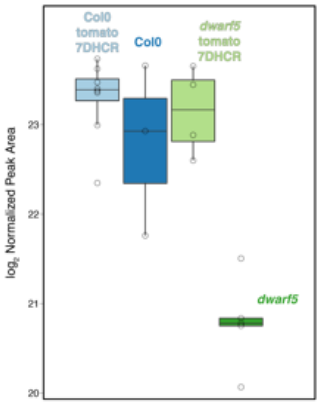

A A A B

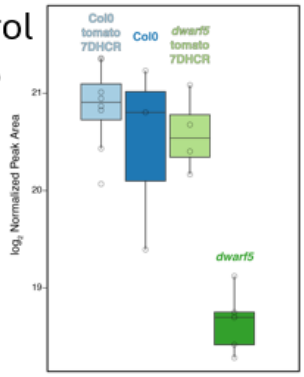

Figure 9 - Pathway of sterol biosynthesis in *Arabidopsis* from squalene to 24-methylenelophenol. Box plots to the side of metabolite names are based on possible metabolite identifications. Numbers in the box plots are the whole number of the neutral mass of the metabolite to which they can be connected to.

Discussion

This work presents evidence for potential *Sl7DHCR* functions beyond the reduction of 7-dehydrocholesterol to cholesterol (Sonawane et al. 2016). Tomato has a branch of its phytosterol pathway that produces cholesterol, which is used to produce the defensive compounds, the steroidal glycoalkaloids (Averello et al., 2024). This branch includes several duplicated genes, including *7DHCR* in the cholesterol branch, reducing 7-dehydrocholesterol to cholesterol, and *DWF5* in the general phytosterol branch, reducing $\Delta^{5,7}$-episterol to 24-methylenecholesterol and $\Delta^{5,7}$-avenasterol to isofucosterol. *Arabidopsis* only has the main phytosterol branch. *dwf5-4* accumulates higher content of early compounds in the pathway, like squalene, while accumulating decreased amounts of compounds after *DWF5*, such as β-sitosterol and campesterol when compared to Col-0, which has a functional *DWF5* allele. When *Sl7DHCR* is expressed in *dwf5-4* lines, the content of these metabolites is changed and more resembles that of Col-0. This leads to the conclusion that *Sl7DHCR* can catalyze reduction reactions with substrates beyond 7-dehydrocholesterol, which was the previous understanding. With the research presented here, the current understanding might be updated to be *Sl-7DHCR* can reduce 7-dehydrocholesterol, 7-dehydrepisterol, and 7-dehydroavensterol while *Sl-DWF5* may only reduce 7-dehydrepisterol and 7-dehydroavensterol. *Sl7DHCR* is capable of reducing a range of sterols, this raises the question of the function of *SlDWF5* (Solyc01g009310). When *Sl7DHCR* was knocked out in tomato, there was no reduction in phytosterol content, suggesting *SlDWF5* catalyzes the other phytosterol reactions in sufficient enough levels to not need *Sl7DHCR* to perform them as well *in vivo* (Li et al 2022). Understanding how *DWF5* and *7DHCR* are differentiated in substrate specificity, tissue specificity, and temporal expression. Using the tomato eFP Browser, there is little relative difference between expression of these two genes in the leaves and higher expression of *DWF5* in the breaker fruit (Waese et al, 2017; Tomato Genome Consortium, 2012). Further experiments to address these questions include knocking out *DWF5* in tomato to understand if *DWF5* is essential to sterol metabolism in tomato, similarly expressing *SlDWF5* in an *Arabidopsis* mutant like *dwf5-4* would also help to understand the substrate specificity of *SlDWF5*. Using a tagging construct such as GFP would allow researchers to understand when and where each *SlDWF5* and *Sl7DHCR* are expressed.

A limitation of this work was the inability to assign features to metabolites. With better identification of metabolites a better understanding of the flux through the pathway may be determined including determining if the substrates of *Sl7DHCR*, $\Delta^{5,7}$-episterol and $\Delta^{5,7}$-avenasterol, accumulate. In the future, better identification may be possible using

MS/MS to fragment the metabolites. Additionally, the use of a CN column may not have effectively separated metabolites as evidenced by 11 of the 16 features analyzed having a retention time between 4.9 minutes and 5.6 minutes. An alternative column may be employed to provide better separation of metabolites, for example a C18 column or a pentafluorophenyl (PFP) column (Della Corte et al, 2015; Helmschrodt et al., 2013; Jäpelt et al 2011; Skubic et al., 2020). These changes may allow better identification of sterols using LC-MS. However, even with these limitations, positively identifying squalene, β-sitosterol, and campesterol, using standard compounds and m/z values allows us to conclude that *Sl7DHCR* has broader substrate specificity than previously understood and leading to more questions about the differentiation between the two branches of the sterol pathway.

Conclusion

In tomato, there is a branch off the main sterol biosynthesis pathway which produces the protective compounds, steroidal glycoalkaloids. Within these branches are several pairs of duplicated genes, one such pair is *SlDWF5* which functions in the main phytosterol pathway, while *Sl7DHCR* functions the SGA branch. *Arabidopsis* only has the main phytosterol pathway, not the SGA pathway. When *Sl7DHCR* is expressed in an *AtDWF5* mutant, there is a change in sterol metabolism that is more like that of a plant with a functional *DWF5* allele than the mutant lines. This finding suggests that *7DHCR* has broader substrate specificity than previously assumed.

References

Abate-Pella, D., D.M. Freund, J.P. Slovin, A.D. Hegeman, J.D. Cohen. 2017. An improved method for fast and selective separation of carotenoids by LC-MS. Journal of Chromatography B 1067: 34-37. doi: 10.1016/j.jchromb.2017.09.039.

Averello, V., A.D. Hegeman, and C. Chen. 2024. Finding the Balance: Modifying the Cholesterol and Steroidal Glycoalkaloid Synthesis Pathway in Tomato (Solanum lycopersicum L.) for human health, fruit flavor, and plant defense. Horticultural Plant Journal. doi: https://doi.org/10.1016/j.hpj.2023.05.019.

Chambers, M.C., B. Maclean, R. Burke, D. Amodei, D.L. Ruderman, S. Neumann, L. Gatto, B. Fischer, B. Pratt, J. Egertson, K. Hoff, D. Kessner, N. Tasman, N. Shulman, B. Frewen, T.A. Baker, M. Brusniak, C. Paulse, D. Creasy, L. Flashner, K. Kani, C. Moulding, S.L. Seymour, L.M. Nuwaysir, B. Lefebvre, B. Connolly, T. Chadick, K. Holly, J. Eckels, E.W. Deutsch, R.L. Moritz, J.K. Katz, D.B. Agus, M. MacCoss, D.L. Tabb and P. Mallick. 2012. A cross-platform toolkit for mass spectrometry and proteomics. Nature Biotechnology 30: 918-920. doi: 10.1038/nbt.2377.

Choe, S., A. Tanaka, T. Noguchi, S. Fujioka, S. Takatsuro, A.S. Ross, F.E. Tex, S. Yoshida, K.A. Feldmann. 2000. Lesions in the sterol Δ^7 reductase gene of *Arabidopsis* cause dwarfism due to a block in the brassinosteroid biosynthesis. The Plant Journal 21: 431-443. doi: 10.1046/j.1365-313x.2000.00693.x.

Chung, M.-H., M.-K. Chen, and S.-M. Pan. 2000. Floral Spray Transformation Can Efficiently Generate Arabidopsis. Transgenic Research 9: 471-486. doi: https://doi.org/10.1023/A:1026522104478

Dalvi, R.R. and W.C. Bowie. 1983. Toxicology of solanine: an overview. Veterinary and Human Toxicology 25: 13-15.PMID: 6338654.

Della Corte, A., G. Chitarrini, I.M. Di Gangi, D. Masuero, E. Soini, F. Mattivi, U. Vrhovsek. 2015. A rapid LC-MS/MS method for quantitative profiling for fatty acids, sterols, glycerolipids, glycerophospholipids and sphingolipids in grapes. Talanta 140: 52-61. doi: 10.1016/j.talanta.2015.03.003.

Friedman, M. 2015. Chemistry and anticarcinogenic mechanisms of glycoalkaloids produced by eggplants, potatoes, and tomatoes. Journal of Agricultural and Food Chemistry 63: 3323-3337. doi: 10.1021/acs.jafc.5b00818.

Ginzberg I., J.G. Tokuhisa, and R.E. Veilleux. 2009. Potato steroidal glycoalkaloids : biosynthesis and genetic manipulation. Potato Research 52: 1-15. doi: 10.1007/s11540-008-9103-4.

Helmschrodt, C., S. Becker, J. Schröter, M. Hecht, G. Aust, J. Thiery, U. Ceglarek. 2013. Fast LC-MS/MS analysis of free oxysterols derived from reactive oxygen species in human plasma and carotid plaque. Clinica Chimica Acta 425: 3-8. doi: 10.1016/j.cca.2013.06.022.

Koressaar T. and M. Remm. 2007. Enhancements and modifications of primer design program Primer3. Bioinformatics 23: 1289-1291. doi: 10.1093/bioinformatics/btm091.

Koressar T., M. Lepamets, L. Kaplinksi, K. Raime, R. Anderson, and M. Remm. 2018. Primer3_masker: integrating masking of template sequence with primer design software. Bioinformatics 34: 1937-1938. doi: 10.1093/bioinformatics/bty036

Li, J., A. Scarano, N. M. Gonzalez, F. D'Orso, Y. Yue, K. Nemeth, G. Saalbach, L. Hill, C. de Oliveira Martins, R. Moran, A. Santino, C. Martin. 2022. Biofortified tomatoes

provide a new route to vitamin D sufficiency. Nature Plants 8: 611-616. doi: 10.1038/s41477-022-01154-6

McKee, R.K. 1959. Factors Affecting the Toxicity of Solanine and Related Alkaloids to *Fusarium caeruleum*. Journal of General Microbiology 20: 686-696. doi: 10.1099/00221287-20-3-686.

McKelvie, A.D. 1961. A list of mutant genes in *Arabidopsis thaliana* (L.) Heynh. Radiation Botany 1: 233-240. doi: 10.1016/S0033-7560(61)80032-X.

Neff, M.M., E. Turk., M. Kalishman. 2002. Web-based primer design for single nucleotide polymorphism analysis. Trends in Genetics 18: 613-615. doi: 10.1016/s0168-9525(02)02820-2.

Jäpelt, R.B., D. Silvestro, J. Smedsgaard, P.E. Jensen, and J. Jakobsen. 2011. LC-MS/MS with atmospheric pressure chemical ionisation to study the effect of UV treatment on the formation of vitamin D_3 and sterols in plants. Food Chemistry 129: 217-225. doi: 10.1016/j.foodchem.2011.04.029.

Inoue, S., N. Iwashita, Y. Takahashi, E. Gotoh, E. Okuma, M. Hayashi,R. Tabata,A. Takemiya, Y. Murata, M. Doi, T. Kinoshita, K. Shimazaki. 2017. Brassinosteroid involvement in *Arabidopsis thaliana* stomatal opening. Plant & Cell Physiology 58: 1048-1058. doi: 10.1093/pcp/pcx049.

Pluskal, T., S. Castillo, A. Villar-Briones, M. Orešič. 2010. MZmine2: Modular framework for processing, visualizing, and analyzing mass spectrometry-based molecular profile data.

Roddick, J.G. 1977. Subcellular localization of steroidal glycoalkaloids in vegetative organs of *Lycopersicon esculentum* and *Solanum tuberosum*. Phytochemistry 16: 805-807. doi: 10.1016/S0031-9422(00)89276-6.

Ruppel, N.J., K. N. Kropp, P.A. Davis, A.E. Martin, D.R. Luesse, R.P. Hangarter. 2013 Mutations in *Geranylgeranyl disphosphate synthase 1* affect chloroplast development in *Arabidopsis thaliana* (Brassicaceae). American Journal of Botany 100: 2074-2084. doi: 10.3732/ajb.1300124.

Skubic, C., I. Vovk, D. Rozman, M. Križman. 2020. Simplified LC-MS Method for Analysis of Sterols in Biological Samples. Molecules 25. doi: 10.3390/molecules25184116

Silvestro, D., T.G. Anderson, H. Schaller, and P.E. Jensen. 2013. Plant Sterol Metabolism. Δ^7-sterol-C_5-desaturase (STE1/DWARF7), $\Delta^{5,7}$-sterol-Δ^7-reductase (DWARF5) and Δ^{24}-sterol-Δ^{24}-reductase (DIMINUTO/DWARF1) show multiple subcellular localization is *Arabidopsis thaliana* (Heynh) L. PLoS One 8. doi:10.1371/journal.pone.0056429.

Sonawane, P.D., J. Pollier, S. Panda, J. Szymanski, H. Massalha, M. Yona, T. Unger, S. Malitsky, P. Ardent, L. Pauwels, E. Almekias-Siegel, I. Rogachev, S. Meir, P.D. Cardenas, M. Athar, M. Petrikov, H. Schaller, A.A. Schaffer, A. Kamble, A.P. Giri, A. Goossens, and A. Aharoni. 2016. Plant cholesterol biosynthetic pathway overlaps with phytosterol metabolism. Nature Plants 3. doi: 10.1038/nplants.2016.205

Untergasser A, I. Cutcutache ,T. Koressaar, J. Ye, B.C. Faircloth, M. Remm and S.G. Rozen. 2012. Primer3– new capabilities and interfaces. Nucleic Acids Research 40. doi: 10.1093/nar/gks596.

Tomato Genome Consortium. 2012 The tomato genome sequence provides insights into fleshy fruit evolution. Nature 485: 635-641. doi: https://doi.org/10.1038/nature11119

Waese, J., J. Fan, A. Pasha, H. Yu, G. Fucile, R. Shi, M. Cummings, L.A. Kelley, M.J. Sternberg, V. Krishnakumar, E. Ferlanti, J. Miller, C. Town, W. Stuerzlinger, N.J. Provart. 2017. ePlant: visualizing and exploring multiple levels of data for hypothesis generation in plant biology. The Plant Cell 29: 1806-1821. doi:10.1105/tpc.17.00073.

Chapter Three: An *Agrobacterium*-mediated transformation protocol of *Jaltomata bohsiana*

Vincenzo Averello IV (ORCID: 0000-0002-5962-9933)[1], Clay Carter (ORCID:0000-0001-9726-1722) [2], Adrian D. Hegeman (ORCID: 0000-00003-1008-6066)[1,2]

1- Department of Horticultural Science, University of Minnesota – Twin Cities, 1970 Folwell Ave, Saint Paul, MN 55108

2- Department of Plant and Microbial Biology, University of Minnesota – Twin Cities, 123 Snyder Ave, Saint Paul, MN 55108

Abstract

Several species in *Jaltomata* produce blood-red nectar, a transformation protocol will enable further research into this trait. Cotyledon and hypocotyl explants were generated from sterile grown seedlings and cocultivated with *Agrobacterium tumefaciens* strain AGL1 containing a T-DNA binary vector based on pDirect_21C which confers resistance to hygromycin B for 48 hours. Explants were transferred to Murashige and Skoog media supplemented with 2 mg/L of *trans*-zeatin to induce shoot growth, 25 mg/L of hygromycin B to select for transformed cells, and 500 mg/L of cefotaxime to remove residual *Agrobacterium*. Explants were maintained on this media for 14 days before being transferred to new media with the same additives, except *trans*-zeatin concentration is reduced to 1 mg/L. A total of 6 calli survived on this media producing 11 shoots. These were transferred to a rooting media that contained 500 mg/L cefotaxime. When sufficient roots had developed, these were transferred to soil. Polymerase chain reaction (PCR) suggested that 3 of these carried the transgene. Further confirmation using Thermal asymmetric interlaced (TAIL) PCR and Sanger sequencing showed T-DNA insertion into the genome of a plant related to *Solanum* (there is only one GenBank entry for *J. bohsiana*, for *waxy*), we conclude the unknown plant sequence to be *J. bohsiana* confirming an insertion event. This transformation protocol should allow research into the genetics of *Jaltomata bohsiana*, including metabolic traits like nectar color or introduction of domestication traits.

Keywords

Jaltomata, *Solanaceae*, AGL1, Hygromycin, TAIL-PCR

Key message

A method for *Agrobacterium mediated* transformation of *Jaltomata bohsiana*. This should enable further genetic research into the species and genus, allowing characterization of traits of interest, such metabolic or domestication traits.

Introduction

Jaltomata bohsiana is a suffruticose plant native to Mexico bearing purple berries (Figure 1a and 1b) (Mione and Spooner, 2010). The leaves and fruits of *Jaltomata* are edible, both eaten unprepared (Davis, 1986; Davis and Bye, 1982). *Jaltomata procumbens* (common name: pipisco) has been found to have antioxidant activity when eaten fresh and when prepared in a sauce (Mendoza-Rodr íguez et al., 2016). All reported chromosome counts for *Jaltomata* are n=12 or 2n=24 and there are no confirmed reports of polyploids (communication with T. Mione). Additionally, all species are reported to be self-compatible (communication with T. Mione). *J. bohsiana* was recently classified as a separate species from *J. procumbens* based on its purple calyx color, smaller fruiting and flower calyx size, and variation in *waxy* sequence (Mione and Spooner, 2010). *Jaltomata bohsiana* is native to Mexico with the type specimen being found in the State of Mexico in a pine forest at 2450m elevation (Mione and Spooner, 2010).

Jaltomata is a genus in Solanaceae, currently classified into tribe Solaneae (Miller et al., 2011; Olmstead et al., 2008). More recent phylogeny based on nuclear genes suggest it may be closer related to the tribes Physalideae and Capsiceae (Huang et al., 2023). Even with whole genome analysis it was difficult to resolve the relationship between *Jaltomata*, *Solanum*, and *Capsicum* (Wu et al., 2019). While colored nectar is relatively rare, at least 13 species in the genus have a red or orange nectar and appears to have evolved up to 8 times (Miller et al., 2011). The red nectar trait was characterized in *J. herrerea* to be caused by nesocodin and the nectar has a relatively high pH (~9) (Roy et al., 2022). Two proteins, α-carbonic anhydrase and sinapyl alcohol oxidase, are present in *J. herrerae* nectar that are hypothesized to be required for a reaction between sinapaldehyde and proline which produces nesocodin (Roy et al., 2022). In *J. procumbens*, the carbonic anhydrase is not present (Roy et al., 2022).

In Solanaceae, *Agrobacterium*-mediated transformation protocols have been developed for many species including tomato, red pepper, groundcherry, eggplant, and petunia (Conner et al., 2009; Khatun et al., 2022; Kumar et al., 2012; Swartwood and Van Eck, 2019; Van Eck et al., 2019). Based on successful methods in these related species, cotyledon and hypocotyl derived explants were chosen for explant tissue source.

Fig. 1 Jaltomata and stages of tissue culture A) *Jaltomata bohsiana* growing outdoors. B) Ripe fruits of *J. bohsiana*. C) Seedlings growing on MS media to produce explants D) Tissue regenerating after co-cultivated with Agrobacterium, arrow pointing toward new shoot development E) Regenerated shoot growing in tissue culture F) Shoot after transplanting to soil

Methods

Regeneration

Because no reported plant regeneration methods for any *Jaltomata* species were found, we began with determining which species and which sources of tissue would be most effective. One option for tissue is the use of leaf tissue. To determine if regeneration is effective from *Jaltomata,* four species were initially selected, *J. bohsiana*, *J. procumbens*, *J. herrerae*, and *J. ventricosa* based on the availability of leaf tissue. Plants were grown in a controlled environment greenhouse in Saint Paul, MN. All leaves collected were 5-8 leaves from the newest growth on a stem. Leaves were placed in sterile water in a Magenta GA-7 (Phytotech Labs, Lenexa, KS) container (hereafter referred to as a magenta box) before being brought to a sterile laminar flow hood. Water was removed by pouring and replaced with a surface sterilization solution of 10% bleach and 0.1% Tween-20. Enough sterilization solution was added to cover all the leaf surface. Magenta boxes were shaken at 100 RPM on an orbital shaker for 12 minutes. Sterilization solution was removed by pouring and replaced by sterile water 3 times.

To produce leaf disk explants, the leaf margin and mid-vein were removed using a curved scalpel blade. Explants were approximately 1.5 cm^2. All cuts were performed in MS-0

liquid media. MS-0 liquid media contains 4.4 g/L basal MS salts, 100 mg/L myo-inositol, 0.4 mg/L thiamine HCl, and 20 g/L sucrose, adjusted to pH 5.8 ± 0.03 with KOH and HCl. Explants were placed on shoot inducing media. Shoot inducing media was 2.2 g/L MS salts, 100 mg/L myo-inositol, 20 g/L sucrose, 1 mL/L of 1000x modified Nitsch vitamin stock with 2 mg/L *trans*-zeatin. 1000x modified Nitsch vitamin stock contains 0.002 g/L of glycine, 0.01 g/L nicotinic acid, 0.0005 g/L pyridoxine HCl, 0.0005 g/L thiamine HCl, 0.0005 g/L folic acid, 0.00004 g/L D-biotin and adjusted to pH 7.0 ± 0.03. Media was adjusted to pH 6.0 ± 0.03 with KOH and then 2 g/L Phytagel™ is added and is sterilized by autoclave. Explants were transferred to new media after 14 days with 1 mg/L of *trans*-zeatin.

To produce cotyledon and hypocotyl explants, *Jaltomata* seeds are first surface sterilized overnight. Seeds were originally purchased from Tradewind Fruits (Santa Rosa, CA) or collected from plants grown from these seeds. 25-35 *Jaltomata bohsiana* seeds were placed in a sterile microcentrifuge tube. 500 uL of sterilization solution was added to each tube. Sterilization solution was 3% sodium hypochlorite with 0.1% Tween-20. Samples were shaken for 7 min on an orbital shaker at 100 RPM. After shaking samples were centrifuged for 2 min at 3000 RPM. The supernatant was removed and replaced with 500 uL of sterile deionized H_2O and centrifuged for 2 min at 2500 RPM. This was replaced with sterile water 4 times total and incubated overnight at 4°C.

The next day, the seeds were transferred by pipette to magenta boxes containing media with 2.2 g/L MS (0.5X) salts (Phytotech Labs, Lenexa, KS), 100 mg/L myo-inositol (Sigma, St. Louis, MO), 2 mg/L thiamine HCl, 0.5 mg/L pyridoxine HCl, 0.5 mg/L nicotinic acid, and 10 g/L sucrose, ph 5.8 and solidified with 8 g/L agar (Figure 1c). Magenta boxes were stored in the dark for 48 hr at 16°C before being moved to 16L/8D at 24°C. When at least 75% of the seeds had germinated in a box and before the 2 true leaf stage, up to 4 explants were generated from each seedling, one from each cotyledon and 2 from the hypocotyl cut laterally (Figure 2). This typically occurred 10-14 days post seeding. For the leaf cotyledon, approximately 1 cm of tissue was removed from the tip and the remaining tissue was removed leaving approximately 1 cm of cotyledon tissue. The hypocotyl explants were generated from the remaining tissue cutting the hypocotyl approximately 3 cm from the meristem. All cuts were made with a curved scalpel blade #10 and were performed with the tissue submerged in liquid MS media. The meristem was then removed from hypocotyl explants.

Approximately 50 explants were placed on each circular petri plate (100 mm x 15 mm) containing media with 2.2 g/L MS salts, 100 mg/L myo-inositol, 20 g/L sucrose, and 1 mL/L of 1000x modified Nitsch vitamin stock. Media was adjusted to pH 6.0±0.03 with KOH and then 2 g/L Phytagel™ is added and is sterilized by autoclave. After sterilization and cooling to a safe pouring temperature (approximately 55°C), 2 mg/L *trans*-zeatin is added. Cotyledon explants were placed adaxial side up, ensuring that cut sides were touching the media. Hypocotyl segments were placed with the cut side touching the media.

Transformation

This transformation protocol was based on those for tomato and *Physallis pruinosa* protocols (Swartwood and Van Eck, 2019; Van Eck et al., 2019). Based on results of regeneration experiments, cotyledon and hypocotyl were chosen as explant sources.

Agrobacterium AGL1 was streaked onto LB media with 25 mg/L Kanamycin and incubated for 48 hours at 28℃. 1 50mL LB liquid culture for each 5 explant plates were prepared and incubated on a shaking incubator at 28℃ overnight until $OD_{600} = 0.6$. Liquid cultures were transferred to 10 mL round bottom culture tubes and centrifuged at 4000 RPM for 20 min. Agrobacterium is resuspended in liquid MS media and transferred to a sterile magenta box, total volume per box is approximately 50 mL. 5 plates of explants are added to each box. Explants were incubated with *Agrobacterium* for 10 minutes with gentle shaking using an orbital shaker.

After this time, explants were removed from the *Agrobacterium* media and briefly placed on sterile paper towels, moistened with MS liquid media. Following this, they were returned to the initial plates, adaxial side down at this point. These plates were sealed with parafilm and stored in the dark at 19℃ for between 48-72 hours.

Following this incubation, explants are transferred to new plates. The media is the same as the co-cultivated media except with the addition of 500 mg/L cefotaxime to control *Agrobacterium* and 25 mg/L Hygromycin B to select for transformants. Explants are transferred to new media every 14 days. These plates are the same as the previous media with the exception that the *trans*-zeatin concentration is reduced from 2 mg/L to 1 mg/L.

When a stem with at least one node develops, it is transferred to a selective rooting media in a sterile magenta box (Figure 1e), transferring to new media every 2 weeks. When roots are fully formed, the plant is transferred to soil to grow (Figure 1f).

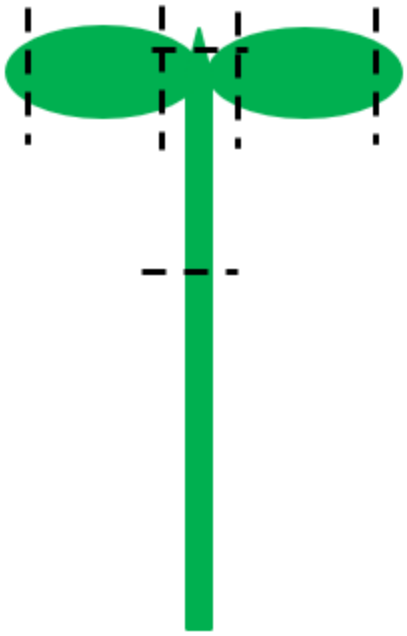

Fig. 2 Diagram of explant sources from *Jaltomata bohsiana* seedling. Each seedling produced at least 3 explants, 1 from each cotyledon, and at least one from the hypocotyl.

Plant Nuclear DNA Extraction

100 mg of leaf tissue was collected in a 1.5 mL tube and flash frozen using liquid nitrogen. This was ground to a fine powder using a pestle. 500 µL of extraction buffer was added to the leaf tissue. The extraction buffer contains 0.05 M ethylenediaminetetraacetic acid (EDTA), 0.1 M Tris-HCl, 0.5 M NaCl, and 2% sodium dodecyl sulfate (SDS). Samples were mixed by vortex and then incubated at 70°C for 60 minutes, mixing by inversion every 15 minutes. After the incubation, 130 µL of ice cold 5 M potassium acetate was added to each sample, which were mixed by inversion and then incubated on ice for 5 min. Samples were centrifuged at 14,000 g for 5 min. Supernatant was collected and transferred to a clean 1.5 mL tube. 30 µL of 3 M Sodium Acetate was added to each sample followed by 330 µL of ice cold 2-propanol. Samples were incubated for 10 min on ice before centrifuging for 5 min at 14,000 g. Supernatant was discarded and replaced with 700 µL of 70% ethanol. Samples were centrifuged for 5 minutes at 14,000 g before supernatant was removed and pellet was allowed to dry for 120 min and resuspended in H_2O. DNA content was determined using a ThermoScientific NanoDrop Spectrophotometer 2000c (Waltham, MA).

Polymerase Chain Reaction (PCR)

Polymerase chain reaction (PCR) was used to determine if insertions were present in *Jaltomata bohisana*. The reaction mixture for PCR was 2.5 µL of 10X NEB ThermoPol Reaction Buffer, 200 µM of dNTPs, 0.2 µM primer M13F, 0.2 µM primer TC320, 1.0 µL of template DNA, 0.625 U of *Taq* polymerase, and a total reaction volume of 25 µL. PCR thermocycling conditions were 95°C for 30 seconds, followed by 30 cycles of 95°C for 15 seconds, 55°C for 30 seconds, 68°C for 1 minute followed by 68°C for 10 minutes before holding at 4°C. PCR products were visualized using a 1% agarose gel with NEB 1 kb DNA Ladder for determining product size. Oligo sequence was from (Cermak et al., 2017) for detecting insertions into the gene editing vector pDIRECT_21C were used here to detect insertions into *Jaltomata bohsiana.* All oligos were synthesized by Integrated DNA Technologies (Coralville, IA).

Table 1- Oligo Sequences

Primer Name	Sequence	Tm (°C)
M13F	GTAAAACGACGGCCAGT	54
TC320	CTAGAAGTAGTCAAGGCGGC	57
AD1	NGTCGASWGANAWGAA	45.6
AD2	TGWGNAGSANCASAGA	49.4
AD3	AGWGNAGWANCAWAGG	44.2
AD6	WGTGNAGWANCANAGA	44.6
LB01	CATATAAGAAACCCTTAGTATGTATTTGTATTTGTA AAATACTTCTATCA	59
LB02	TGAGTAGTTCCCAGATAAGGGAATTAGGGTTCC	63

Primer Name	Sequence	Tm (°C)
M13F	GTAAAACGACGGCCAGT	54
TC320	CTAGAAGTAGTCAAGGCGGC	57
AD1	NGTCGASWGANAWGAA	45.6
AD2	TGWGNAGSANCASAGA	49.4
LB03	GATCGACAAGCTCGAGTTTCTCCATAATAATGTG	62

TAIL-PCR

Thermal asymmetric interlaced PCR (TAIL-PCR) was used to determine if insertions were present after cocultivation with *Agrobacterium*. TAIL-PCR was performed in 3 stages. The primers specific to pDIRECT_21C were designed in SnapGene® Viewer software (Dotmatics, Boston, MA) with each primer selected based on criteria in (Singer and Burke, 2003) with decreasing distance from insertion site (Cermak et al., 2017). AD1, AD2, AD3, and AD6 were combined into 4X AD primer pool with AD1, AD2, and AD3 at a concentration of 12 µM, and AD6 at a concentration of 16µM. The reaction mixture for the first stage of TAIL-PCR contained 1µL 10X Thermopol Reaction Buffer, 0.2 mM dNTPs, 0.2 µM LB03 primer, 2.5 µL of 4X AD primer pool (final concentration of AD1, AD2, and AD3 being 3 µM and AD6 being 4µM), 0.5 U of *Taq* DNA polymerase, and 1 µL of template DNA, with a total reaction volume of 10 µL. DNA was used directly from DNA extraction without dilution unless initial concentration was greater than 100 ng/µL, in which case it was diluted 1:10 before use in TAIL-PCR. The cycling conditions for the first stage are 94℃ for 15 minutes, 5 cycles of 94℃ for 30 seconds, 62℃ for 1 minute, and 72℃ for 2:30 minutes, followed by 94℃ for 30 seconds, and 2 cycles of 25℃ decreasing by 0.4℃/minute for 3 minutes and 72℃ decreasing by 0.3℃/minute, this is followed by 15 cycles of 94℃ for 10 seconds, 68℃ for 1 minute, 72℃ for 2:30 minute, 94℃ for 10 seconds, 68℃ for 1 minute, 72℃ for 2:30 minute, 94℃ for 10 seconds, 44℃ for 1 minutes, and 72℃ for 2:30, before a final 72℃ for 5 minutes and hold at 4℃.

The second PCR contained 1 µL 10x Thermopol Reaction Buffer, 0.2 mM dNTPs, 0.2 µM LB02 primer, 1.5 µL of 4X AD primer pool (final concentration of AD1, AD2, and AD3 being 1.8 µM and AD6 being 2.4 µM), 0.5 U of *Taq* DNA polymerase, and 1 µL of 1:100 diluted PCR product from the first PCR. The cycle for the second PCR reaction was 94℃ for 15 minutes, five cycles of 94℃ for 10 seconds, 64℃ for 1 minute and 72℃ for 2:30, followed by 15 cycles of 94℃ for 10 seconds, 64℃ for 1 minutes, 72℃ for 2:30, 15 cycles of 94℃ for 10 seconds, 64℃ for 1 minutes, 72℃ for 2:30, 94℃ for 10 seconds, 64℃ for 1 minutes, 72℃ for 2:30, 94℃ for 10 seconds, 44℃ for 1 minutes, and 72℃ for 2:30, followed by 5 cycles of 94℃ for 10 seconds, 44℃ for 1 minute, and 72℃ for 3 minutes, followed by a final extension at 72℃ for 5 minutes and hold at 4℃.

The third PCR reaction mixture contained 2µL 10x Thermopol Reaction Buffer, 0.2 mM dNTPs, 0.2 µM LB01 primer, 5 µL 4x AD primer pool (final concentration of AD1, AD2, and AD3 being 3 µM and AD6 being 4µM), 0.5 U of *Taq* polymerase and 1 µL of 1:50 diluted PCR from the 2nd PCR. with a total volume of 20 µL. The program for the third PCR reaction was 94℃ for 15 minutes, followed by 20 cycles of 94℃ for 10 seconds, 44℃ for 1 minute, 72℃ for 2 minutes, then a final extension at 72℃ for 5 minutes, and hold at 4℃. PCR product from this reaction was separated and visualized on 1% agarose gel with ethidium bromide. Bands were extracted from agarose gel using a Qiagen QIAQuick Gel Extraction Kit (Germantown, MD) using manufacturer's instructions.

Gene Cloning and Sequencing

The purified bands were cloned into a pGEM-T vector using the pGEM-T Vector System II (Promega Corporation, Madison, WI) following manufacturer's instructions. White colonies were streaked to ensure only a single colony was present. DNA was extracted from liquid colonies using a New England Biolabs Monarch Plasmid Miniprep Kit (Ipswich, MA) following manufacturer's instructions. Sanger sequencing was performed by Azenta.

Results

Approximately 200 leaf discs of each species, *Jaltomata bohsiana*, *Jaltomata procumbens*, *Jaltomata herrerea*, *Jaltomata ventricosa*, were placed on shoot inducing media. While some of these produced calli, no calli produced shoots even after 2 months on culture medium. Based on this result, leaf discs were not considered effective for explant production going forward.

Approximately 100 seeds were germinated on MS germination media producing approximately 200 cotyledon explants and 100 hypocotyl explants. A total of 6 explants produced calli. All calli produced were from the root end of the hypocotyl, consistent with the findings for regeneration of *Physallis pruinosa*. These produced a total of 12 shoots, one

of which died in the magenta box due to fungal contamination. These were separated from the callus and allowed to produce roots, all of which readily produced roots on media before being transferred to soil in a greenhouse. Initial PCR suggested that 3 of these shoots carried the insertion (Figure 3). Samples 1D, 1E1 and 2 amplified the expected 609 bp fragment. As this approach is only sensitive to the presence or absence of the T-DNA, a positive result could be due to residual *Agrobacterium* and does not necessarily confirm T-DNA insertion into the plant genome.

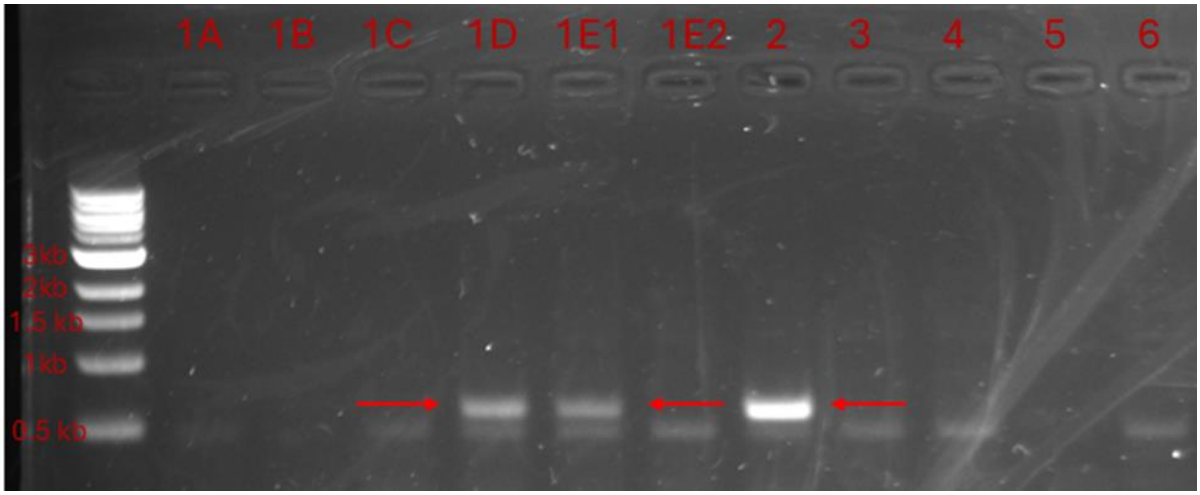

Fig 3 1% agarose gel to detect presence of DNA insertion into *J. bohsiana*. Arrows indicate bands of interest

To further confirm the insertion, TAIL-PCR was performed on all samples and visualized on a 1% agarose gel (figure 4). TAIL-PCR produces a product that includes both T-DNA sequence and plant sequence. Like the previous PCR, samples 1D, 1E-1, and 2 have PCR bands that suggest the presence of an insertion, as well as sample 5. When these bands were extracted and cloned into a vector for Sanger sequencing. Sample 1D was successfully cloned and sequenced. Samples 1E-1, 2, and 5 were not successfully cloned into the TA vector at this time.

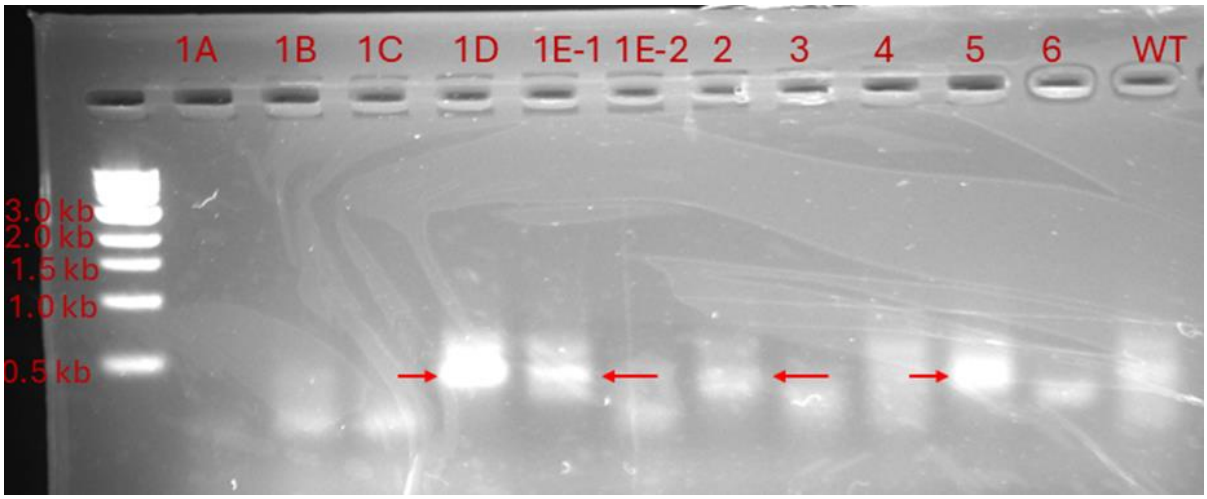

Fig 4 1% agarose gel of J. bohsiana TAIL-PCR. Arrows indicate bands of interest.

One of these, 1D, was successfully cloned and sequenced. The sequence was analyzed to identify sections from the pGEM-T and pDIRECT_21C (Figure 5). The remaining sequence was used for a BLAST against the non-redundant nucleotide database using BLASTN (performed on September 19, 2024). Of the 97 hits, 96 were to accessions in subfamily Solanoideae, with 94 being to *Solanum* and 2 to *Capsicum rhomboideum*, the remaining hit was to the insect *Aphideta obliterata*. The top 5 of these are summarized in Table 3, with the highest significant alignment to *Solanum nigrum* (Figure 6). While TAIL-PCR is usually used to map an insertion into a genome, in this situation, it is used to determine if the insertion is in the plant genome. There is currently one GenBank accession attributed to *J. bohsiana* (GU256349.1), it is unlikely that the short sequence detected by TAIL-PCR would match to that entry. Because the TAIL-PCR product contains sequence which matches to the T-DNA vector and to a plant sequence it can be concluded the T-DNA was inserted into the genome of *Jaltomata bohsisana*.

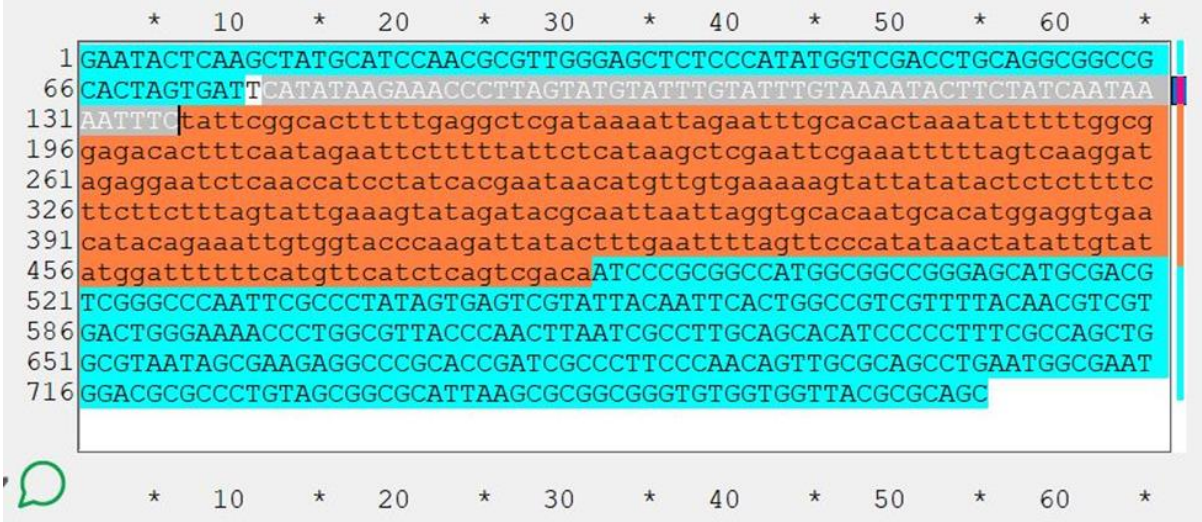

Fig 5 Sequence of clone from sample 1D. ApE was used to color sections, cyan is from pGEM-T, grey matches pDIRECT_21C, and orange is assumed to be Jaltomata sequence based on BLAST results

Table 2- Five highest results of BLASTN of non-redundant nucleotide database

Description	Scientific Name	Max Score	Total Score	Query Cover	E value	Percent identity	Access ion
Solanum nigrum genome assembly, chromosome: 28	*Solanum nigrum*	126	250	90%	1e-23	68.9	OZ176 039.1
Solanum dulcamara genome assembly, chromosome: 8	*Solanum dulcamara*	123	123	31%	1e-22	83.62	OX35 9259.1
Solanum nigrum genome assembly, chromosome: 32	*Solanum nigrum*	122	122	38%	1e-22	81.75	OZ176 043.1

Solanum nigrum genome assembly, chromosome: 33	*Solanum nigrum*	121	121	40%	4e-22	79.19	OZ176044.1
Solanum dulcamara genome assembly, chromosome: 4	*Solanum dulcamara*	84.2	84.2	26%	3e-11	80.65	OX359255.1

Solanum nigrum genome assembly, chromosome: 28

Sequence ID: OZ176039.1 Length: 75158893 Number of Matches: 3

Range 1: 64888055 to 64888378 GenBank Graphics ▼ Next Match ▲ Previous Match

Score	Expect	Identities	Gaps	Strand
126 bits(139)	1e-23	237/344(69%)	46/344(13%)	Plus/Plus

```
Query  15        TGAGGCTCGATAAAATTAGAATT--TGCACACTA-AAT--ATTTTTGGCGGAGACACTTT  69
                 ||||| | ||| ||||||||||  ||||   || |||  | |||| |  | ||| ||||
Sbjct  64888055  TGAGGTTTGATTAAATTAGAATTCATGCATTGTAGAATTCAATTTTAGAAGTGACGCTTT  64888114

Query  70        CAATAGAATTCTTTTTATTCTCATAAGC--TCGAATTCGAAATTTTTAGTCAAGGATA-G  126
                 ||| |  ||| |||| ||| ||||| |   | ||||  ||||  | |  | |||  |  |
Sbjct  64888115  CAACAAGATTTTTTTCATTTTCATAGGGATTTGAATATGAAACCTCTGATTAAGAGTGTG  64888174

Query  127       AGGA-ATCTCAACCATCCTATCAC--------------GAATAACATGTTGTGAAAAAGT  171
                 |||| || | |||| | ||| |||              || ||||| |||  || |||||
Sbjct  64888175  AGGAGATTTTAACCGTTCTACCACAATCTATGTTTATAGATTAACAAGTTACGAGAAAGT  64888234

Query  172       ATTATATACTCTCTTTTCTTCTTCTTTAGTATTGAAAGTATAGATACGCAATTAATTAGG  231
                 |||||||| |              |  | |||||||||| |||| ||||||||||   |||
Sbjct  64888235  ATTATATAAT------------TAATGAGTATTGAAAATATAAATACGCAATTA---AGG  64888279

Query  232       TGCACAATGCACATGGAGGTGAACATACAGAAATTGTGGTACCCAAG---ATTATACTTT  288
                 ||||||||||||||||||  |||||||  |||||||| |||||||   ||||| |  |
Sbjct  64888280  TGCACAATGCACATGGAGGT--ACATACATGAATTGTGGCACCCAAGATTATTATGCGAT  64888337

Query  289       GAATTTTAGTTCCCATATAACTATATTGTATATGGATTTTTTCA  332
                 |||||| |||| ||||||   | |||  |||||| ||||||| ||
Sbjct  64888338  GAATTTCAGTTTCCATAT---TGTATAATATATGCATTTTTCCA  64888378
```

Range 2: 2754494 to 2754587 GenBank Graphics ▼ Next Match ▲ Previous Match ▲ First Match

Score	Expect	Identities	Gaps	Strand
65.3 bits(71)	3e-05	75/100(75%)	6/100(6%)	Plus/Minus

```
Query  50        ATTTTTGGCGGAGACACTTTCAATAGAATTCTTTTTATTCTCATAAGCTCGAATTCGAAA  109
                 |||| ||| || ||| ||| ||| |      ||||| |||| | | ||||||| || |||
Sbjct  2754587   ATTTCTGGAGGTGACGCTTCCAACAA-----TTTTTTTTCTAAGA-GCTCGAACTCAAAA  2754534

Query  110       TTTTTAGTCAAGGATAGAGGAATCTCAACCATCCTATCAC  149
                 ||| || | ||  |||||||||||| |||| ||||||||||
Sbjct  2754533   TTTCTAATTAAAAATAGAGGAATCCCAACTATCCTATCAC  2754494
```

Range 3: 72646403 to 72646467 GenBank Graphics ▼ Next Match ▲ Previous Match ▲ First Match

Score	Expect	Identities	Gaps	Strand
58.1 bits(63)	0.004	53/66(80%)	1/66(1%)	Plus/Plus

```
Query  59        GGAGACACTTTCAATAGAATTCTTTTTATTCTCATAAGCTCGAATTCGAAATTTTTAGTC  118
                 || |||||||  |||||||||| |||| || | || | ||||||||||||||| | |  |
Sbjct  72646403  GGTGACACTTCCAATAGAATTTTTTTCATACCCAGA-GCTCGAATTCGAAATCTCTGATT  72646461

Query  119       AAGGAT  124
                 ||||||
Sbjct  72646462  AAGGAT  72646467
```

Fig 6 Blast alignment to *Solanum nigrum* chromosome 28, the accession with the highest E-value of BLAST Search hits

Discussion

A transformation protocol for *Jaltomata bohsiana* will enable further genetic research into this species as well as others in the genus, including *Jaltomata sinuosa* and *Jaltomata hererrea*. The chemical characterization of *J. hererrea*'s nectar can be furthered with genetic knock-outs of candidate genes related to this red nectar trait. Additionally, the genes that have been suggested to encode the red nectar trait are not present in *J. bohsiana* and could be transformed to attempt to produce the red nectar color, characterizing the genetics of the trait.

Initial regeneration and transformation experiments were limited by the availability of seed. Due to this, a leaf disk method was initially attempted for four *Jaltomata* species, *J. bohsiana*, *J. herrareae*, *J. procumbens,* and *J. ventricosa*. However, while callus was observed in all species tested, there was no formation of shoots even without selective pressure. When enough seed was available for *J. bohsiana*, *J. procumbens*, and *J. herrareae* these were used to generate explants for transformation. Both *J. bohsiana* and *J. procumbens* germinated on seeding media at high enough frequency, *J. herrareae* did not. Options to improve seed germination in *J. herrareae* include treating see with GA3 or as was reported in *J. procumbens*, KNO_3 (Flores-S ánchez et al., 2022). Because this protocol is very similar to previously published protocols for other Solanaceae species, it is hopeful that this protocol can be applied and adapted to other *Jaltomata* species. If we consider the hypocotyl of *J.bohsiana* to the be best source of explants producing a total of six independent calli, which produced 12 shoots. However, our current understanding This transformation protocol was developed using a T-DNA vector that carries the HygR gene, which confers resistance to hygromycin B. While this is effective, if other antibiotic selectable markers are used, there will be need to research to determine effective concentrations for selection. While a total of 12 shoots were produced from 6 calli, only 4 potentially carry a T-DNA insert. With a high escape rate, a higher HygB rate may be tested in future *Jaltomata* transformation protocol development. Similar considerations should be made if using a different antibiotic than cefotaxime to control *Agrobacterium* after cocultivation. While we have shoots that survived on HygB, there was a large number of escapes, however, 2 DNA based methods, one targeting the T-DNA sequence and TAIL-PCR, which produced a sequence including binary vector sequence and plant DNA sequence, lead to the conclusion this is a transformation event. Further confirmation of this transformation will be the heritability of T-DNA. However, at this time, none of the likely transformed plants have produced fruit.

Two of the requirements for gene editing are well annotated genomes and effective transformation protocols. This work represents one part of that, an effective transformation protocol for *Jaltomata bohsiana*. Further work to develop well annotated genomes for *Jaltomata* will be needed for effective gene editing and prime editing as it becomes adapted to dicots (Vu et al., 2024).

There are several interesting classes of metabolites that are common in *Solanum* such as steroidal glycoalkaloids and acylsugars that have a wide diversity of forms (Averello et al., 2024; Kerwin et al., 2024; Zhao et al., 2021). Little is known about *Jaltomata*'s production of these specialized metabolites. If steroidal glycoalkaloids are produced, it would be important to understand the production of these and how similar they are to *Solanum* species or if different SGAs are produced than those found in *Solanum.*

As *Jaltomata procumbens* is eaten as food, there may be interest in growing it in more places. At this time, there is little information on the cultivation and horticultural traits of *Jaltomata bohsiana*, however, it is possible it has several weedy traits that may limit its use. Gene editing could be a way to quickly generate plants that have been moved closer to domestication (Lemmon et al., 2019).

Conclusion

The transformation of *J. bohsiana* represents the first reported genetic modification in *J. bohsiana* and the genus *Jaltomata*. This method was based on previous reports for tomato and *Physallis pruinosa*. As with *Physallis pruinosa*, hypocotyl explants were the most effective source of material to transform and should be considered for other Solanaceous species when developing transformation protocols. With this protocol, researchers will be better enabled to understand the production of metabolic traits like the red nectar seen in *Jaltomata herrearae* or if there is interest in cultivation and domestication, transformation and gene editing can be effective to introduce domestication traits.

Works Cited

Averello, V., A.D. Hegeman, and C. Chen. 2024. Finding the Balance: Modifying the Cholesterol and Steroidal Glycoalkaloid Synthesis Pathway in Tomato (Solanum lycopersicum L.) for human health, fruit flavor, and plant defense. Horticultural Plant Journal. doi: https://doi.org/10.1016/j.hpj.2023.05.019.

Cermak, T., S.J. Curtin, J. Gil-Humanes, R. Čegan, T.J.Y. Kono, E. Konečná, J.J. Belanto, C.G. Starker, J.W. Mathre, R.L. Greenstein, and D.F. Voytas. 2017. A multi-purpose toolkit to enable advanced genome engineering in plants. The Plant Cell 29:tpc.00922.02016-tpc.00922.02016. doi: 10.1105/tpc.16.00922.

Conner, A.J., N.W. Albert, and S.C. Deroles. 2009. Transformation and Regeneration of Petunia. In: T. Gerats and J. Strommer (eds.). Petunia. Springer, New York, NY. doi: https://doi-org.ezp1.lib.umn.edu/10.1007/978-0-387-84796-2_19.

Davis, T. 1986. *Jaltomata* and the Tarahumara Indian Region of Northern Mexico. In: W.G. D'Arcy (ed.). Solanaceae: Biology and Systematics. Columbia University Press, New York.

Davis, T. and R.A. Bye. 1982. Ethnobotany and progressive domestication of *Jaltomata* (Solanaceae) in Mexico and Central America. Economic Botany 36:225-241. doi: https://doi-org.ezp1.lib.umn.edu/10.1007/BF02858722.

Flores-Sánchez, I.D.í., M. Sandoval-Villa, and E. Uscanga-Mortera. 2022. Breaking seed dormancy of *Jaltomata procumbens* (Cav.) J.L. Gentry Seeds with the use of KNO_3. Crops 2:99-110. doi: https://doi.org/10.3390/crops2020008.

Huang, J., W. Xu, J. Zhai, Y. Hu, J. Guo, C. Zhang, Y. Zhao, L. Zhang, C. Martine, H. Ma, and C.-H. Huang. 2023. Nuclear phylogeny and insights into whole-genome duplications and reproductive development of Solanaceae plants. Plant Communications 4. doi: https://doi.org/10.1016/j.xplc.2023.100595.

Kerwin, R.E., J.E. Hart, P.D. Fiesel, Y.-R. Lou, P. Fan, A.D. Jones, and R.L. Last. 2024. Tomato root specialized metabolites evolved through gene duplication and regulatory divergence within a biosynthetic gene cluster. Science Advances 10. doi: DOI:10.1126/sciadv.adn3991.

Khatun, M., B. Borphukan, I. Alam, C.A. Keya, H. Khan, M.K. Reddy, and M. Salimullah. 2022. An improved *Agrobacterium* mediated transformation and regeneration protocol for successful genetic engineering and genome editing in eggplant. Scientia Horticulturae 293. doi: https://doi.org/10.1016/j.scienta.2021.110716.

Kumar, R.V., V.K. Sharma, B. Chattopadhyay, and S. Chakraborty. 2012. An improved plant regeneration and *Agrobacterium*-mediated transformation of red pepper (*Capsicum annuum* L.). Physiology and Molecular Biology of Plants 18:357-364.

Lemmon, Z. H., N. T. Reem, J. Dalrymple, S. Soyk., K.E. Swartwood, D. Rodriquez-Leal., J. Van Eck., and Z. Lippman. 2018. Rapid improvement of domestication traits in an orphan

crop by genome editing. Nature Plants 4: 766-770. doi: https://doi.org/10.1038/s41477-018-0259-x.
Mendoza-Rodríguez, M.N., L. González-Barraza, L. Argüelles-Martínez, I. Hernández-Ramírez, M. Cervantes-Rodríguez, O. Rodríguez-Salazar, A. Aguilar-Paredes, and D. Méndez-Iturbide. 2016. Antioxidant capacity of the wild fruit pipisco (*Jaltomata procumbens)*, and its application in the preparation of a sauce. Mexican Journal of Biotechnology 1:83-96. doi: https://doi.org/10.29267/mxjb.2016.1.2.83.

Miller, R.J., T. Mione, H.-L. Phan, and R.G. Olmstead. 2011. Color by Numbers: Nuclear Gene Phylogeny of Jaltomata (Solanaceae),Sister Genus to Solanum , Supports Three Clades Differing in Fruit Color. Systematic Botany 36 153-162. doi: DOI 10.1600/036364411X553243.
Mione, T. and D.M. Spooner. 2010. *Jaltomata bohsiana*: A New Species and Key to the *Jaltomata* (Solanaceae) of Mexico. Novon: A Journal for Botanical Nomenclature 20:186-198. doi: https://doi.org/10.3417/2009025.
Olmstead, R.G., L. Bohs, H.A. Migid, E. Santiago-Valentin, V.F. Garcia, and S.M. Collier. 2008. A molecular phylogeny of the Solanaceae. Taxon 57:1159-1181. doi: 10.1002/tax.574010.
Roy, R., N. Moreno, S.A. Brockman, A. Kostanecki, A. Zambre, C. Holl, E.M. Solhaug, A. Minami, E.C. Snell-Rood, M. Hampton, M.A. Bee, Y. Chiari, A.D. Hegeman, and C.J. Carter. 2022. Convergent evolution of a blood-red nectar pigment in vertebrate-pollinated flowers. Proceedings of the National Academy 119. doi: https://doi.org/10.1073/pnas.2114420119.
Singer, T. and E. Burke. 2003. High-Throughput TAIL-PCR as a Tool to Identify DNA Flanking Insertions, p. 241-271. In: E. Grotewold (ed.). Plant Functional Genomics. Methods in Molecular Biology. Humana Press, Totowa, NJ. doi: https://doi-org.ezp3.lib.umn.edu/10.1385/1-59259-413-1:241.
Swartwood, K. and J. Van Eck. 2019. Development of plant regeneration and *Agrobacterium tumefaciens*-mediated transformation methodology for *Physalis pruinosa*. Plant Cell, Tissue and Organ Culture (PCTOC) 137:465-472.
Van Eck, J., P. Keen, and M. Tjahjadi. 2019. Agrobacterium tumefaciens-Mediated Transformation of Tomato, p. 225-234. In: S. Kumar, P. Barone, and M. Smith (eds.). Agrobacterium Protocols: Methods and Protocols. Humana Press, New York, NY.
Vu, T.V., N.T. Nguyen, J. Kim, Y.J. Song, T.H. Nguyen, and J.-Y. Kim. 2024. Optimized dicot prime editing enables heritable desired edits in tomato and *Arabidopsis*. Nature Plants. doi: https://doi-org.ezp3.lib.umn.edu/10.1038/s41477-024-01786-w.
Wu, M., J.L. Kostyun, and L.C. Moyle. 2019. Genome sequence of *Jaltomata* addresses rapid reproductive trait evolution and enhances comparative genomics in the hyper-diverse Solanaceae. Genome Biology and Evolution 11:335-349. doi: 10.1093/gbe/evy274.

Zhao, D.-K., Y. Zhao, S.-Y. Chen, and E.J. Kennelly. 2021. *Solanum* steroidal glycoalkaloids: structural diversity, biological activities, and biosynthesis. Natural Product Reports 38:1423-1444. doi: 10.1039/D1NP00001B.

Conclusion

As we elucidate the biosynthesis of more specialized metabolites, we can better understand each enzyme in these pathways. In chapter one, I reviewed the current literature about the production of steroidal glycoalkaloids in tomato. When there are multiple copies of a gene as was discussed in chapter two, it is important to determine how these enzymes behave differently. In the case of tomato, there are two genes that perform sterol Δ^7 reduction. In tomato, the understanding was that one of these *7-dehydrocholesterol reductase* (*7DHCR*) reduces 7-dehydrocholesterol to cholesterol while *DWARF5* is assumed to perform any other sterol Δ^7 reductions. When *Sl7DHCR* was expressed in *dwf5 Arabidopsis* plants, there was an increase of β-sitosterol and campesterol compared to the *dwf5* mutant. While *7DHCR* may primarily use 7-dehydrocholesterol as a substrate, our results show it can perform this reaction with other $\Delta^{5,7}$ sterols. With this however, there is the need to further research *SlDWF5* to better understand how these two genes have differentiated functions.

Unlike tomato, which has abundant genomic and genetic resources, the closely related genus *Jaltomata* does not. In chapter three, this is advanced in the description of an *Agrobacterium* mediated transformation protocol. As there is more research into the genus and the species it contains, *Agrobacterium* mediated transformation protocols can assist and improve research in many ways. When applied to plant metabolomics, simple, effective protocols can rapidly advance research when combined with genomic data and gene editing. In the example of *Jaltomata*, with the protocol described earlier it should enable us to continue research in the production of red nectar in the species and the mechanism of alkalinization in the nectar.

Plant genetics research of specialized metabolism allows heterologous expression of genes as was performed with *Sl7DHCR* in *Arabidopsis* which has helped to inform us about the substrate specificity of *Sl7DHCR*. With this information there could be a re-evaluation of the tomato sterol biosynthesis pathway. Similarly, *Jaltomata* nectar contains specialized metabolites and proteins. With a transformation protocol, the genes that encode these proteins can be further characterized. The exciting biochemistry of *Jaltomata* red nectar exemplifies the need for development of genetic manipulation techniques along with genomic data to investigate specialized metabolic traits in Solanaceae.